# Dielectric Sorption Analysis
# on
# Polymer Films

Proefschrift

ter verkrijging van de graad van doctor
aan de Technische Universiteit Delft,
op gezag van de Rector Magnificus Prof.dr.ir. J.T. Fokkema,
voorzitter van het College voor Promoties,
in het openbaar te verdedigen
op maandag 15 oktober 2007 om 15:00 uur
door:

Massimiliano GIACOMELLI PENON

materiaalkundig ingenieur
geboren te ‘s-Gravenhage

Dit proefschrift is goedgekeurd door de promotor:

Prof. dr. S.J. Picken

Samenstelling promotiecommissie:

| | |
|---|---|
| Rector Magnificus | Voorzitter |
| Prof. dr. S.J. Picken | Technische Universiteit Delft, promotor |
| Prof. dr. J. van Turnhout | Technische Universiteit Delft |
| Prof. dr. M. Wübbenhorst | Katholieke Universiteit Leuven |
| Prof. dr. J.H.W. de Wit | Technische Universiteit Delft |
| Ing. L.G.J. van der Ven | Akzo Nobel |
| Prof. B. de With | Technische Universiteit Eindhoven |
| Prof. dr. M.Wessling | Universiteit Twente |
| Prof. dr. F. Kapteijn | Technische Universiteit Delft, reservelid |

Het onderzoek beschreven in dit proefschrift is onderdeel van het onderzoeksprogramma van het SenterNovem, IOP oppervlaktetechnologie, project nr. IOT99001

De publicatie van dit proefschrift is financieel gesteund door SigmaKalon

ISBN 978-90-9022356-8

Keywords: polymer coatings, films, water sorption, dielectric analysis, diffusion coefficient, UV degradation, elevated pressure

Cover design: Massimiliano Giacomelli Penon
Cover: SEM picture of an epoxy clear coating

# Contents

## Chapter 1 INTRODUCTION

1.1 General introduction 9
1.2 Research aim 10
1.3 Research approach 11
*1.3.1 Preview of the following chapters 12*

## Chapter 2 BACKGROUND

2.1 Brief introduction 13
2.2 Coatings 13
*2.2.1 Composition 13*
*2.2.2 Types 15*
*2.2.3 Solvent types 16*
*2.2.4 Nanoparticle in coatings 18*
2.3 Coating degradation 18
*2.3.1 Natural coating degradation 18*
*2.3.2 Analysis of coating degradation 19*
*2.3.3 Exposure – natural weathering 21*
*2.3.4 Exposure – natural accelerated weathering 22*
*2.3.5 Exposure – Accelerated degradation techniques 23*
*2.3.6 Discrepancy between natural and accelerated coating degradation 24*
*2.3.7 Further developments in coating degradation 26*
*2.3.8 Brief discussion 32*
2.4 Dielectric measurements – introduction – models – technique 32
*2.4.1 Dielectric the basics 32*
*2.4.2 Dielectric models 34*
*2.4.3 Mixing theories 34*
*2.4.4 Dielectric spectroscopy vs EIS 35*
*2.5 Water sorption in polymers 36*
2.6 Dielectric Sorption Analysis 37
References 39

## **Chapter 3 DIELECTRIC WATER SORPTION ANALYSIS**

3.1 Introduction 41
3.2 Experimental 42
*3.2.1 Materials 42*
*3.2.2 Experimental set-up 42*
*3.2.3 Gravimetric experiments 44*
*3.2.4 Humidity measurement 44*
3.3 Results 45
*3.3.1 Validation of switching behaviour and stability 45*
*3.3.2 Comparison between DSA results and gravimetric measurements 47*
3.4 Conclusions 50
References 51
Appendix 1 52
Appendix 2 53

## **Chapter 4 VAPOUR DIFFUSION IN POROUS/ NON POROUS POLYMER COATINGS BY DIELECTRIC SORPTION ANALYSIS**

4.1 Introduction 55
4.2 Experimental 56
*4.2.1 Materials 56*
*4.2.2 DSA set-up 57*
*4.2.3 Gravimetric experiments 57*
4.3 Results and discussion 58
*4.3.1 Comparison of films 58*
*4.3.1.1 Films - various frequencies 58*
*4.3.1.2 Films - 1 kHz 60*
*4.3.1.3 Gravimetric measurements 62*
*4.3.2 Comparison of filters 63*
*4.3.2.1 Filters - various frequencies 63*
*4.3.2.2 Filters - 1 kHz 66*
4.4 Conclusions and outlook 68
References 70

**Chapter 5 WATER SORPTION IN UV DEGRADED CLEAR & PIGMENTED EPOXY COATINGS BY DIELECTRIC SORPTION ANALYSIS**

5.1 Introduction 71
5.2 Experimental 72
*5.2.1 Materials 72*
*5.2.2 DSA set-up 73*
*5.2.3 Degradation set up 73*
5.3 Results 74
*5.3.1 DSA measurements on degraded samples 74*
5.4. Conclusions 84
References 85

**Chapter 6 DIELECTRIC SORPTION ANALYSIS OF UV DEGRADED PIGMENTED EPOXY COATINGS AT ELEVATED PRESSURES**

6.1 Introduction 87
6.2 Experimental 88
*6.2.1 Materials 88*
*6.2.2 DSA set-up 89*
*6.2.3 High pressure degradation set up 89*
6.3 Results and discussion 90
*6.3.1 DSA measurements on degraded samples 90*
6.4 Conclusions 102
References 105

**Chapter 7 WATER SORPTION IN UV DEGRADED NANOCOMPOSITE ALKYD COATINGS BY DIELECTRIC SORPTION ANALYSIS**

7.1 Introduction 107
7.2 Experimental 107
*7.2.1 Preparation of nanocomposite coating 107*
*7.2.2 UV degradation of nanocomposite coating 109*
*7.2.3 Expansion measurements 109*
*7.2.4 DSA measurements 109*
*7.2.5 Contact angle measurements 110*

*7.2.6 Ultra Violet – (Visible) spectroscopy (UV-VIS) 110*
*7.2.7 Attenuated Total Reflectance – Fourier Transformed Infrared spectroscopy (ATR – FTIR) 110*
7.3 Results 111
*7.3.1 Expansion measurements 111*
*7.3.2 DSA measurements 112*
*7.3.2.1 DSA measurements on undegraded nanocomposite coatings 112*
*7.3.2.2 DSA measurements on degraded nanocomposite coatings 113*
*7.3.2.3 Calculation of % of water uptake 115*
*7.3.2.4 Sorption models 117*
*7.3.3 Contact angle measurements 121*
*7.3.4 UV-VIS measurements 122*
*7.3.4.1 Effect of solid content: (addition of Laponite nanoparticles) 122*
*7.3.4.2 Effect of UV degradation 123*
*7.3.5 ATR-FTIR measurements 125*
7.4 Conclusions and discussion 126
References 127

**Chapter 8 WATER SORPTION IN NATURALLY DEGRADED COILCOATINGS BY DIELECTRIC SORPTION ANALYSIS**

8.1 Introduction 129
8.2 Experimental 130
*8.2.1 Materials 130*
*8.2.2 DSA set-up 130*
*8.2.3 Natural degradation 130*
*8.2.4 Micro ATR-FTIR 131*
*8.2.5 SEM 131*
8.3 Results 131
*8.3.1 DSA 131*
*8.3.2 ATR-FTIR 135*
8.4 Conclusions and outlook 136
References 137

**Chapter 9 CONCLUSIONS AND OUTLOOK**

9.1 Conclusions 139
9.2 Outlook 140

**SUMMARY 141**
**SAMENVATTING 144**
**Curriculum Vitae 148**
**Acknowledgements 149**
**List of publications 152**

# Chapter 1

# INTRODUCTION

## 1.1 General introduction

The use of paint already appeared during the Stone Age, where cavemen painted animals on a wall in their cave. The Egyptians used paint for the graves of their pharaohs where their customs and gods are illustrated on the walls of the tomb. Surprisingly, these paintings can still be visited and are still in pretty good condition, taken into account that they are several thousand years old. But due to the large number of visitors, the quality of the paintings is diminishing. The humidity, temperature and light cycles are the main cause of this degradation, and action has been undertaken to prevent further loss of these cultural treasures by closure.

In former days paint was used for decoration, but nowadays protection of the substrate plays a very important role besides decoration. Coatings are not designed to last forever, but they preferably last as long as the lifetime of the product. Even this preference is a demanding one, because often coatings degrade and loose their protective qualities before the product is at the end of its lifecycle. A few examples are coatings used on bridges, gates, monuments, ships, automotive coatings, coated roof plates, window frames, etc (fig. 1). The parameters that cause this degradation are light, temperature, water, oxygen and other chemical substances that appear in water (NaCl, acid rain) or the atmosphere ($NO_x$, $SO_3$, $O_3$,).

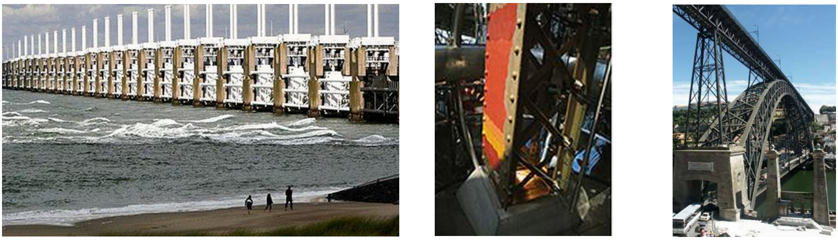

*Fig. 1 Photo's of: the Deltaworks (left); Eiffel tower (middle); ponte Dom Luis (Oporto) (right).*

The coating industry continuously improves their coatings and is doing much research to comply with the demands of the customer and government. Rheology, levelling, adhesion, curing and processing techniques are important research issues; for most coatings the lifetime as a function of the weathering or exposure condition is a research item as well. The service life is not only important for the customer, but also for the coating industry, which needs this information to innovate and improve their coatings, in order to remain competitive on the market.

The experimental tests used to predict the lifetime of a coating can be divided in two categories: accelerated and natural exposure. In short, accelerated exposure is done on a laboratory scale and tries to mimic and accelerate the natural weather. Natural exposure is putting the coating system (plus substrate) outside under a certain angle, certain direction and often at a specific location and monitoring the changes.

Accelerated exposure is preferable to natural exposure, because the parameters are controllable and accelerable, while outdoor weathering is not constant, uncontrollable, and varies throughout the world. With outdoor weathering the producer also has to wait 10 to 15 years to evaluate the performance of his coating, which is not acceptable and competitive.

Thus it seems straightforward to perform accelerated exposure experiments. However, a major problem is that it has not yet been possible to correlate accelerated exposure with natural exposure. There are several reasons for this and these will be briefly pointed out in the following chapter. Much research is done to correlate natural and accelerated exposure, but the fundamentals are missing.

## 1.2 Research aim

The goal of this thesis is to improve the understanding, between natural and accelerated degradation of coatings in such a way that it becomes possible to predict life-time expectance of organic coatings. Although this is a very prestigious objective, already discovering an early warning method, or showing why and how it can be improved is helpful. From the start of this research more or less a carte-blanche was given in order to approach this subject in a fresh and different approach.

## 1.3 Research approach

Due to this freedom of approach, two different routes have been chosen in order to improve the success-rate. In principle this research can be approached from two sides: first the sensitivity of the measurement techniques can be improved or a new way of detecting and quantifying “degradation” can be developed. And secondly the accelerated degradation devices can be improved or developed. In the first phase of the project a measurement device DSA – Dielectric Sorption Analysis has been developed that analyzes the degradation grade in a different and (hopefully) earlier way (early warning detection). The set up and its measurement principle is described in chapter 3, along with measurements which are compared to gravimetric measurements as proof of concept. Chapter 4 shows that the device is not limited only to measurements on coatings and paints, but also membranes, filters and other organic systems. Due to these results, the broad application of the DSA becomes clear. Also frequency sweeps can show whether there is interaction or not between watermolecules and the matrix. Chapter 5 discusses DSA measurements on UV degraded samples. The measurements showed that the DSA was able to detect differences between varying degradation times.

The second approach was focused on the accelerating degradation devices, which have been critically analyzed for further improvement. In chapter 6 an accelerating parameter is investigated which had not been used before in the accelerating degradation devices, which is the atmospheric pressure. The known devices use intensified doses of the parameters that are responsible for coating degradation, which are UV, humidity and temperature. Pressure has never been actively investigated as an accelerated degradation parameter. Chapter 6 shows that various pressures, in combination with UV, has a clear effect on the humidity sorption of coatings.

During the project it became clear that the use of nano-particles in waterborne coatings is an interesting topic. In chapter 7 DSA measurements are described on degraded, and undegraded, laponite filled alkyd coatings. The effect of various % of laponite in the alkyd coating is also discussed.

The final chapter 8, discusses DSA measurements on naturally degraded coilcoatings. Initially the measurements had been performed to correlate between natural and accelerated degraded coatings. Unfortunately running out of budget and time prohibited this, and instead it was shown that the DSA device can detect naturally degraded coatings.

### 1.3.1 Preview of the following chapters

Chapter 2 gives the necessary background information on coating degradation and related topics. Chapter 3 discusses a home build device used for Dielectric Sorption Analysis (DSA). Chapter 4 extends the applicability of the DSA by investigating various organic coating samples. Chapter 5 shows that the DSA is able to measure sorption differences between degraded and undegraded coatings. In chapter 6 pressure is used as degradation parameter in combination with UV. In chapter 7 various %'s of nanoclay filled alkyd coatings have been degraded and measured with the DSA to investigate the influence of clay. Chapter 8 shows some preliminary results of DSA measurements on naturally degraded coilcoatings.

# Chapter 2

## BACKGROUND

## 2.1 Brief introduction

During this research roughly four areas of expertise have been covered. These areas are, coatings and paints (composition and types), degradation of coatings and paints (natural and accelerated + analysis of degradation), dielectrical measurements (DRS / EIS) and water sorption in polymer coatings. In this chapter the fundamental basics, and to a certain extent, the latest developments on these four fields will be briefly described. It must be made clear that this introduction is by no means a complete overview of the topics that are being discussed, and has been written only to give an impression of the fields of interest.

## 2.2 Coatings

### 2.2.1 Composition

Organic coatings are composed of the following ingredients:

- Binder
- Solvent
- Pigments and extenders
- Additives

The binder is the component that makes the coating; it is a high molecular weight, or a crosslinked, polymer that binds the other components. The binder co-determines the mechanical properties of the coating. The binder also determines largely the adhesion on the substrate.

The solvent is important in solvent-based coatings. The solvent should dissolve the binder and be a dispersion agent for all other components. During application the coating must wet the surface, have the right viscosity in order not to sag or slump and it must be able to level after application.

Pigments are used to give the coating its appearance (colour), but also to protect and cover the substrate. To a certain extent, pigments protect the coating from degradation and embrittlement. The pigments also play an important role in the coatings hardness and its durability. In fact next to the binder the pigments form one of the most important components of the coating. Extenders (eg. talc) are used to reduce the raw-material costs of the paint formulation, and may have some influence on some other paint properties.

Additives are only used in small amounts in coating systems. Commonly used types of additives are: catalytically active additives, surface modifiers, thickeners, surface-active agents, levelling and coalescing agents, and special-effect additives. A few examples of additives are: adhesion promotors, levelling agents, viscosity control, fire-retardants, anti-fungal, stabilizers, etc.

Important additives to improve the durability of the coating are the light stabilizers. These additives slow down the degradation of the binder due to exposition to UV. The principle of these additives will be described briefly. An excellent explanation of how these additives function can be found in by J. Bieleman, ref.1.

Light stabilizers can be classified into four classes: UV absorbers, quenchers, radical scavengers and peroxide decomposers. Each class has its own function; UV absorbers try to absorb UV light in competition with the “chromophores” (this is a functional group in the polymer, which is able to absorb UV light and initiate degradation). Quenchers accept the energy of the excited chromophores and release the energy as harmless heat or radiation. Radical scavengers (e.g. HALS [hindered amine light stabilizer]) interrupt the chain reaction of the polymer degradation by disproportionation and combination; these scavengers are also named primary antioxidants. And finally the peroxide decomposers destroy the hydroperoxides into harmless products by oxidation, or they interfere directly with chain propagation steps; these are also called secondary antioxidants.

An example of the relative proportions of ingredients in coatings are shown in Table 1, the left column shows the coating with solvent and water and the right column when the coating is completely dried.

*Table 1. Weight fraction of ingredients in coatings (solved and dried).*

| Paint raw material | Quantity in wt% (dissolved/dispersed) | Quantity in wt% (dried) |
|---|---|---|
| Binder | 29.5 | 47.6 |
| Solvent | 27.4 | 0 |
| Water | 10.6 | 0 |
| Pigments | 18.7 | 30.2 |
| Extenders | 12.3 | 19.8 |
| Additives | 1.5 | 2.4 |
| Total | 100 | 100 |

In the dried state the coating consists of almost 50 wt% binder and 50 wt% pigment and extender, and a very small amount of additives. Of course, the pigments also play a part in the protection of the binder by screening, but it is surprising that the small amount of stabilizers pay an essential contribution to the durability of a coating (of course pigments have a higher density, which results in a different volume distribution).

### 2.2.2 Types

The difference between coating types is mainly due to the binder, or in other words the polymer. Every polymer has different properties and because of this the coating can be used for different applications.

A brief summary of the various coatings types is presented below, along with their possible applications. A more thorough review about polymerisation of coatings and its applications is given in Surface Coatings by Swarej Paul, ref. 2.

| | |
|---|---|
| Alkyds and polyesters | wood, lacquer, traffic paints, venetian blinds, floor paints, swimming-pool, marine, coil coating, automotive, aircraft |
| Formaldehyde-based polymers | varnishes, automotive, metal containers, marine, |

| | |
|---|---|
| | printing |
| Epoxy resins | industrial maintenance, container coatings, marine applications, trade sales coatings |
| Silicone resins | coating binders, coating additives |
| Chlorinated rubber | chemical-corrosion resistant coatings, marine, building, masonry and swimming-pool paints, traffic paints, fire-retardant |
| Polyurethanes | wood, metal, electrical, concrete, flexible substrates, aircraft, automotive |
| Acrylic resins | automotive, aircraft, wood, lacquer, steel |
| Hydrocarbon resins | adhesives, paints, printing inks, flooring |
| Fluoropolymers | cooking pans, anti-fouling, fire-retardant, high temperature application |
| Vinyl resins | food cans, metal foils, wire coatings, paper |

As one can see the use of coatings is very broad and diverse. This makes it important that during the development of a coating for a new application, the coating is tested for its functionality and durability.

### 2.2.3 Solvent types

There are different ways of applying the paint to a substrate, which varies with the type of coating: solvent borne, water borne or solvent free coatings.

Until recently the most commonly used paints or coatings were the solvent borne type of coatings. Dependent on the type of coating a specific solvent is used to dissolve the binder and disperse the pigments and other additives. Possible solvents are hydrocarbon (aliphatic, chlorinated, aromatic), alcohols, esters, ethers and ketones.

However, due to more stringent demands for environmental reasons, the use of solvent borne coatings is becoming more and more restricted. For industrial use it is still allowed, if the coating is applied in a closed system, where the vaporized solvent is extracted and burned. For commercial use the solvent borne coatings are more and more restricted. Therefore water borne, high solids and solvent free coatings have been developed to meet the legal requirements.

Water borne coatings are coatings where the binder, pigments and its additives are dispersed in water. In water borne coatings co-solvents are being added and emulsifiers to keep the ingredients dispersed in water. Water borne coatings are susceptible to sag and in water only a low solid substance content is possible.

The ideal coating would be a solvent free coating, in this way no ingredients have to be dissolved or dispersed in a solvent. Solvent free coatings are also available in the form of powder coatings. At the moment these coatings are mainly used for metal substrates, and a method to apply these coatings are by electrostatic spraying. Thin layers are not possible, and high temperatures are necessary to allow the coating to spread. In figure 1 a few examples are given for the application of different coating types.

*Fig. 1 Photo's of: an old fashioned (solvent) paint line (left); water borne paint line (midddle); powder coating line (right).*

### 2.2.4 Nanoparticle in coatings

The use of nanoparticles in coatings does not yet have a long established history. Around 2001 Yeh discovered that the use of clay montmorillonite in a PMMA coating, improved the corrosion resistance significantly. Due to the use of, especially disk shaped, nanoparticles; the tortuous path for a permeant (gas or liquid) was increased. This was already known for normal (micrometer-scale) fillers, but at nanoscale the area is significantly larger and therefore more efficient. Rapidly after this discovery, the benefits of nanoparticles in coatings became clear; the colloidal stability of emulsions[3] improved, the nanofilled coating had a better fire-retardancy and the mechanical strength increased[4-9]. These particles can vary in size and composition, and the shape can be spherical, needle or platelet-like. It seems likely that more research on this topic will be done in the near future.

## 2.3 Coating degradation

### 2.3.1 Natural coating degradation

The ingredients that are necessary to form a coating, the types of coatings, and their application, have been discussed. The main question now is how does a coating degrade, or what causes a coating to degrade? In this case only degradation due to outdoor influences are meant, thus degradation caused by outdoor weathering.

Factors that cause a coating to degrade are: UV, water, oxygen, temperature cycles, chemical attack, dirt, biological fouling and internal and external stresses. These factors are induced by the weather or by normal outdoor use of the system, namely: sunlight; rain; day and night time temperature; acid rain or solvents, exhaust gasses, etc.; sand, tar; fungi; summer and winter, external abrasion or impact from stones etc. It becomes clear from the amount of factors that cause a coating to degrade, quite a number of degradation parameters have to be taken into account.

Coating degradation can be divided into three types of degradation: chemical, physical and aesthetic degradation. Chemical degradation is the actual breakdown of the polymer (binder) by UV, water (hydrolysis)

*Fig. 2 Photo's of coating degradation. Left: coating degradation leading to corrosion. Right: coating degradation leading to flaking of coating.*

and other components. Mechanical degradation occurs due to large temperature cycles, swelling and shrinking due to humidity changes, damage due to external force (falling objects, scratching, etc.). This causes the coating to chip, blister, microcrack or crack. Aesthetic degradation is caused by dirt retention or fungal growth, but of course also mechanical and or chemical degradation can, or does, take place. It is definitely not the case that the coating is subject to only one type of degradation; it is always a combination of degradation processes that are taking place at the same time. For example chemical degradation causes embrittlement of the coating, which can be made more severe by weathering cycles that induce mechanical degradation of the coating. Therefore it is very difficult to determine the actual cause for the degradation of a coating; in figure 2 pictures are shown of naturally degraded coatings.

The degradation types discussed in this chapter are common and not specific for a type of coating. Much research has been done to determine the relationship, or ratio, between factors that accelerate or slow down the degradation of organic coatings. This research is performed with artificial degradation techniques on laboratoy scale, because then the parameters are controlled.

### 2.3.2 Analysis of coating degradation

Before natural weathering and artificial exposure are discussed, an overview will be given of the measuring methods that can detect the grade of degradation, or the reaction mechanisms involved during degradation.

Already various measurement techniques have been used and developed to detect or measure the grade of degradation of the coating. The effects on a coating due to degradation by weathering are: loss of adhesion, chalking, loss of gloss, environmental etching, chemical breakdown and (micro)-cracking.

The order of degradation of a coating by weathering is typically as follows,

- Gloss reduction, where the surface loses more of the "body" of the binder, and more stable pigments become concentrated.
- Chalking is the result of the release of non-bound powdery pigment particles on the surface of the film.
- Loss of dry film thickness, this is the shrinking of the film due to formation of smaller, and volatile, molecules.
- Embrittlement, caused by cross-linking of the binder.
- Formation of cracks, due to the enhanced embrittlement of the binder, and decrease in the size of the molecules.
- Peeling and flaking, happens when the cracks have reached the substrate.

Entities that can be measured as a function of the degradation are: mechanic modulus (stiffness), heat conductivity, heat capacity, strength, chemical structure and optical appearance (gloss, transparency, yellowing etc.).

A list of measurement techniques that are being used to evaluate coating degradation is given below:

Light microscopy, SEM (Scanning Electron Microscope), AFM (Atomic Force Microscope), UV-VIS analysis (Ultraviolet Visible analysis), FT-IR (Fourier Transformed – Infrared Spectroscopy) and its derivations (PAS "photocacoustic spectroscopy", ATR "attenuated total reflectance", grazing angle etc.), EIS (Electrochemical impedance spectroscopy), DSC (Differential scanning calorimetry), XPS (X-ray photoelectron spectroscopy), Tensile testing, Micro/ nano indentation, DMA (dynamic mechanical analyser), GC (gas chromatography), GPC (gel permeation chromatography), contact angle measurements, NMR (nuclear magnetic resonance), Raman spectroscopy, ESP (electron spin polarization), ESR spectroscopy (electron spin resonance), XMA (X-ray microanalysis),

RAIR (reflection absorption infrared spectroscopy), DMTA (dynamic mechanical thermal analysis), TMA (thermal mechanical analysis), EPMA (electron probe microanalysis), Chemiluminence, Fluorescence, TEM (transmission electron microscopy), and more techniques.
So it becomes clear that for coating investigation all possible techniques are being explored.

### 2.3.3 Exposure – natural weathering

The most simple and most frequently used natural exposure procedure would be the use of exposure frames. Exposure frames are aluminium / steel / wood racks where the samples can be clamped to, and left for outside exposure (see figure 3). These racks can be placed at different angles in order to achieve the most effect of the sun, or the amount of time the sample remains wet from rainfall or dew. Common angles are: 45 degrees south, 5 degrees south, 90 degrees racks, station latitude and variable angle[10]. The choice of angle depends on which parameter is considered as most important.

A variant to this is the "black box", which is used for recreating the conditions found on flat surfaces of an automobile. It consists of a simple black box with an open top side, where the panels are placed over the open top side. In this way a higher temperature of the coated samples is reached.

*Fig. 3 Natural weathering in Florida.*

### 2.3.4 Exposure – natural accelerated weathering

Coating degradation under normal natural weathering, might take a very long time. Therefore there is a desire to speed up the degradation rates by aggravating the degradation parameters that are involved.
In order not to loose contact with reality, these parameters are increased while the samples are exposed outside.
The black box is one example for raising the temperature of a sample; even heating elements can be incorporated in order to maintain a high temperature.

Salt spray, which is also referred to as scab test, is sprayed (5% sodium chloride) at regular intervals. This is a good method to determining the corrosion resistance of automotive coatings. Of course, the salt spray can also be done without sodium chloride, this is the normal spray test.
The racks can also be motorized in such way that it follows the path of the sun, in this way the solar radiation is increased with up to 10%.

Another way to increase solar radiation is by Fresnel reflector concentration (see figure 4), these are mirrors that reflect the sunlight back on the samples (also called EMMA or EMMAQUA (when water is involved)[10].

A problem with accelerating parameters is that only one parameter is increased while others remain the same. Even when all parameters are increased it is necessary to make sure that those parameters have the correct ratio to each other, compared to natural weathering.

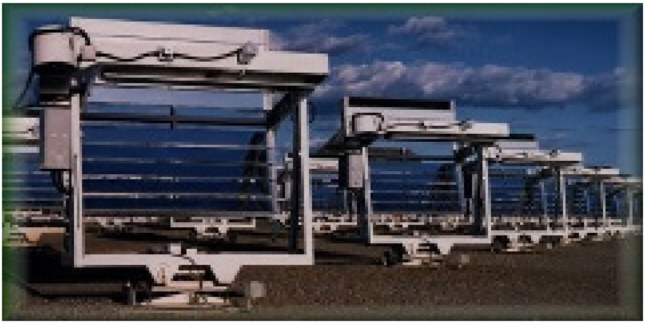

*Fig. 4 Natural accelerated weathering in Florida, a Fresnel reflector.*

### 2.3.5 Exposure - Accelerated degradation techniques

The time to degrade a coating via the natural way, or accelerated natural way takes often too much time. Therefore artificial weathering devices (figure 5) have been made in order to speed up the degradation, but also to find out how the different parameters correlate with each other. Still it has not been possible to obtain the same type of coating degradation on a laboratory scale compared to natural weathering.

First a light source has to be found which reproduces the spectrum of the sunlight; this already is a difficult task on itself. The first light source was the enclosed carbon arc in 1918, which was used to accelerate weathering and light fastness. Except it has very low output below 350 nm and two large spikes around 360 and 380 nm.

The open flame carbon arc appeared in 1933. This was a large improvement, but still a large spike around 390 nm appeared and it radiates UV wavelengths between 260 and 320 nm, which natural sunlight (UV from 290 nm) does not show. It must be avoided that low (short wavelength) UV radiation is used, because this introduces abnormal degradation that does not occur during natural weathering.

The Xenon arc (1954) with two borosilicate filters showed a very good simulation, where the cut off is around 280 nm, but decays during use, see also figure 6 for its spectrum.

Fluorescent UV lamps only reproduce the lower spectrum of the sun, thus the UV region.

*Fig. 5 Accelererated degradation technique: Weather-o-meter (WOM).*

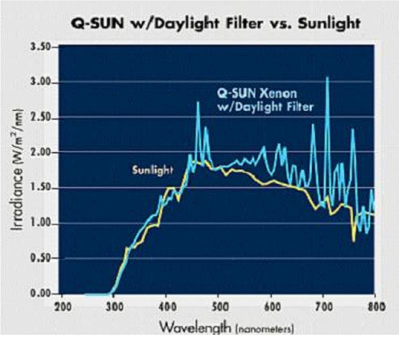

*Fig. 6 Spectrum of sun compared to that of a Xenon light source with daylight filter.*

F40-UVB and UVB-313 have UV regions that are lower than sunlight, and are not really reproducing sunlight. The UVA-340 shows much better reproduction of the UV region, from 290 nm up to around 340 nm, after 340 nm the spectrum of the lamp decays until 400 nm. More information about these light sources can be found in ref. 10.

Moisture can simply be reproduced by water spray, condensation, fog or immersion. Of course cycles can be done with dry and wet periods in order to induce stresses.

The temperature is a parameter that should be monitored, because it must be avoided that too high temperatures are used during accelerated weathering. Slightly higher temperatures already accelerate the degradation rate, but much higher temperatures might introduce degradation mechanisms that normally do not occur.
It is also possible to introduce a higher concentration of oxygen or ozone to the samples, to accelerate the oxidation rate.

### 2.3.6 Discrepancy between natural and accelerated coating degradation

A large advantage of laboratory weathering is that the parameters are controllable and can be varied in a reproducible manner, which is not the case for natural weathering. However ASTM G 90 already states that: ‘no accelerated exposure test can be specified as a total simulation of natural field exposures’.

All these laboratory devices are used to accelerate the degradation of coatings and, although they do not correlate with real natural degradation, the results are used in combination with the results obtained from natural weathering. Both data, natural and accelerated, complement each other in order to determine whether the coating can withstand the conditions what it is designed for. In fact, customers of the paint industry demand that the coatings are tested, both naturally and accelerated.

One explanation for the fact that accelerated and natural weathering do not correlate, is that every different coating (polyester/ polyurethane / epoxy), and formulation (pigments, additives), shows different acceleration factors. This makes it nearly impossible to fine-tune the acceleration factors for all different coating formulations. Another point, which was already mentioned before, is that it is not possible to mimic weather; because the weather is not constant and does not repeat itself. Imagine that ten years of natural weathering has to be compressed into a few months of accelerated weathering; this cannot simply be done by boosting all parameters to a certain level, without taking their ratios into account and the variability of the weather. During accelerating, e.g. high dose of UV, also far more radicals are formed than ever will happen during natural weathering.

When accelerated degraded coatings and naturally degraded coatings are compared to each other, the discrepancy becomes clear. For example the values of the Young's modulus, or $T_g$, increase far more in accelerated than natural weathering[11]. For some of the results it can be explained that light sources were used that have UV (wavelength) radiation below that of sunlight, and causes unnatural degradation of coatings. In other cases too high intensity of the UV source was used, causing unnatural light dosages. However, an investigation showed that it seemed that short exposure at a high intensity may be equivalent to very long exposure times at its average intensity value[11]. These controversies make it very difficult to develop an accelerated degradation device that correlates perfectly to nature.

Besides tuning the accelerated weathering devices also care must be taken with identical specimens exposed to the same exposure conditions, because these also may vary. This variation could be caused by systematic errors in the laboratory exposure equipment (cleaning filters, changing light sources, rotation, ambient conditions). Besides this, coatings are heterogeneous, which causes aqueous pathways surrounded by regions of lower transport rates. Pigments and fillers reduce these pathways tremendously. It was also found that the degradation response of polymeric materials exposed under well-controlled exposure conditions does not show a linear response[12].

One way to find a solution for this stalemate is by developing new and highly sensitive measurement devices, which can detect changes much earlier than the conventional ones. The degradation rate can then be determined at an early state during natural weathering, and also compared with accelerated weathering. In order to mimic natural weathering it might be interesting to introduce chemical resistance tests into the accelerated weathering devices; which are up to now still tested separately.

### 2.3.7 Further developments in coating degradation

Below a number of alternative techniques for accelerated weathering are mentioned, which deviate from the normal accelerating weathering techniques. First a number of different exposure methods is summarized, followed by a few approaches which are more innovative.

Different exposure methods,

- Thermal degradation of coatings is stimulated in an oven at 150 °C.
- Determining the oxygen uptake during degradation. For this the coating is put in a closed system with 100% oxygen. The coating is irradiated with a high-pressure mercury lamp with a pyrex glass filter (> 300 nm). Furthermore, exposure in a closed system with air at 100% humidity and irradiation by a Xenon lamp (290-400 nm, 55 W/m$^2$); the $CO_2$ production can be measured[13].
  A similar experiment has been done as described above[13], but in this case a mercury lamp has been used[14] and a variety of exposure cycles and times were used.
- The effect of degradation of a coating in aggressive media is stimulated by 1008 hrs of UV radiation (LRF250E40, 300-460nm)

and after that 1008 hrs of immersion in a 5% $H_2SO_4$ / NaOH / KOH[15].

- The thermo-oxidative degradation of a coating is studied by placing the coating in a closed vessel with 100% oxygen, and immersion in an oil bath at 140 °C[15].
- Accelerated (thermal) degradation is induced by 3% NaCl (in $H_2O$) immersion between 20 and 65 °C. In this way thermal shocks are generated[16].
- Hydrolysis of polyester coatings is accelerated by immersion in 3 mol/l NaOH[17], which is called a base-catalyzed hydrolysis.
- Acid rain[18] is simulated in a 24 hr cycle: 1st spraying of acid dew (fog, the acid is 1:0.3:0.17 parts by weight, sulphuric:nitric: hydrochloric acid, pH 1.5 and 2.5) with continuous irradiation by a fluorescent UV-lamp (ISO 4892-3, no UV below 295 nm, 45 $W/m^2$). Next 14 hr dry (9 hr, 35 °C/ 30% RH, 5 hr 60 °C/ 5% RH) followed by 4 hr rain (demineralized water 35 °C) and 6 hr dry 60 °C/ 5% RH). When this is done for 5 cycles, 2 cycles follow without acid spray[19].

  Another similar experiment has been done with acid rain, where the coating was exposed to the SAE J1960 method, but now with acid rain[20]. The composition of acid rain is: sulfuric acid, nitric acid, hydrochloric acid (1:0.3:0.17; weight) and pH=3.2.

A few studies, with a rather different approach towards accelerated weathering, are discussed more in detail below.

Bauer[21,22] presented two papers in which he tries to find a correlation between natural and accelerated weathering. In his first paper[21] he developed a photo-oxidation model where total light dose and mean daily high air temperatures for all four seasons in all geographical locations of the US are taken into account. With this model degradation, due to natural weathering, can be predicted. This model mainly aimed at the car industry.

The model comprises UV load (which varies for each location and also each period), scattering of UV, seasonal variations, cloud cover and temperature. Monitoring UVA (an ultraviolet absorber, like HALS) depletion, which shows the rate of photo-oxidation, can be compared with the model. When the amount of time the car will be outside in the sun, and if where the car will be used (US, Europe) is known, a prediction can be made with the model. Wavelength dependence, paint surface temperature and humidity correction was estimated. The rate of photo-oxidation is related to the wavelength cut off of UV. At low declination angles the rate of photo-oxidation is higher than at high angles (up to 5%). The temperature of the sample also changes constantly, during sunrise and sunset, the Arrhenius equation is used to account for the temperature. Finally moisture, which is responsible for extraction and roughening of the surface, is also incorporated in the model.

The model can predict fairly well lifetimes of coatings, but still much more experimental data are necessary, on a year-to-year basis. Also climate-variations cause large errors in this model. Furthermore exposing coatings in wet and dry locations is necessary to guarantee a certain minimum lifetime to the customer. This model could become useful in the future for determining acceleration factors/ parameters in coatings.

Another interesting article by Burch et al.[23] describes a computer model for degradation of a coating. In this model the heat and moisture transfer is incorporated as shown below (more specific details are given in Burch's article).

$$\frac{\partial}{\partial y}(\mu \frac{\partial p}{\partial y}) + \frac{\partial}{\partial y}(\rho_d D' \frac{\partial s}{\partial y}) = \rho_d \frac{\partial y}{\partial t} \qquad \text{moisture distribution}$$

$$\frac{\partial}{\partial y}(k \frac{\partial T}{\partial y}) + h_{lv} \frac{\partial}{\partial y}(\mu \frac{\partial p}{\partial y}) = \rho_d (c_d + \gamma c_w) \frac{\partial T}{\partial t} \qquad \text{temperature distribution}$$

The model comprises water vapour transfer rate, liquid transfer rate, relative saturation and the heat transfer rate. From these laws a moisture distribution and a temperature distribution can be derived. The first term of the moisture equation represents water vapour distribution, the second one the capillary (liquid) transfer and the right term the moisture storage. For the temperature distribution the first term is the conduction, the second the latent heat transfer and the right side the storage of heat. These equations can be solved by an efficient tridiagonal matrix solution technique. Furthermore algorithms are incorporated to deal with surface wetting by rain and dew condensation, variable convection as a function of wind speed, sky temperature and variable permeability paint layers. Finally damage indices are used to predict the severity of damage due to radiation, temperature and moisture; these are, mean diurnal temperature change index, relative humidity change index and time of wetness index.

With this model simulation runs are made and it is planned to compare this with experimental results.

Nichols et al.[24] have approached the long-term weathering endurance of a coating with fracture mechanics. During weathering the mechanical properties of a coating change, and by measuring the fracture energy and stress the performance can be predicted. Tension tests are done to obtain the modulus and the strain at which cracks appear in the clearcoat. The thermal expansion coefficient is determined by TMA. Then the complete paint system can be modelled using finite element analysis (FEA).

Coatings may crack or delaminate from each other; in both cases a crack is propagating. The conclusions are that channelling (cracks going inside the coating) requires a higher energy than surface cracking, and thin clearcoats have a higher resistance to cracking. Furthermore fast cycles in environmental conditions lead to enhanced stresses at the surface of the clearcoat. This in combination with the fact that thermal expansion coefficients increase during weathering, a higher hygroscopicity (higher humidity-induced stresses) of the coating, an increase of $T_g$ which can magnify thermal stresses and a densification of the clearcoat creating internal stresses and embrittlement of the surface layer during weathering; may lead to cracking of the clearcoat.

Fracture mechanics could be used in the future to predict the long-term weathering performance of clearcoat / basecoat systems.

Adamsons[25] used a microtome to remove thin slices (10 micrometer) from the top of the coating. Then before weathering, UV-VIS spectroscopy is done to measure the UVA content of those slices. After weathering the same procedure is done and the difference is measured. The result of this experiment was that there is a UVA gradient (low UVA concentration at the top which increases to normal concentration in the bulk). ATR-FTIR (measuring the infrared absorption of the surface of a coating) also showed that the top is hydrophilic, which shows that hydrolysis takes place, while the bulk material remains more hydrophobic. Furthermore with optical microscopy and IR analysis the decrease in thickness is monitored during exposure, which occurs due to loss of volatiles from the bulk (Over time the melamine crosslinker releases methanol, butanol and formaldehyde). Then photo-oxidation and hydrolysis become apparent and this might cause a further reduction in thickness.

In another article, by Palm et al.[26], a coating system was exposed to an accelerated weathering program (SAE J1960); but instead of exposing the coating to the usual water spray, they used acid rain (which is mimicked by sulfurid acid, nitrid acid, hydrochloric acid 1:0.3:0.17) weight and pH=3.2). The frequency of acid rain cycles appeared to be of importance and a Weibull function was used to find the optimum. In addition, an ELD model (effective light dose model) has been derived in order to correlate accelerated and natural weathering. The ELD model is derived from the ELD factor; the ELD factor is the ratio between the light dose required to cause 75% gloss retention in Florida and in the accelerated test program. Also a constant rate of gloss loss is assumed. First a prediction is made, with the model, for the gloss retention after 12 months exposure in Florida; then the actual gloss and the predicted gloss are compared. Also the accelerated weathering results are compared to 24 months exposure in Miami (EMMAQUA), to see whether the acceleration factors are correct, and the outcome is that the use of acid rain in the accelerated tests gave a better correlation than the standard ISO 4892-2 without acid rain. Also acid etch pits appeared on many coatings due to the acid rain exposure, but according to the author this had a negligible effect on gloss.

Sugiura et al[27] used “derivatization-electron probe X-ray microanalysis” (in short: derivatization-XMA) instead of IR spectroscopy in order to obtain information about the chemical structure of the (degraded) coating. With this derivatization-XMA technique a reagent is used which is highly selective to functional groups in polymers, and

highly sensitive to XMA.
Conclusion: XMA has a 2-6 times higher sensitivity than the micro-IR. Also degradation occurs from the surface and rain extracts oxidation products generated near the surface.

An important experiment was done by Boxhammer[28]; he investigated the colour difference at various levels of irradiance and sample surface temperature.
The conclusion was that, keeping the temperature constant, increasing irradiance levels up to three times, gives a good correlation between exposure and colour changes. But when the temperature is varied to increase the degradation rate, different results are obtained. Alkyd-melamine behaves linear, while in polystyrene (exposed close to $T_g$) the mobility of the chains and radicals increased, resulting in a change in oxygen diffusion coefficient. PVC showed a very complex ageing process. Conclusion: a case-to-case decision has to be made in order to find out the effect of higher temperatures on the degradation level.

One of the most recent models is described by Martin[29], where he assumes a cumulative damage process. In his experimental set-up he irradiates 12 different coatings at different UV-wavelengths at closely controlled humidity and temperature parameters. UV-VIS and IR spectroscopy were used to detect degradation to detect the damage for all coatings at different wavelengths.

To take all wavelengths into account, Martin defines a total effective dosage, which is the total number of absorbed photons that contribute to the photo-degradation of a material during an exposure period. The total effective dosage has had extensive application in the biological community in order to link field and laboratory experiments. It is based upon the fact that it is not the goal to simulate the outdoors, but to cover the range of exposure conditions that a polymeric product will be exposed to in service. The connection between field and laboratory exposure is made through a cumulative damage model, instead of using correlation techniques.
In conclusion: the total effective model is a good model to connect between field and laboratory exposure results. However, estimates of the

total effective dosage and spectral quantum yield are still sensitive to a number of experimental variables (initial UV-absorbance, formation of coating degradation products, UV-visible and FTIR measurements errors).

### 2.3.8 Brief discussion

It can be seen that even after more than 50 years of modern paint development, little success has been booked in predicting the lifetime of a coating, using accelerating weathering techniques. In addition a detailed understanding of mechanisms is often lacking. Cycles have been incorporated, new parameters are used like acid rain; our meteorological knowledge has grown, improved and new measuring techniques are used, large amounts of databases of the past 50 years are at hand and correlation and cumulative models are developed. This makes it clear that, the lifetime prediction of a coating is very complex. Along with this, the coating industry is constantly changing and improving their coatings, which makes it even more difficult. This means that the practical development is a giant leap ahead of fundamental research, when it concerns improving coating lifetime.

## 2.4 Dielectric measurements – introduction – models – technique

### 2.4.1 Dielectric the basics

The principle of broadband dielectric spectroscopy (figure 7) is known for more than a 100 years, and it is still an expanding field of research. Ion-conducting solids , polymers and mesophases, nanocomposites, liquid and colloidal systems. It is clear that the semi-conductor industry, chemical research, pharmaceutical industries, corrosion investigation, paint companies, etc… has a large benefit with this technique. The principle behind this technique is very simple, a (polar or non-polar, although a non-polar material will not result in large differences during a frequency sweep) material of interest is placed between two electrodes and a varying electrical field is applied. By changing the frequencies of the electrical field and performing this at different temperatures the dielectric response of the material is monitored. If the dipoles follow the electrical field perfectly, no signal loss will occur and the material is said to be a perfect capacitor. However, in general most (investigated) materials some loss will occur due to the fact that the dipole is forced to move in accordance with the electrical field and this costs energy. The resultant signal therefore, can be split into two parts. One part is the real permittivity ($\varepsilon'$) and the other is the dielectric loss ($\varepsilon''$). Debije was one of the first to systematically investigate molecular processes at various frequencies and temperatures[30]. He also figured out that dielectric relaxation (dispersion of real permittivity ($\varepsilon'$) and the occurance of dielectric absorption ($\varepsilon''$) in the frequency domain was due to the reorientation of the molecular dipoles in the material. The mobility of dipolar groups and the link with the dielectric constant made it possible to determine the molecular structure. Dielectric relaxation studies have a long and well recorded history in studying molecular dynamics, and the frequencies ranges from $10^{-7}$-$10^{11}$ Hz. Roughly it can be said that, below $10^{3}$ Hz ionic movement occurs in materials, between frequency range $10^{3}$-$10^{10}$ Hz dipole orientation, between $10^{9}$-$10^{15}$ Hz atomic orientation, between $10^{15}$-$10^{18}$ Hz electronic orientation and above $10^{18}$ Hz it is expected that there is no field response anymore. Dielectric equipment nowadays is still being developed and improved; producers are for example, Novocontrol, HP, Autolab, Ivium and Andeen Hagerling.

*Fig. 7 Broadband Dielectric Spectroscopy set up.*

### 2.4.2 Dielectric models

The dielectric response can be analyzed by a number of models that have been developed by a number of researchers. Debije, Cole/Cole, Cole/Davidson, and Havriliak/Negami models are used to model the frequency response at various temperatures. Debije was the first one to establish this relationship and the other researchers refined his theory for specific cases which have other relaxation time distributions.

Arrhenius, Vogel-Fulcher-Tammann (VFT) and mode-coupling theory (MCT) are used for fitting dielectric data at a certain frequency for a temperature sweep in glass-forming dynamics. Arrhenius is the most simple model and uses the normal Boltzmann distribution, whereas VFT is based upon a free volume theory (Boltzmann distribution normalized by the total free volume of the system), and MCT uses a non-linear oscillator equation. An informative book on this topic is Broadband Dielectric Spectroscopy (Kremer-Schonhals editors), which covers the basics up to the latest developments into dielectric spectroscopy (2002)[31]. Nowadays measurements of (polymer) materials focus on biomaterials, nanocomposites, nanofilms and liquid crystalline polymers (LCP's)[32-35].

### 2.4.3 Mixing theories

Also the morphology can be investigated by dielectric spectroscopy. Blending two different polymers, adding pigments to a resin, changing the shape of the added particle in the resins, phase separation in block-copolymers, sorption of liquid into polymers etc. can be investigated and modeled. Since the different phases do not have the same permittivity, mixing theories have been developed to predict the dielectric response of these composites when they have different shapes or various ratios. It all started with the well known theory of Maxwell-Garnett[36], or the Clausius-Mossotti equation. Since this theory was only valid for low volume fractions, particle interaction was neglected and the theory showed a non-linear behavior of the volume fraction for large dielectric contrasts (causing a non-symmetrical model); other theories followed based upon Maxwell-Garnett. Bruggeman assumed that the composite should be seen as a homogenized medium, and derived a symmetrical model; making his model valid for higher volume fractions. Others models where derived by Fricke and Looyenga-Landau-Lifschitz, and are also known as effective medium theories (EMT); because they calculate the effective field across the matrix with inclusions. Others models exist, different from EMT, such as multi-scattering models; but mostly EMT models are used. Further information on this subject can be found in Handbook of Electromagnetic Materials by Neelakanta[36] and Electromagnetic mixing formulas and applications by Sihvola[37].

Mixing theories are used for modeling nanocomposites, nanofilms and liquid crystalline polymers[38-40].

### 2.4.4 Dielectric spectroscopy vs EIS

Besides DRS (dielectric relaxation spectroscopy) or BDS (broadband dielectric spectroscopy), which focuses on evaluating the dielectric properties of various materials, there is also EIS or electrochemical impedance spectroscopy. EIS based on the same measurement principle as DRS, except the frequency range of interest is below 1 MHz. Furthermore the analysis of the data is different, DRS uses the real and imaginary permittivity $\varepsilon$' and $\varepsilon$'' whereas EIS makes use of the real and imaginary impedance Z' and Z'' (ohm). Both permittivity and impedance are mathematically dependent on each other. The difference appears when the data is analyzed. With permittivity data, the dielectric characteristics of the material is usually calculated; whereas with the impedance data the material is compared with a model electronic circuit, containing resistors, capacitors and inductors. EIS is interesting when the investigated material changes its dielectric characteristics in time, or when the electode(s) during the dielectric measurement is a conductive liquid, instead of metal contact electrodes (since it introduces and extra resistor). Examples can be found in corrosion processes and other layer-formation processes, curing of polymer resins, water sorption into polymer coatings and degradation of polymer coating onto metallic substrates. It becomes clear that during these changes the equivalent circuit parameter changes their values, or the circuit expands into more (or less) components. With this (fitted) information the molecular processes that occur (in time) can be described. An introduction into this subject is given in Impedance

Spectroscopy (J.R. Macdonald) – emphasizing solid materials and systems[41].

## 2.5 Water sorption in polymers

Polymers are not impermeable to water due to the fact that polymer has 2 to 3% free volume which are interconnected, and the polymer chains are flexible enough to allow the water molecules to enter[42] and may even swell.

Diffusion is the transport of particles driven by concentration differences. Therefore, a polymer coating in contact with water (or water vapor) causes the water molecules to diffuse into the coating. The famous equation for this particle transport was given by Fick, who used the heat transport equations of Fourier[43] to derive Fick's first law[44].

$$F = -D\frac{\partial C}{\partial x}$$

This first law states that the particle current density is proportional to the gradient of the particle concentration. If one is interested in the concentration of particles as function of position and time during a diffusion process, then Fick's second law becomes more useful for constant diffusion coefficient ($D$).

$$\frac{\partial C}{\partial t} = D\left(\frac{\partial^2 C}{\partial x^2} + \frac{\partial^2 C}{\partial y^2} + \frac{\partial^2 C}{\partial z^2}\right)$$

For coatings Fick's second law simplifies to one dimensional diffusion, and the solution for this (and other geometries) is described in Crank[42].

Straightforward methods to measure the overall water uptake in coatings are permeability, gravimetric and impedance measurements. With the last two techniques the coating can be on a substrate.

In general diffusion into polymer coatings does not show a perfect Fickian diffusion profile (and therefore not a constant diffusion coefficient ($D$) in time), where there is a square root time dependency to the (mass) water uptake until saturation. Fickian diffusion only prevails when polymer chain rearrangement (relaxation) takes place at the same rate as sorption, and this occurs to be possible above the $T_g$. Anomalous diffusion behavior has been described as two-stage, sigmoidal and case II sorption. Two-stage sorption can be identified as a curve that seems to be composed of two different curves, a fast Fickian curve and a slow non-Fickian curve. The non-Fickian part occurs due to polymer relaxations and was described by Berens and Hopfenberg[45]. A sigmoidal diffusion curve has a S shaped curve from the beginning and was explained by slow establishment of equilibrium at the surface of the coating[46]. A variable surface concentration (VCS) model was able to fit the curve. Finally case II sorption has a mass uptake proportional to time, and Thomas and Windle explained this effect by stating that the first molecules that enter the coating provide an easy path for the following ones[47].

The water that resides inside the polymer matrix can be present in three different states, single water molecules, aggregated water molecules and localized interactions. As single water molecule there is not much interaction. Aggregated water molecules are grouped together and form clusters. And for the final state, the water molecules interact with polymer groups of the matrix.

Due to the diffusion of water molecules into pre-existing spaces between polymer chains, swelling is caused by an increased distance of separation between polymer molecules due to large scale segmental motion. Swelling is a result of relaxation of stress in the polymer matrix. The stresses in the matrix are a result of fabrication process (extruding, cross-linking), crystallization processes, mechanical deformations, etc. Even nowadays modeling of non-Fickian diffusion into polymers is of interest[48,49].

## 2.6 Dielectric Sorption Analysis

For this research a home build device has been build. In principle it is a combination of aspects discussed in paragraph 2.4 (dielectric measurements) and 2.5 (water sorption in polymers). By using the fact that the dielectric permittivity of water is ~80 and that of an organic coating between 2-7; the absorption of water in an organic coating, even if it is only a small amount, can easily be detected by dielectric means. Using this fact, a dielectric measurement device has been build with a porous top electrode. By flowing a humid medium across the porous electrode, the organic coating is able to absorb the water. Real time water absorption can now be monitored dielectrically, making it possible to investigate the absorption of water into an organic coating on a second interval or even less.

## References

1. J. Bieleman ed., Additives for coatings, (2000) Wiley, -
2. P. Swaraj ed., Surface coatings: Science and Technology 2nd ed., (1996) Wiley
3. Y.S. Choi, M. Xu, I.J. Chung, Polymer **46**, 531 (2005)
4. T.H. Kim, L.W. Jang, D.C. Lee, H.J. Choi, M.S. Jhon, Macromol. Rapid Commun **23**, 191 (2002)
5. J. Yeh, S. Liou, C. Lai, P. Wu, Chem. Mater. **13**, 1131 (2001)
6. J. Yeh, S. Liou, C. Lai, P. Wu, Chem. Mater. **14**, 154 (2002)
7. K.E. Strawhecker, E. Manias, Chem. Mater. **14**, 2943 (2000)
8. D. Wang, J. Zhu, Q. Yao, C.A. Wilkie, Chem. Mater. **14**, 3837 (2002)
9. Y.K. Kim, Y.S. Choi, K.H. Wang, I.J. Chung, Chem. Mater. **14**, 4990 (2002)
10. Z.W. Wicks, Jr. F. N. Jones, S.P. Pappas, J. Coat. Techn, 71, 889 (1999)
11. J.V. Koleske, Paint and coating testing manual 14th ed., (1995) ASTM International
12. E.V. Schmid ed., Exterior durability of organic coatings, (1988) FMJ Inter national
13. R.A. Rynz ed., Plastics & coatings Durability, Stabilization, and Testing, (2001) Hanser Gardner
14. P. Vink, T.P.M. Koster, H.F.N. Fontijn, A. Mackor, Pol. Degr. Stab. **48**, 155 (1995)
15. D. Kotnarowska, Progr. Org. Coat. **37**, 149 (1999)
16. G. Botelho, A. Queiros, P. Gijsman, Pol. Degr. and Stab. **73**, 431 (2001)
17. A. Miszczyk, K. Darowicki, Corr. Science **43**, 1337 (2001)
18. X. Gu, D. Raghavan, T. Nguyen, M.R. VanLandingham, D. Yebassa, Pol. Degr. Stab. **74**, 139 (2001)
19. U. Schulz, P. Trubiroha, U. Schernau, H. Baumgart, Progr. Org. Coat. **40**, 51 (2000)
20. M. Palm, B. Carlsson , J. Coat. Techn. **74**, 69 (2002)
21. D.R. Bauer, Polym. Degr. Stab. **69**, 306 (2000)
22. D.R. Bauer, Polym. Degr. Stab. **69**, 307 (2000)
23. D. Burch, J.W. Martin, M.R. VanLandingham, J. Coat. Techn. **75** (2002)
24. M.E. Nichols, J.L. Gerlock, C.A. Smith, C.A. Darr, Progr. Org. Coat. **35**, 114 (1999)
25. K. Adamsons, J. Coat. Techn. **74**, 47 (2002)
26. M. Palm, B. Carlsson, J. Coat. Techn. **74**, 69 (2002)
27. M. Sagiura, T. Mitsuoka, A. Murase, Polym. Journ. **33**, 617 (2001)
28. J. Boxhammer, Polym. Test. **20**, 719 (2001)
29. J.W. Martin, T. Nguyen, E. Byrd, B. Dickens, N. Embree, Polym. Degr. **75**, 193 (2002)
30. P.W. Debije, Polar Molecules; Chemical Catalog Co. New York (1927)
31. F. Kremer, A. Schonhals eds., Broadband Dielectric Spectroscopy (2003)

Springer
32. V. Lupascu, H. Huth, C. Schick, M. Wubbenhorst, Thermochimica Acta **432**, 222 (2005)
33. R.D. Davis, A.J. Bur, M. McBrearty, Y-H. Lee, J.W. Gilman, P.R. Start, Polymer **45**, 6487 (2004)
34. S.D. Figueiróa, A.A.M. Macêdoa, M.R.S. Meloa, A.L.P. Freitasa, R.A. Moreiraa, R.S. de Oliveirab, c, J.C. Góesc, A.S.B. Sombrac, Biophysical Chemistry **120**, 154 (2006)
35. Z. Yildirim, M. Wübbenhorst, E. Mendes, S.J. Picken, I. Paraschiv, A.T.M. Marcelis, H. Zuilhof, E.J.R. Sudhölter, J. of Non-Cryst. Solids **351**, 2622 (2005)
36. A. Sihvola, Electromagnetic Mixing Formulas and Applications (1999) IEE
37. P.S. Neelakanta, Handbook of Electromagnetic Materials (1995) CRC, -
38. M.C.W. van Boxtel, M. Wübbenhorst, J. van Turnhout, C.W.M. Bastiaansen, D.J. Broer, Liquid Crystals **30**, 235 (2003)
39. A. M. Zheltikov, J. of Exp. and Theor. Physics **99**, 37 (2006)
40. H. Du, , J.Q. Xiao, Y.S. Zou, T.G. Wang, J. Gong, C. Sun, L.S. Wen, Optical Materials **28**, 944 (2006)
41. J.R. McDonald ed., Impedance Spectroscopy (1987) Wiley
42. J. Crank, The Mathematics of Diffusion 2nd edition (1975) Oxford
43. J.B.J. Fourier, Theorie Analytique de la chaleur (1822)
44. A. Fick, Pogg. Ann. **94**, 59 (1855)
45. A.R. Berens, H.B. Hopfenberg, Polymer **19**, 489 (1978)
46. F.A. Long, D. Richman, J. Am. Chem. Soc. **82**, 513 (1960)
47. N.L. Thomas, A.H. Windle, Polymer **23**, 529 (1982)
48. A. El Afif, M. Grmela, J. Rheol. **46**, 591 (2002)
49. J.S. Vrentas, C. M. Vrentas, J. Polym. Sci.: Part B **39**, 1529 (2001)

# Chapter 3

## DIELECTRIC WATER SORPTION ANALYSIS *

*This chapter has been published in Review of Scientific Instruments: M. Giacomelli Penon, S.J. Picken, M. Wübbenhorst, G. de Vos, J. van Turnhout, Rev. of Sci. Instr., 2006, 77, 115107.

### 3.1 Introduction

Mass transport properties of organic coatings are important for several applications, like food packaging, beverage cans, protective paints, or composite materials[1-3]. A measure for the barrier or permeation behaviour of a coating is the time lag, i.e. the diffusion time for gasses or liquids to propagate through a film of a given thickness *d*[4], which depends on the solubility *S* (sorption) and the diffusion constant *D*. These two material properties depend on both the coating material and the permeant (e.g. methane, benzene, gasoline, oil etc)[5].

The techniques used most frequently to investigate sorption and diffusion properties are isothermal weight measurements, thermogravimetric (TGA) analysis and permeability ($P=DS$) measurements. For the latter, typically two-chamber cells are used, which are separated by the membrane to be tested. Monitoring the time evolution of the gas flow or the pressure difference allows the determination of the dynamic (*D*) and static (*S*, *P*) transport properties. A good review of the current state-of-the-art techniques is given by Rabek[6]. Gravimetric measurements are the most straightforward methods to determine the sorption behaviour of coatings. The mass increase is monitored while the coating is exposed to the gas/liquid of interest under isothermal conditions.

The main disadvantage of the above-mentioned techniques is the inability to monitor the very first seconds of the dynamic transport characteristics. The inability to use a substrate is another disadvantage for some of the techniques. This makes it difficult to characterize paints or samples of which the top micrometer layer has been chemically or physically modified, e.g. by weathering or oxidation.

Therefore we propose an alternative approach that aims to measure water sorption with a high sensitivity and with a fast acquisition rate using a capacitive measurement[7]. The high sensitivity stems from the fact that water has a large dipole moment and high relative dielectric constant[8] causing a significant change of the dielectric constant at low moisture levels i.e. when water starts to penetrate into the organic coating. The basic principles of the technique are described and validated by measuring the water vapour sorption of a Kapton® polyimide coating. It will become clear that measurements can be done over both short and long times. The former provides a particular advantage if the transport phenomena in surface layers are to be studied.

## 3.2 Experimental

### 3.2.1 Materials

To test our dielectric sorption set-up we have used polyimide films (Kapton®, Du Pont) with a thickness of 50µm. These films have a uniform thickness and their properties are stable. The chemical structure is shown in figure 1, where n represents the number of repeating units.

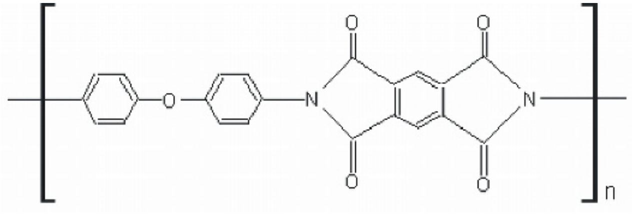

*Fig. 1 Chemical structure of Kapton®.*

### 3.2.2 Experimental set-up

The dielectric sorption technique is schematically shown in Figure 2 and comprises the following components: A humidifier, a two-way gas switch, the measurement cell and a dielectric analyser. Gaseous nitrogen, originating from a liquid nitrogen source, is used as the working

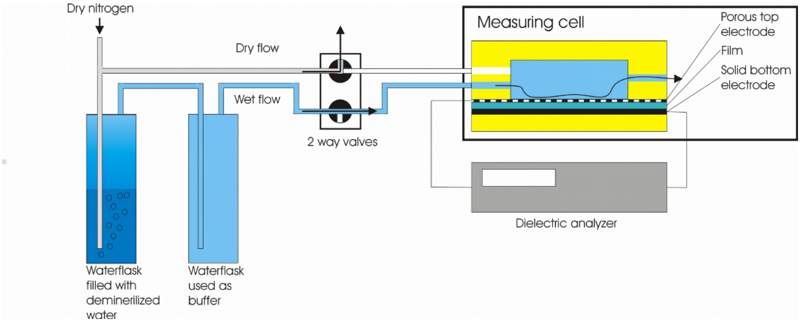

*Fig. 2 Schematic drawing of the DSA set-up.*

gas with a controlled temperature and flow rate. The dry gas is either moisturized in a humidifier (waterflask + buffer reservoir) or bypassed to the sample cell using two fast electro-mechanical two-way valves [type Alcon 220 V]. The measuring cell consists of a closed compartment, in which the organic film is sandwiched between a porous top electrode, and a solid bottom electrode, which are connected to a dielectric analyser (Andeen Hagerling high precision 1 kHz bridge, type 2500A). The gas inlets for dry and moisturized nitrogen are located close to the “quasi-free” sample surface to ensure an effective and fast gas exchange.

Several measures have been taken to ensure mechanical stability and reliable electrical contacts. Furthermore water absorption on tube and cell surfaces is avoided in order to obtain good reproducibility. Teflon tubes have been used in the entire flow circuit, the sample cell is made from a low permittivity based polymer (Delrin®, DuPont) and all electrodes are coated with a gold layer. For the porous top electrode, a crucial component, an off the shelf sheet of gold layered perforated steel 100 μm thick was used with holes of 100 μm diameter at an average spacing of 115 μm (see figure 3).

To ensure good contact between the porous top electrode and the coating, a constant load is applied with a weight with a value that depends on the type of coating. For Kapton® films a constant stress of about 20 kPa is the maximum. Higher stresses result in plastic deformation causing a permanent imprint of the top electrode in the film. Lower stress values may give rise to poor contact of the electrodes with the film and an air gap will remain.

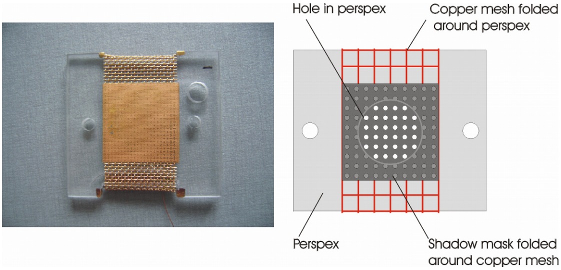

*Fig. 3  Photograph and schematic representation of the porous screen used as top electrode in the DSA set-up.*

The bottom surface of the Kapton® film was coated with gold by vapour deposition to eliminate the influence of the air gap between the film and bottom electrode. The gold layer also blocks the uptake of water at the bottom surface.

Due to the small gas exchange volume (~ 1ml) and a nitrogen flow of up to 7 ml/s, a refreshment rate of about 5 times per second was realised.

The set-up is placed in a temperature conditioned room at about 24.5 ºC (±1 ºC) ambient temperature.

### 3.2.3 Gravimetric experiments

For the validation of the DSA results, gravimetric measurements were performed. The Kapton® samples were dried in dry nitrogen at RT for 5 days and then weighed on a precision balance. Subsequently, the sample was stored in a flow cell that was continuously flushed with moisturized nitrogen at 88% RH (at RT). The mass was measured by taking the sample out for a few seconds every 15 minutes (1st hour), 20 minutes (2nd and 3rd hour) and finally every 30 minutes until saturation of the sample mass was observed.

### 3.2.4 Humidity measurement

The humidity and the temperature of the dry and humidified nitrogen were monitored real time with a humidity meter (Testo 177-H1). This real time measurement was achieved by splitting the gas inlets just before they enter the measurement cell, and not in the cell itself as otherwise the humidity meter would have disturbed the sensitive dielectric measurements.

## 3.3 Results

### 3.3.1 Validation of switching behaviour and stability

**Conditions**

The temperature and the gas flow rate of the dry and humidified nitrogen were monitored real-time. The temperature was constant 27 °C (+/-1 °C), while the flow rate stayed constant. The humidity of the wet nitrogen flow was stable at 86 % RH (+/-1 % RH).

**Response time**

The response time of the dielectric bridge (Andeen Hagerling high precision 1 kHz bridge, type 2500A) was about 1 second; this was checked by rapidly removing a glass fibre from between two brass electrodes, which gave a sharp stepwise change in the measured capacity.

To test whether a sharp square humidity profile wave was generated, when switching between dry and wet nitrogen, an empty electrode system was used.

As shown in figure 4a, at room temperature a sharp square wave

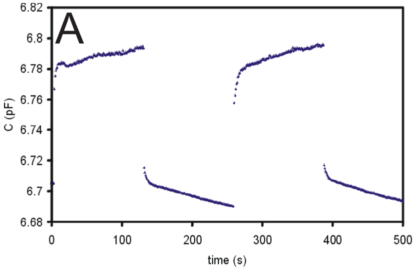

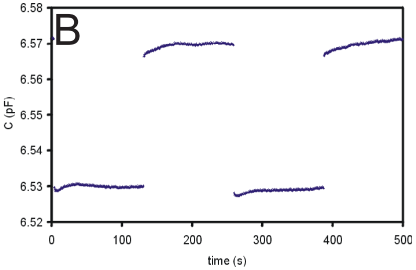

*Fig. 4a Generation of a block wave between the empty electrode system at room temperature.*

*Fig. 4b Generation of a block wave between the empty electrode system at 60˚C.*

is not observed when switching from dry to wet nitrogen. However, when the electrodes were heated to 60 ºC a nice square wave was found (figure 4b). We believe that at room temperature a thin water-layer is formed on the electrodes[9], while at 60 °C this layer is not present on the electrodes. A water layer can not be formed on the electrodes, if a sample is placed between them.

In conclusion the measured response time of the dielectric analyser was found to be in good relation with the gas exchange rate (7 times a second) of the meas.

### Stability

The stability of the measurement cell was monitored using a piezoelectric force transducer. The transducer was placed on top of the cell, and directly after inserting a Kapton® film in the set-up, a decrease of load was registered. This decrease was due to the settling of the film between the two electrodes and thermal and mechanical adjustments of the device as a whole. Therefore before actually starting the measurement, dry nitrogen was passed through the DSA set-up for about 4 hours.

### Reproducibility

After verification and characterizing the "empty" DSA equipment, a Kapton® film was repeatedly measured (seven times) for about 1800 seconds. The results are shown in figure 5. After each measurement the Kapton® film was kept under ambient conditions for one day before starting the next measurement; therefore the coating initially was not entirely dry.

These results indicate that it is possible to obtain good and

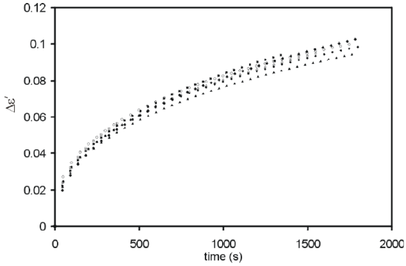

*Fig. 5 Increase in dielectric permittivity with time of Kapton® for short times.*

reproducible sample handling with the DSA . In addition the sample response showed that no chemical or physical changes occurred during the seven measurements.

To analyse the capacitive response, we use expression 1,

$$\varepsilon' = \frac{C' \cdot d}{\varepsilon_0 \cdot A} \tag{1}$$

where $\varepsilon'$ is the dielectric permittivity of the sample, $C'$ is the real part of the capacitance [F], $d$ the thickness of the sample [m], $\varepsilon_0$ the permittivity of vacuum [$J^{-1}C^2m^{-1}$] and $A$ the measured Kapton® area [$m^2$].

Sorption of water in the coating causes swelling of the coating[10]. The resulting increase in $d$ gives a decrease in the capacitance (see equation 1). But in view of the small water uptake of Kapton® (~2 vol% in our case) this decrease is negligible in comparison to the increase in $\varepsilon'$ as caused by the high dielectric constant of the penetrating water.

Since we are interested in changes of the dielectric constant as the result of water absorption it is useful to present the difference $\varepsilon'(t) - \varepsilon'(t = 0)$, where $\varepsilon'(t = 0)$ is the initial value of $\varepsilon'$ in the dry state at the start of the measurement; as shown in figure 5.

### 3.3.2 Comparison between DSA results and gravimetric measurements

Now a direct comparison between the DSA response and the gravimetric data of the Kapton® samples can be made.

The results of the gravimetric measurements are displayed in figure 6a. The mass increase levels off, when the saturation concentration is reached. The data in figure 6a have been normalised by showing $\Delta M_t / \Delta M_{sat}$.

The DSA results are displayed in figure 6b, where similar normalisation has been applied to the capacitive response ($\Delta\varepsilon'_t / \Delta\varepsilon'_{sat}$ ).

To relate the dielectric response to the actual mass increase, which is assumed to be solely due to the water uptake, we have to model the

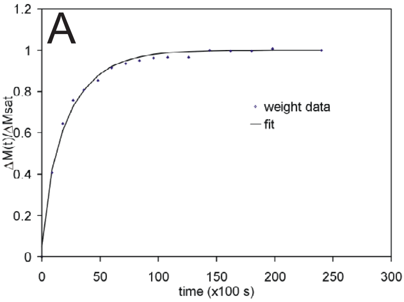

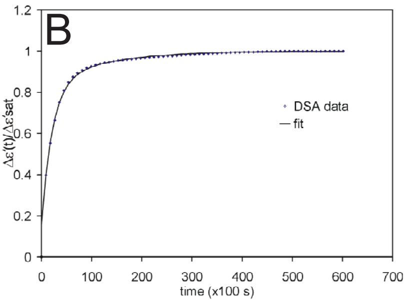

*Fig. 6a Normalized weight increase of Kapton® at 86% RH and room temperature. The solid line represents the fit to the data using eq. 2.*
*Fig. 6b Normalized DSA data for Kapton® at 86% RH and room temperature. The solid line represents the fit with eq. 2.*

dielectric response and the mass response. For this a two-stage sorption model[11] with a relaxation term is used[12], shown in equation (2).

$$\frac{\Delta M_t}{\Delta M_{sat}} = \Phi\left(1-\frac{8}{\pi^2}\sum_{n=0}^{\infty}\frac{1}{(2n+1)^2}\exp\left(-\left(2n+1^2\right)\frac{\pi^2 Dt}{4d^2}\right)\right)+(1-\Phi)\left[1-\exp(-kt)\right] \qquad (2)$$

The two-stage sorption model is used, because the diffusion coeffient is not constant in time. The first term in equation (2) represents the “perfect” Fickian diffusion of water into a sample and the second term, which accounts for the time dependency of the diffusion coefficient, is the additional gradual uptake brought about by the long-term relaxation of the sample due to structural rearrangements induced by the diffusing medium, in this case water.

$M_t$ is the weight increase in time, $M_{sat}$ the weight increase at saturation, $d$ the half thickness [m], $D$ the diffusion coefficient [$m^2s^{-1}$], $t$ the time [s], $\Phi$ the equilibrium ratio constant which represents the ratio of the equilibriums of the first stage to that of the second stage in the sorption, and $k$ the rate constant of the relaxation process [$s^{-1}$]. Note that the exponential series in eq. 2 converges quickly, and using the first three terms therefore suffices. Crank[11] and Talbot[17] derived an approximation to the inverse of the exponential part in eq. 2. This greatly simplifies the calculation of $D$, cf. appendix 1 at the end of this chapter.

Fitting eq. 2 to the weight results gives a diffusion coefficient of

$4.8\times10^{-13}$ $m^2s^{-1}$ (according to the literature $D$ varies between 2–4 $\times10^{-13}$ $m^2s^{-1}$ at 50 °C and 80% RH[13]). Already Pethrick[19] has assumed that $\Delta\varepsilon'_t$ is linearly dependent on $M_t$ and $\Delta\varepsilon'_{sat}$ on $M_{sat}$ for his dielectric measurements (the validity of these assumptions is addressed in appendix 2 at the end of this chapter) Using this assumption a diffusion coefficient of $5.0\times10^{-13}$ $m^2s^{-1}$ is obtained for the DSA measurements. The resulting fit curves are shown in figures 6a and 6b. This indicates that there is excellent agreement between the DSA results and the mass uptake curve.

The weight percentage of the saturation water content can be calculated from the mass measurements by $M_{sat}/M_{dry}$, resulting in 1.6% w/w (at RT and 86% RH). For DSA a dielectric mixing rule is necessary to account for the heterogeneous nature of a dielectric material containing a dispersed phase of a second component, in this case water[14,17]. Lindqvist[18] compared 5 formulas of mixing on various coatings for impedance measurements. We use a model, which assumes that the water (-molecule) is dispersed in the matrix as spherical (or randomly dispersed ellipsoidal) clusters, resulting in the following relationship known as the Landau, Lifschitz, Looyenga (LLL) relation[15,16] (equation 3).

$$\varepsilon_t'^{1/3} = \nu_w \cdot \varepsilon_w'^{1/3} + (1-\nu_w)\cdot \varepsilon_d'^{1/3} \tag{3}$$

$\varepsilon_t'$ is the total dielectric permittivity of the saturated signal (water + Kapton®, which is 2.593), $\varepsilon_w'$ the dielectric permittivity of water (assumed to be 80), $\varepsilon_d'$ is the dielectric permittivity of dry Kapton® (derived from measurements, 2.238) and $v_w$ the volume fraction of water at saturation. The volume percentage of water in Kapton® found using this model is 2.2% v/v (@ RT and 86% RH). This corresponds to a weight percentage of 1.56% w/w, since the specific density of Kapton® is 1.42 g/ml.

The results of 1.6% w/w and 1.56% w/w indicate a good agreement between the direct (gravimetric) and the indirect (DSA) approach. According to Dupont the water uptake in Kapton® is about 4% w/w in 100% water at 40 °C.

## 3.4 Conclusions

The basics of the DSA technique have been described together with the experimental details and characteristics of the set-up. First results on Kapton® films have demonstrated the reproducibility and sensitivity of the DSA technique for the measurement of  water vapour absorption in thin polymer films.

Direct comparison of the capacitive response with gravimetric results revealed a linear relationship between the two quantities, which emphasises the suitability of the DSA technique for the quantitative measurement of mass transport properties of polymer films.

Another feature of the DSA technique is its ability to monitor transport phenomena on a broad time scale varying from seconds to even days (up to saturation). Particularly its fast response time allows future study of highly permeable systems (filters and membranes); and as well as the initial (possibly variable) stages of diffusion that gives insight in surface properties of coatings or other polymer films. Because with most other sorption analyzing techniques, the first seconds of sorption into polymer films are difficult to monitor.

To exploit the potential of the new technique in the field of non-destructive coating inspection and early warning testing, future work will be dedicated to investigation of other types of polymer films. In addition, UV degradation will be inflicted on epoxy coatings to determine the sensitivity of the DSA to detect chemical surface changes.

Clearly, the DSA technique can be used with different gases than the present combination (nitrogen, moisturized nitrogen).

## References

1. O.G. Piringer, A.L. Baner, Plastic Packaging Materials for Food: Barrier Function, Mass Transport, Quality Assurance, and Legislation (Wiley, 2000).
2. J.W. Chin, T. Nguyen, K. Aouadi, J. Appl. Pol. Sci. **71**, 483 (1999).
3. P. Marcus, J. Oudar, Corrosion mechanisms in theory and practice, (Dekker, 1995), p. 581.
4. J. Crank and G.S. Park, Diffusion in Polymers, (Academic Press, 1968), p. 260.
5. J. Comijn, Polymer Permeability, (Elsevier, 1985), p. 11.
6. J.F. Rabek, Experimental methods in polymer chemistry (Wiley, 1980), p. 601.
7. M.F. García-Sánchez, J. M´Peko, A.R. Ruiz-Salvador, G. Rodríguez-Gattorno, Y. Echevarría, J. Chem. Educ. **80**, 1062 (2003).
8. R. Buchner, J. Barthel, J. Stauber, Chem. Phys. Lett. **30**, 57 (1999).
9. M. Heim, R. Eschrich, A. Hillebrand, H.F. Knapp, R. Guckenberger, J. Vac. Sci. Technol. B **14**, 1498 (1996).
10. G. Wypych, Handbook of solvents (Chemtec, 2001), p. 305.
11. J. Crank, The mathematics of diffusion (Clarendon Press, 1975), p. 44.
12. Y. Sun, Polymer **37**, 3921 (1996).
13. K.I. Okamoto, N. Tanihara, H. Watanabe, K. Tanaka, H. Kita, A. Nakamura, Y. Kusuki, K. Nakagawa, J. Polym. Sci.: Polym. Phys. B **30**, 1223 (1992)
14. P.A.M. Steemann, J. van Turnhout: in Kremer F., Schönhals A. eds., Broadband Dielectric Spectroscopy (Springer, 2003), p. 495.
15. L.D. Landau, E.M. Lifshitz, Electrodynamics of continuous media (Pergamon, 1960), p. 46.
16. H. Looyenga, Physica **31**, 401 (1965).
17. A. Talbot, J.A. Kitchener, Brit. J. Appl. Phys. **7**, 96 (1956).
18. S.A. Lindqvist, Nat. Ass. of Corr. Eng. **41**, 69 (1985).
19. D. Hayward, R.A.Pethrick, Polymer **38**, 1151 (1997)

## Appendix 1

Talbot solved equation (2), without viscoelastic term (thus only the 1st term, the "perfect" Fickian term), graphically by using the following approximation, putting,

$$\frac{\pi^2 M_t}{8 M_{sat}} = x$$

$$\theta = -\ln x + \frac{q}{p} + \frac{r \cdot q^2}{2 \cdot p^3} \tag{4}$$

where

$$\theta = \frac{\pi^2 D t}{4 l^2}$$

$$p = 1 + x^8 + x^{24}$$

$$q = \frac{1}{9} x^8 + \frac{1}{25} x^{24}$$

$$r = 1 + 9x^8 + 25x^{24}$$

*D* is the diffusion coefficient ($m^2/s$), *t* is time (s) and *l* is thickness (m). This graphical solution is correct up to four significant digits when $M_t/M_{sat} < 2/3$.

## Appendix 2

The capacitance of a dry coating is given by,

$$C_0 = \frac{\varepsilon_d \varepsilon_0 A}{d} \tag{5}$$

$C_0$ is the capacitance of dry coating (F), $\varepsilon_d$ is the dielectric permittivity of the dry coating, $\varepsilon_0$ the permittivity of vacuum [$J^{-1}C^2m^{-1}$], $A$ the measured Kapton® film area [$m^2$] and $d$ the thickness of the coating (m).
When from time t=0 water starts to penetrate from the top of the coating, then there is a wet top layer and a dry bulk layer, which changes in time. The series arrangement of a wet and dry layer changing in time is given by,

$$\frac{1}{C_t} = \frac{d_t}{\varepsilon_0 \varepsilon_w A} + \frac{d - d_t}{\varepsilon_0 \varepsilon_d A} \tag{6}$$

$C_t$ is the resultant capacitance of the coating (F), $\varepsilon_w$ is the dielectric permittivity of the wet coating, $d_t$ the thickness of the wet part of the coating [m].
Because we are interested in the difference of capacitance, just like the difference in mass for gravimetric measurements, we can subtract (6) from (5).

$$\frac{1}{C_t} - \frac{1}{C_0} = \frac{d_t}{\varepsilon_0 A}\left(\frac{1}{\varepsilon_w} - \frac{1}{\varepsilon_d}\right) \Rightarrow 1 - \frac{C_0}{C_t} = \frac{d_t}{d}\left(1 - \frac{\varepsilon_w}{\varepsilon_d}\right) \tag{7}$$

If we assume a simplified diffusion equation,

$$d_t = \sqrt{Dt} \tag{8}$$

$D$ is the diffusion coefficient ($m^2/s$), $t$ is time (s).
Replacing $d_t$ by equation (8) the resulting equation then becomes:

$$1 - \frac{C_0}{C_t} = \frac{\sqrt{Dt}}{d}\left(1 - \frac{\varepsilon_w}{\varepsilon_d}\right) \tag{9}$$

Equation (9) shows that the change of capacitance, due to water ingress, is basically diffusion related and therefore the assumption can be made that $\Delta M_t$ can be substituted by $\Delta\varepsilon'_t$, and $\Delta M_{sat}$ by $\Delta\varepsilon'_{sat}$.

# Chapter 4

# VAPOUR DIFFUSION IN POROUS/ NON POROUS POLYMER COATINGS BY DIELECTRIC SORPTION ANALYSIS[*]

[*]This chapter has been published in Journal of Applied Polymer Science: M. Giacomelli Penon, S.J. Picken, M. Wübbenhorst, J. van Turnhout, *J. Appl. Sci.*, **105**, (2007), 1471-1479.

## 4.1 Introduction

Sorption of vapour or liquid into coatings is an interesting issue for food packaging, beverage cans, pipes and tubes in process plants, protective paints and composite materials in the aerospace industry[1-3]. Not only the diffusion coefficient (how quick the polymer absorbs) is of importance, but also the total sorption into the bulk material. For example, if in one case the rate of absorption is very high and the total absorption is not higher than 0.1%, it will have little effect on the ultimate material properties. A more serious change in material properties will be caused when the rate of absorption is very low, but eventually the total absorption is more than 8%[4-6].

In a previous paper[7], the concept of DSA (Dielectric Sorption Analysis) has been introduced as a useful method to investigate the sorption of vapour into Kapton® films by means of dielectric changes; instead of the more traditional techniques (isothermal weight measurements, thermogravimetric analysis and permeability measurements[8]). The high sensitivity stems from the fact that water has a large dipole moment and large dielectric constant[9] causing a significant dielectric change at low moisture levels i.e. when water starts to penetrate into the organic coating. This paper will illustrate the full potential of the DSA by measuring a range of various organic coatings and filters/membranes. The DSA results show clear differences between all investigated organic films (and filters), by the maximum sorption and the calculated diffusion coefficients. For the filters an interesting desorption profile can be detected, where the filter first absorbs vapour and then, after some time, releases it. It will also become clear that measuring with the dielectric analyser at different frequencies is an important and powerful tool to discover interactions of water with the polymer bulk material. The results in this paper opens the possibility to investigate in the near future degraded coatings, in order to detect the differences in vapour sorption compared to undegraded coatings. Besides measuring differences in degraded an undegraded coatings, also the sensitivity of the DSA will be an interesting issue.

## 4.2 Experimental

### 4.2.1 Materials

To test the range of DSA we used the following, with decreasing affinity towards water, films: Polyamide 6.6 (PA6.6), polymethyl methacrylate (PMMA), Polyimide (PI), epoxy resin, and low density polyethylene (LDPE).

The epoxy resin was received from Akzo Nobel, which is used as marine protective coatings with a thickness of 116 µm. Kapton® (Du Pont) of 50 µm thickness was used as PI. PA6.6 (75 µm), PMMA (39 µm) and LDPE (82 µm) films were made by pressing granules at 250 ºC, 250 ºC and 190 ºC respectively.

To expand the possibilities of the DSA we also used the following, with increasing pore sizes, filters (all from Millipore, except porous polyethylene and cotton linters): nitro cellulose (pore size 0.05 µm, thickness 76 µm) type VM; Durapore polyvinylidene fluoride (PVDF) membrane (pore size 0.22 µm, thickness 117 µm) Millex GV; Durapore polyvinylidene fluoride (PVDF) membrane (pore size 0.45 µm, thickness 96 µm) Millex HV; poly-tetra-fluoro-ethylene (PTFE) (pore size 5 µm, thickness 133 µm) Mitex type LS; porous polyethylene (porous PE) Solupor Solupor:3p07A from DSM (thickness 20 µm) and cotton linters (which have the appearance of normal paper filters) from Schleicher&Schell Gmbh 595 (thickness 100 µm). (It should be mentioned that for the last two filters the pore sizes are unknown, but by light microscopy it became clear that they were larger as compared to the other filters, porous PE ~ 10 µm, cotton linter ~ 20 µm).

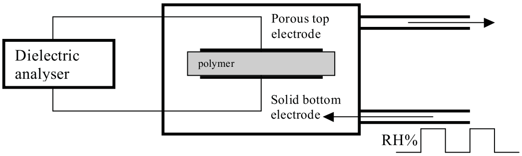

*Fig. 1  Schematic of DSA set up*

### 4.2.2 DSA set-up

The DSA set up, schematically shown in figure 1, has been described more in detail in a previous article[7]. With DSA it is possible to measure the moisture uptake and drying of organic coatings by dielectric means, making use of a porous top electrode.

The dry flow was gaseous nitrogen and the “wet” flow gaseous nitrogen, humidified by passing the flow through a water flask. The flow speed of both dry and wet nitrogen flow was 7 ml/s. The gas temperature was 27 ºC, the dry gas was about 2% RH and the wet gas was 86% RH. The dry and wet flow was controlled by a two-way valve, which leads either the dry or the wet flow across the sample. The sample was sandwiched between a solid bottom electrode and a porous electrode placed in a closed compartment.

The dielectric analyser used for these experiments was a HP frequency analyser with a frequency range between 20 Hz until 1 MHz. The set up was placed in a temperature conditioned room of 24.5 ºC (±1 ºC).

### 4.2.3 Gravimetric experiments

For the validation of the DSA results, additional gravimetric measurements were performed. The epoxy samples were dried in dry nitrogen at RT for 5 days and then weighed by means of a precision balance. Subsequently, the sample was stored in a flow cell that was continuously flushed with moisturized nitrogen at 88% RH (at RT). The mass was measured by taking out the sample for a few seconds every 15 minutes (1st hour), 20 minutes (2nd and 3rd hour) and finally every 30 minutes until saturation of the mass was observed.

## 4.3 Results and discussion

### 4.3.1 Comparison of films

Frequency sweeps are shown for all films in order to discover whether interactions between water and polymer matrix occurs. Then, to illustrate the differences between the samples, PI, PA6.6, LDPE, epoxy and PMMA are compared at 1 kHz, followed by gravimetric measurements on an epoxy coating. Besides gravimetric measurements, the second part (3.2) discusses all of the above for porous PVDF 0.22 µm, PVDF 0.45 µm, PTFE, nitro cellulose and cotton linter samples.

#### 4.3.1.1 Films - various frequencies

For all samples the difference in capacitance ($\Delta C'$) is used to plot the data. To compare the frequencies, the data has been normalized with respect to the saturation values (1). $|C'|$ is the normalized capacitance, $\Delta C_t'$ is the difference in capacitance ($C_t'$-$C_0'$) between time $t$ and $t$=0

$$\left|C'\right| = \frac{\Delta C_t'}{\Delta C_{sat}'} \qquad (1)$$

(pF), $\Delta C_{sat}'$ is the difference in capacitance ($C_\infty'$-$C_0'$) at saturation (pF). Presenting data this way will clarify whether vapour diffuses uniformly (with / without interaction) into the polymer matrix, or not.

The normalized capacitance vs. frequency can be found in figure 2 for various polymer films. For PI, PMMA, epoxy and LDPE it is clear that the data overlap perfectly, indicating that the vapour penetrates the matrix uniformly and does not interact with the polymer matrix. From these results it can be seen that, at the frequencies used, no dominant relaxation processes, and no polymer-water interactions, are detected. Only PA6.6 shows a deviation from this behaviour that has a non-Fickian, more sigmoidal diffusion profile. This diffusion profile is present at all frequencies, where it is assumed that a slow establishment of equilibrium takes place at the surface of the film[10]. This slow establishment of equilibrium for nylon 6.6 can be explained by the fact that nylon is highly hydrophilic. From lower frequencies (50 Hz) up to high (1 MHz) a peak starts to appear at around 5.000 seconds; whereas from 10.000 seconds

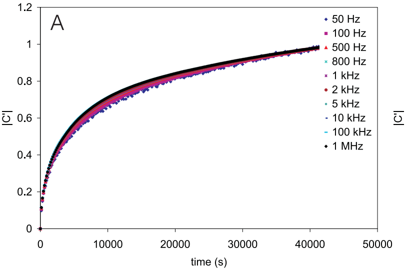

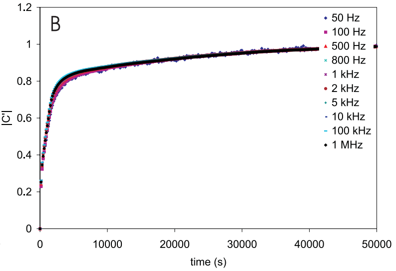

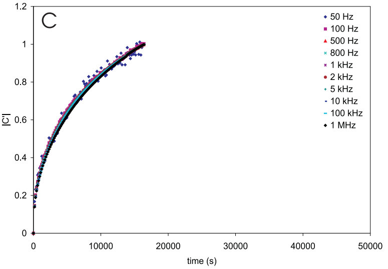

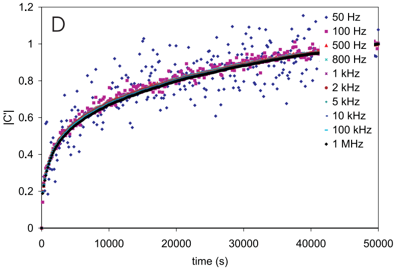

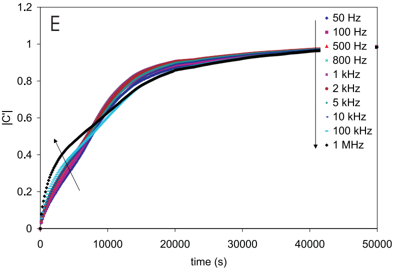

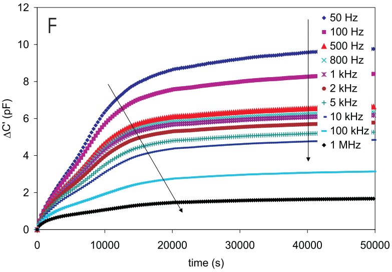

*Fig. 2a Normalized frequency sweeps of PI.*
*Fig. 2b Normalized frequency sweeps of PMMA.*
*Fig. 2c Normalized frequency sweeps of epoxy.*
*Fig. 2d Normalized frequency sweeps of LDPE.*
*Fig. 2e Normalized frequency sweeps of PA6.6.*
*Fig. 2f Non-normalized frequency sweeps of PA6.6.*

on the diffusion behaves uniformly again. When the non-normalized data is shown (figure 2f), it becomes clear why the "bump" appears. Due to the high values of ΔC' at low frequencies, normalizing the data results in a more pronounced signal at 1 MHz. We believe that at lower frequencies polarization is taking place at the electrodes, due to the high water uptake (up to 8-10%)[11].

### 4.3.1.2 Films - 1 kHz

Comparison between the films is not straightforward, since the thickness is not the same for all coatings; therefore corrections have to be made for the maximum sorption. In figure 3a the data is shown without correction, in figure 3b a thickness correction (all coatings have been corrected to 100 µm) is made for the maximum sorption. The equation used for maximum sorption correction is shown below (2).

$$C_1 = \frac{\varepsilon_r \varepsilon_0 A}{d_1}, C_2 = \frac{\varepsilon_r \varepsilon_0 A}{d_2} \Rightarrow C_1 = \frac{C_2 d_2}{d_1} \qquad (2)$$

$C_1'$ ($C_2'$) is the capacitance for coating 1 (2) (F), $\varepsilon_r$ is the dielectric permittivity, $\varepsilon_0$ is the permittivity of vacuum ($8.85 \times 10^{-12}$ F/m), $A$ the measured area of coating 1 ($m^2$), $d_1$ ($d_2$) thickness of coating 1 (2) (m). No error is introduced by the different dielectric permittivity values of the coatings, because the difference in capacitance signal is used.

As can be seen in figure 3b no large changes can be seen after the correction, except PMMA and PI for which $\Delta C_t'$ became larger. As expected PA6.6 has the highest absorption, followed by PMMA, PI, epoxy and LDPE.

To relate the dielectric response to the actual mass increase, which is assumed to be solely due to an increase by the water uptake, we have to model the dielectric response and the mass response. A two-stage sorption model (equation (3)) with a relaxation term is used for this[12]. The first term in equation (3) represents the “perfect” Fickian diffusion of water into a sample and the second term is the additional gradual

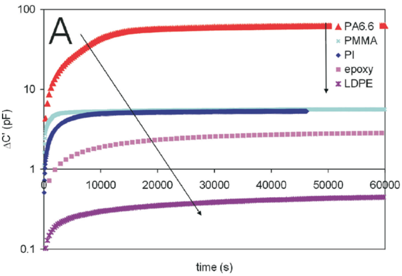

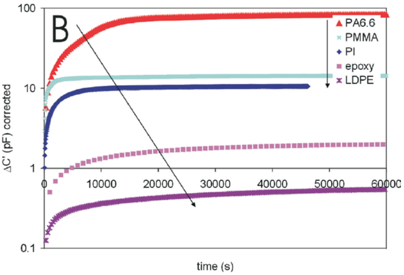

*Fig. 3a Film comparison at 1 kHz: uncorrected.*

*Fig. 3b Film comparison at 1kHz: thickness corrected (100 µm).*

$$M_t = M_{\infty,F} \cdot \left(1 - \frac{8}{\pi^2} \sum_{n=0}^{\infty} \frac{1}{(2n+1)^2} \exp\left(-(2n+1^2)\frac{\pi^2 Dt}{4d^2}\right)\right) + \sum_i M_{\infty,i}\left[1 - \exp(-k_i t)\right] \qquad (3)$$

uptake caused by the long-term relaxation of the sample due to structural rearrangements induced by the uptake of water. $M_t$ is the weight increase in time, $M_{\infty,F}$ is the equilibrium amount of sorption in the unrelaxed polymer [mg/g], $d$ the half thickness [m], $D$ the diffusion coefficient [$m^2s^{-1}$], $t$ the time [s], $M_{\infty,i}$ the equilibrium sorption of the ith relaxation process [mg/g], and $k_i$ the relaxation rate constant of the ith relaxation process [$s^{-1}$]. Note that the exponential series in eq. 3 converges fast, and a limited sum of three terms therefore suffices for the Fickian term. Only one relaxation process is assumed to take place in the polymer matrix, therefore only one relaxation term (equation (3)) is used.

In figure 4 a fit is shown for dielectric data of epoxy with eq. 3, assuming that the capacitance is linear dependent on weight; with a diffusion coefficient of $3.1 \times 10^{-12}$ $m^2s^{-1}$. For the gravimetric data of epoxy the fit results in a diffusion coefficient of $2.2 \times 10^{-12}$ $m^2s^{-1}$. For the other films the diffusion coefficients are given in table 1, along with the model parameters. For PA 6.6, the sigmoidal part of the sorption curve could not be fitted as perfectly as for the other films, therefore other diffusion models will have to be checked in the future (e.g. variable surface concentration model[10]). The lowest rate of sorption is found for PA6.6, which in turn has the highest sorption, indicating that both maximum sorption and sorption rate are necessary and important parameters.

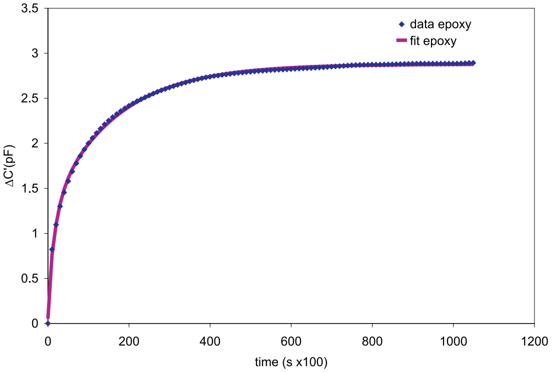

*Fig. 4 Fit of epoxy data with viscoelastic diffusion model (eq. 3).*

The maximum sorption is a good indicator for the affinity, and wet ability, of the polymer towards water (vapor); and the sorption rate shows how easy the water penetrates first the free volume of the polymer, followed by polymeric relaxation processes to increase its uptake (also linked with the wet ability).

From the DSA measurements maximum sorption values can be calculated by the following equation[7], which is known as the Landau, Lifschitz, Looyenga (LLL) relation[13, 14] (4).

$$\varepsilon_t^{'1/3} = \nu_w \cdot \varepsilon_w^{'1/3} + (1 - \nu_w) \cdot \varepsilon_d^{'1/3} \tag{4}$$

$\varepsilon_t$' is the total dielectric permittivity of the saturated signal (water+polymer), $\varepsilon_w$' the dielectric permittivity of water (assumed to be 80), $\varepsilon_d$' is the dielectric permittivity of dry polymer; and $v_w$ the volume fraction of water at saturation. The values of the calculated volume percentages of water in films can be found in table 1.

Weight measurements of (0.6533 g dry) epoxy show a mass water uptake of $8.7 \times 10^{-3}$ g, which results in 1.3 wt% (1.5 vol%) vapour uptake. For DSA measurements the vapour uptake is 2.1 vol% calculated with equation (4), which is in reasonable agreement with the weight measurements. Due to electrode polarization a too high value for water sorption in PA6.6 is calculated, whereas the other values are acceptable values for vapour sorption in polymer films[15].

| **Film** | **Diffusion coefficient ($\times 10^{-12}$ $m^2s^{-1}$)** | **$M_{\infty,F}$ [mg/g]** | **$M_1$ [mg/g]** | **$k_1$ [$s^{-1}$]** | **Vol % DSA** | **(vol% weight)** |
|---|---|---|---|---|---|---|
| Epoxy | 3.1 | 1.24 | 1.64 | 0.00622 | 2.1 | (1.5) |
| PI | 0.44 | 4.60 | 0.72 | 0.00758 | 2 | (2.2) |
| PMMA | 1 | 4.94 | 0.68 | 0.00688 | 1.8 | (-) |
| LDPE | 1.2 | 0.26 | 0.29 | 0.00178 | 0.17 | (-) |
| PA6.6 | 0.01 | 4.57 | 60.37 | 0.01189 | 21 | (-) |

*Table 1 Diffusion coefficients, model parameters, and total sorption calculated for films.*

### 4.3.1.3 Gravimetric measurements

A direct comparison between the DSA response and the gravimetric data of the epoxy samples will be made. The gravimetric

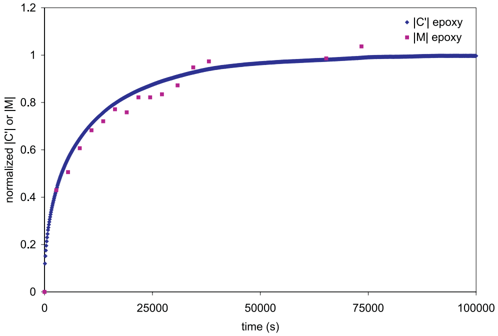

*Fig. 5 Gravimetric measurement vs. dielectric measurement epoxy (1 kHz).*

measurements were performed with epoxy coatings on a glass substrate in order to prevent double sided diffusion. In a previous article[7] it was observed that Kapton® dielectric data was similar to weight (absorption) data.

The results of the normalized gravimetric ($|M|=\Delta M_t/\Delta M_{sat}$) and dielectric ($|C'|=\Delta C_t'/\Delta C_{sat}'$) measurements are displayed in figure 5. The dielectric data can be treated as weight data, since the dielectric curve overlaps the mass curve.

### 4.3.2 Comparison of filters

In this section the results for filters are discussed and the same approach is used as for films (3.1). First an evaluation on measurements done at various frequencies has been done, followed by comparison of various filters at 1 kHz. Gravimetric measurements were not possible for filters due to too rapid desorption on removal from the flow cell flushed with moisturized nitrogen.

#### 4.3.2.1 Filters - various frequencies

The normalized results for filters are shown at various frequencies in figure 6. For the filters another effect takes place during vapour uptake than the films. For porous PE and cotton linter a clear peak appears, which becomes smaller at higher frequencies. Berens and Hopfenberg found such behaviour for sorption of methanol in PVC[12]. The assumption

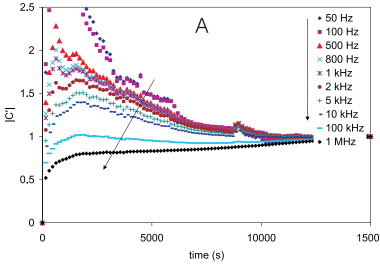

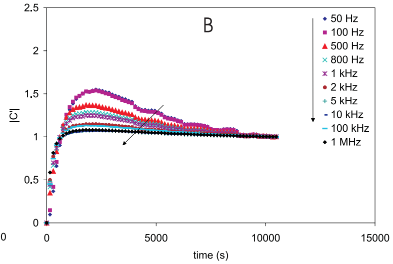

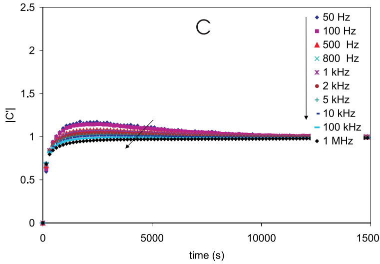

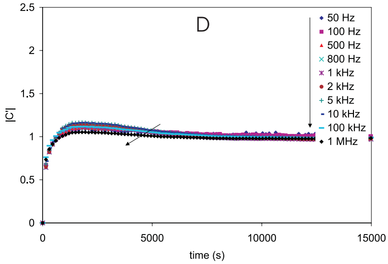

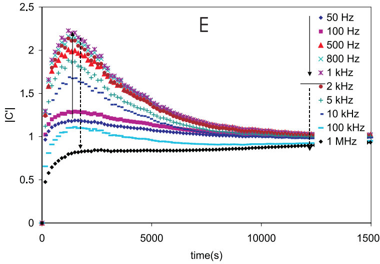

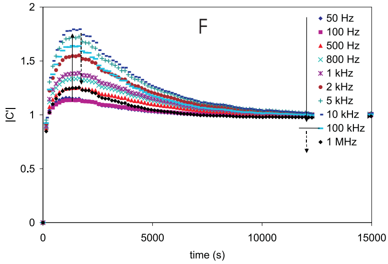

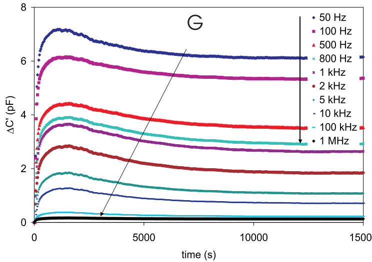

*Fig. 6a Normalized frequency sweeps of porous PE.*

*Fig. 6b Normalized frequency sweeps of cotton linter.*

*Fig. 6c Normalized frequency sweeps of nitro cellulose 0.05 μm.*

*Fig. 6d Normalized frequency sweeps of PTFE 5 μm.*

*Fig. 6e Normalized frequency sweeps of PVDF 0.45 μm.*

*Fig. 6f Normalized frequency sweeps of PVDF 0.22 μm.*

*Fig. 6g Non-normalized frequency sweeps of PVDF 0.22 μm.*

involves desorption of methanol due to collapse or deswelling of the glassy structure of PVC. It is not unlikely that also in this case desorption occurs for cotton linter, which is hydrophilic, due to softening (and finally collapse) of the matrix. On the other hand, for porous PE strong capillary forces caused by water, and strong hydrophobicity, deswells the structure. Porous PE has a low weight per surface area (3 g/m$^2$) and is hydrophobic with a thickness of 20 μm, whereas cotton linter has a higher weight per surface area (78 g/m$^2$), is hydrophilic and has a thickness of 100 μm.

Despite the fact that porous PE is hydrophobic, the low weight per surface area and small thickness causes electrode polarization. In some of the measurements nearly (the measurement was then stopped) short-circuiting occurred, especially at low frequencies. Due to the low absorption of water in the PE polymer matrix, the water forms a thin layer in the continuous open structure of the pores. This also explains the fact that the peak becomes smaller from low to high frequencies due to polarization (decreasing from low to high frequencies). The same holds for the cotton linter, except in this case no short-circuiting appears due to the fact that the vapour easily penetrates the cotton, in combination with the higher thickness of the filter.

Nitro cellulose and PTFE shows a similar behaviour, albeit to a much smaller extent than porous PE and cotton linter. Nitro cellulose is slightly hydrophilic and has pores of about 0.05 μm diameter. The formation of a water layer on the pore walls causes polarization at lower frequencies and finally due to swelling of the polymer matrix the pores tend to close causing desorption of the water in the pores.

PTFE, a fibre structure (like cotton linters) and hydrophobic of nature, did not show polarization, observing the overlap at all frequencies, probably due to denser structure than porous PE; but desorption still occurs.

Finally PVDF 0.22 μm (pore size) and PVDF 0.45 μm (pore size) has a trend that starts with a low peak at low frequencies (50-500 Hz), to a maximum at higher frequencies (0.8-2/10 kHz) and ending low at the highest frequencies (0.05/0.1-1 MHz). This behaviour is obviously not the result of polarization, which should increase with decreasing frequency. The structure is continuous and the matrix is hydrophilic PVDF. This material behaves similar to cotton linter, except the pore size is much smaller for PVDF. PVDF has been made hydrophilic, therefore the frequency has an important effect on the interaction of water to the matrix and finally the height of the peak, in this case the highest for PVDF between 2-10 kHz.

In figure 6g the non-normalized data can be found for PVDF 0.22 µm. There is a general decreasing trend from high to low frequencies and also the peak has the same height over the frequency range 50 Hz-10 kHz. Compared to the other filters, PVDF, PTFE and nitro cellulose show similar results. Cotton linter and porous PE show the trend from low to high frequency a high to low peak height, due to polarization.

Polarization does not play a role for PVDF, PTFE and nitro cellulose, because the peak heights are the same between 50 Hz-10 kHz; therefore the peak is likely an effect of desorption due to collapse of the matrix. The fact that higher frequencies (100 kHz-1 Mhz) show a smaller effect can be explained by different distribution of water, bulk water and bound water, in the polymer.

### 4.3.2.2 Filters - 1 kHz

For filters the same data presentation is used as for films, where in figure 7a the data is plotted without any correction. In 7b the maximum sorption correction (eq. (2)) is given and 7c displays the normalized data for all filters.

Without maximum sorption correction (figure 7a) the order from high to low peak is: PVDF 0.22µm, cotton linter, PVDF 0.45 µm, porous PE, nitro cellulose and PTFE. Corrected for the thickness this becomes now (figure 7b): porous PE, cotton linter, PVDF 0.22 µm, PVDF 0.45 µm, nitro cellulose and PTFE. The most porous system (porous PE) and most hydrophilic (cotton linter) have the highest sorption; whereas the most hydrophobic (PTFE) has the lowest sorption, followed by the more hydrophilic nitro cellulose. The fact that PVDF 0.45 µm has 1.5 times higher density than PVDF 0.22 µm could explain higher water uptake of PVDF 0.22 µm.

The normalized graph (figure 7c) shows that porous PE and PVDF 0.45 µm have the largest desorption peaks. This large desorption peak might be the cause of high water uptake due to high porosity, causing electrode polarization on the electrodes and is followed by, for PVDF, a collapse of the matrix due to softening of the polymer; whereas for PE strong capillary forces and hydrophobicity causes the matrix to deswell. PVDF 0.45 µm has a higher density, but the pores are larger than that of PVDF 0.22 µm, resulting in larger electrode polarization for PVDF 0.45 µm.

Interestingly, the desorption peaks for all filters occur around the same time: 1000-2000 seconds (figure 7c). A plausible explanation might be that the vapour penetrates the pores of all filters at the same rate, followed by diffusion in the polymer filter material causing the desorption peak to disappear due to swelling or collapse. This would only be plausible if the pore characteristics are similar (size, size distribution, connectivity), and therefore this observation can be seen as a coincidence.

The diffusion coefficient has been calculated with the same fitting equation (3), where the only difference is that two relaxation terms were used: one to account for the desorption process, and one for the normal

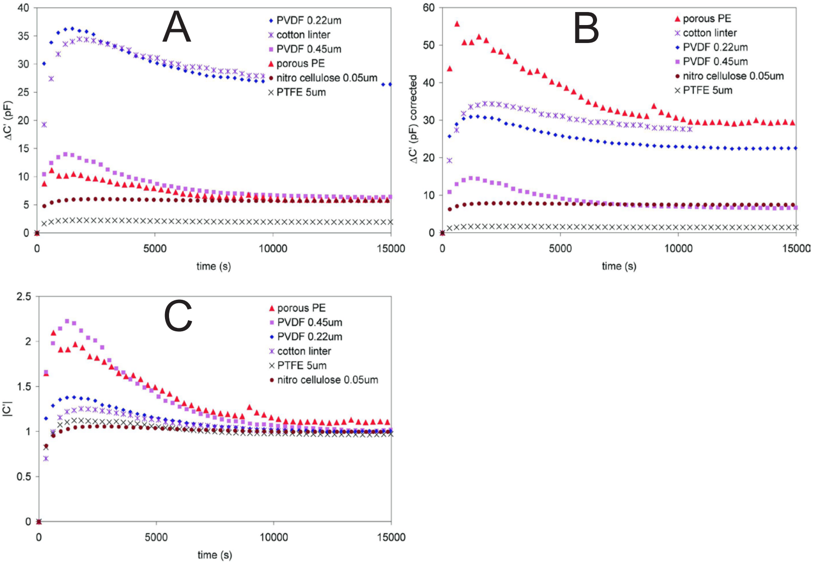

*Fig. 7a Filter comparison at 1 kHz: uncorrected.*
*Fig. 7b Filter comparison at 1 kHz: thickness corrected (100 µm).*
*Fig. 7c Filter comparison at 1 kHz: normalized.*

structural relaxation of the polymer matrix. In figure 8 the fit is shown of PVDF 0.45 μm, resulting in a diffusion coefficient of 5.2x10$^{-12}$ m$^2$s$^{-1}$. The diffusion coefficients for the filter membranes are shown in table 2, along with the model parameters.

The most interesting result from the calculated diffusion coefficients in table 2 is, that it seems that they seem to represent the diffusion coefficients for the bulk polymer. This means that equation (3) corrects the porous structure into a bulk polymer by using the two relaxation terms. This can be seen when the diffusion coefficient of PE (in table 1) is compared with porous PE (table II), which are nearly the same. Also PVDF 0.22 μm and PVDF 0.45 μm have the same diffusion coefficients, although the pore sizes are different. More experiments are necessary to verify this.

| **Filter** | **Diffusion coefficient (x10$^{-12}$ m$^2$s$^{-1}$)** | **$M_{\infty,F}$ [mg/g]** | **$M_{\infty,1}$ [mg/g]** | **$k_1$ [s$^{-1}$]** | **$M_{\infty,2}$ [mg/g]** | **$k_2$ [s$^{-1}$]** |
|---|---|---|---|---|---|---|
| Porous PE | 1.7 | 6.64 | 9.26 | 0.59 | -10.25 | 0.031 |
| Cotton linter | 2.9 | 5.90 | 35.23 | 0.24 | -15.28 | 0.021 |
| PVDF 0.22μm | 5.5 | 25.79 | 25.32 | 0.68 | -24.97 | 0.035 |
| PVDF 0.45μm | 5.2 | 18.34 | 3.79 | 0.95 | -15.88 | 0.036 |
| Nitro cellulose | 0.15 | 2.75 | 4.27 | 0.76 | -1.37 | 0.035 |
| PTFE | 0.53 | 7.19 | 1.30 | 0.59 | -5.97 | 0.0099 |

*Table 2 Diffusion coefficients calculated for filters, along with model parameters.*

## 4.4 Conclusions and outlook

The DSA is able to distinguish between all types of films and filters; which illustrates the capability of the device. The dielectric data can be used as mass data to calculate diffusion coefficients, since a good overlap was found when comparing gravimetric measurements and DSA measurements for an epoxy film (and also for PI). The diffusion coefficient can be determined by using a Fickian diffusion equation combined with a relaxation parameter. The maximum sorption can be determined by using a dielectric mixing-rule given by Landau, Lifschitz, Looyenga (LLL).

Frequency analysis showed that for polymer films the vapour penetrates the organic coating without interacting with the polymer. For PA6.6 this was not the case, where likely electrode polarization takes place due to the high water uptake of this material. Therefore, care should be taken with interpretation of the results for total water sorption. Also other diffusion models will have to be tried, to see whether the sigmoidal fit can be fitted better.

First observation of the DSA filter measurements showed that desorption seemed to occur. The largest desorption was found for the most porous systems (porous PE & cotton linter), and the smallest desorption for the least porous systems (nitro cellulose & PTFE). The relation between the size of the desorption peak and the porosity could indicate that electrode polarization occurs for the most porous systems and decreases for less porous systems.

Due to the high hydrophobicity of PTFE and small pore size of nitro cellulose, a negligible frequency effect (no interaction between water and polymer) of PTFE and nitro cellulose was found. For porous PE and cotton linter the electrode polarization takes place due to the high porosity of both materials. The intermediate case holds for PVDF 0.22 µm and PVDF 0.45 µm, where the frequency analysis show, that with increasing frequency first a rising and then a decrease in desorption peak size. This could be explained by the fact that the material is made hydrophilic, resulting in a frequency dependency with water. Also no electrode polarization occurred because the pore sizes are between porous PE/cotton linter and PTFE/nitro cellulose.

Clearly DSA is a powerful technique for measuring vapour sorption rates in a wide range of polymer materials and filters. For films with defects (pinholes, etc.) the DSA technique can be useful. Also, due to the possibility of frequency analysis, more complicated water sorption processes can be investigated in some detail as is demonstrated for PA6.6, and the porous filter materials, where “bulk” and absorbed water contribute to the response.

To establish the potential of the new technique in the field of non-destructive coating inspection and early warning testing, future work will be done on other types of polymer films. In addition UV degradation will be inflicted on epoxy coatings to determine the sensitivity of the DSA to detect chemical surface changes.

## References

1. Piringer O.G., Baner A.L., Plastic Packaging Materials for Food: Barrier Function, Mass Transport, Quality Assurance, and Legislation. Wiley, 2000.
2. Chin J.W., Nguyen T., Aouadi K., J. Appl. Pol. Sci.1999;71:483-492.
3. Marcus P., Oudar J., Corrosion mechanisms in theory and practice. Dekker, 1995. pp. 581-628.
4. Berger C.M., Henderson C.L., Polymer 2003; 44: 2101-2108.
5. Nogueira P., Ramirez C., Torres A., Abad M..J, Cano J., Lopez J., Lopez-Bueno I, Barral L, J. Appl. Polym. Sci. 2001 ;80:71-80.
6. Chin J.W., Nguyen T., Aouadi K., J. Appl. Polym. Sci. 999;71:483-492.
7. Giacomelli Penon M., Picken S.J., Wübbenhorst M., de Vos G., van Turnhout J.. Rev. Sci. Instr. 2006;77:115107.
8. Rabek J.F., Experimental methods in polymer chemistry. Wiley, 1980. pp. 601-614.
9. Buchner R., Barthel J., Stauber J., Chem. Phys. Lett. 1999;30:57-63.
10. Long F.A., Richman D., J. Am. Chem. Soc. 1960;82:513-519.
11. Schönhals A., Kremer F: in Kremer F, Schönhals A eds.; Broadband Dielectric Spectroscopy. Springer 2003. pp. 59-98.
12. Berens A.R., Hopfenberg H.B., Polymer 1978;19:489-496.
13. Landau L.D, Lifshitz E.M., Electrodynamics of continuous media. Pergamon 1960. pp. 46.
14. Looyenga H., Physica 1965;31:401-406.
15. Kohan M.I.., Nylon Plastics Handbook: Carl Hanser Verlag, 1995.

# Chapter 5

# WATER SORPTION IN UV DEGRADED CLEAR&PIGMENTED EPOXY COATINGS BY DIELECTRIC SORPTION ANALYSIS[*]

[*]This chapter has been published in Polymer Degradation and Stability: M. Giacomelli Penon, S.J. Picken, M. Wübbenhorst, and J. van Turnhout. Pol. Degr. Stab., **92**, (2007), 1247-1254.

## 5.1 Introduction

Life time prediction of organic coatings plays an important role in today's world. From around 1950-1960 scientists and industries started to bring more coherence in coating degradation[1-11], and tried to find methods to estimate when their coating or paint should be replaced. Also the consumer expects a ranking or indication from the paint industry of how good their coating is in comparison to their competitors (clearly the paint industry also would like to know this). For this accelerated test facilities have been built to speed up degradation and get fast results, like the weather-o-meter , QUV, salt spray test and others[12], dependent on the conditions the coating likely will experience. Of course also the traditional long term exposures are still performed in exotic places like (the most famous one) in Florida, Australia, and nowadays all over the world[13-16]. After extensive trials to compare the accelerated degraded coatings with the naturally degraded coatings[17-24], it became clear that most likely due to nature's irreproducibility (and laboratory's reproducibility) and the interaction and interaction change upon acceleration, the link between both is very difficult to be made. Still, in order to give a quality indication of the coating, and to keep paint development going, the paint industry uses the accelerated weathering tests on large scale in combination with natural weathering tests.

Besides various ways of degrading the coating naturally or accelerated, numerous methods of analysing the degree of degradation (involving different fields of expertise: chemists, mathematicians, physicists, material scientists, mechanical engineers, etc.) have been performed over time. There is gloss, hardness, rheometric, UV-VIS, WAXS, DSC, FTIR, AFM, SEM, DRS, etc.[25-32]. Unfortunately all these results have been performed separately on different coatings, resulting in a scattered whole. Following the trend of articles though, it becomes clear that the degradation should be detected at an earlier level, and therefore more sensitive equipment is used (like the AFM and micro ATR-FTIR).

Previous articles[33-34] have shown that the dielectric sorption analyser is suitable in measuring sorption curves for various organic coatings and filters. UV degraded clear and pigmented coatings were chosen to investigate sorption differences. From the results in this paper it will follow that the DSA shows clear trends with increasing degradation times. Also a desorption mechanism is found that occurs after a certain amount of degradation time. This desorption phenomenon has already been shown for DSA measurements on filters[34], and will be extended with model systems in this paper. A dielectric frequency sweep with DSA measurements resulted in a higher sensitivity at lower frequencies. It will become clear that the advantage of DSA over most other measurements devices is the non-destructive aspect and the fact that both surface and the whole coating is measured (in time).

## 5.2 Experimental

### 5.2.1 Materials

An epoxy clear coating (resin) and a fully commercial pigmented epoxy coating, both received from Akzo Nobel, has been used for UV degradation. The clear coating contains only surfactant and defoamer as additives. The pigmented coating is chemically similar to the clear coating, but is in commercial state (which means more additives, and pigments added); and is used as marine protective coating.

Both coatings were air sprayed on glass plates, cured at ambient conditions, and end cured for 30 minutes at 110 ºC. DSC measurement were done to make sure the coatings were fully cured. The coatings are then released from the glass and dried under a dry nitrogen flow. The clear coatings have an average thickness of 100 μm and the pigmented coatings 60 μm.

### 5.2.2 DSA set-up

An extensive description involving the principles of the dielectric sorption analysis can be found in a previous article[33]. The main advantage of this technique involves the possibility of measuring real time the change in dielectric properties of the coating during moisture uptake.
Gaseous nitrogen (2% RH at 27 ºC) represents the dry flow and the “wet” flow is humidified gaseous nitrogen (86% RH at 27 ºC), with a flow speed of 7 ml/s.
(Dry or wet) gaseous nitrogen absorption by the sample is achieved by a porous top electrode and a solid bottom electrode; the whole is place in a closed compartment.
The dielectric analysers used for these experiments are an Andeen Hagerling (high precision 1 kHz bridge, type 2500A) and a Hewlett Packard (HP 4284A precision LCR meter) frequency analyser with a frequency range between 20 Hz until 1 MHz.

### 5.2.3 Degradation set up

A closed system was built, to degrade the coatings under controlled parameters. Basically it is a closed box with a quartz window for UV degradation; a heat element is used to adjust the temperature, and the medium is dry air (<25 vpm). The UV source is a Philips PL lamp, of which the difference in spectrum and intensity becomes clear in figure 1,

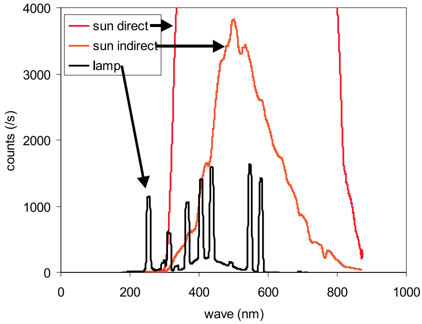

*Fig. 1 Spectrum of UV source used for degradation, compared with sunlight.*

when compared to the sun (direct and indirect). The indirect spectrum is measured by exposing the spectrometer at such an small angle to the sun, that the CCD of the meter was no longer over saturated; and is just shown as comparison.

The clear coatings were UV degraded in two ways. For the first method one coating was degraded cumulatively for 0, 1, 2, 4, 8 and 16 days. The second method a new clear coating was used for each separate degradation (0, 2, 4, 14, 20 and 40 days). The pigmented coatings were degraded for 0, 2, 4 and 40 days (a fresh coating for each degradation).

## 5.3 Results

### 5.3.1 DSA measurements on degraded samples

### Clear coating

The DSA results for the cumulative degraded clear coating are shown in figure 2. Figure 2a shows the difference $\Delta C'$ ($C_t'$-$C_{sat}'$), which is the capacitative part of the signal; and 2b the difference $\Delta C''$ ($C_t''$-$C_{sat}''$), which is the resistive part of the signal.

Interestingly, the differences in $\Delta C'$ in figure 2a between 0, 2 and 4 days are not significant. A difference can be seen for 1 day degraded, which is characterized by a higher water uptake. Increased hydrophilic behaviour is caused by scission (and oxidation) of bonds in the polymer, which could explain this higher water uptake. In comparison with the

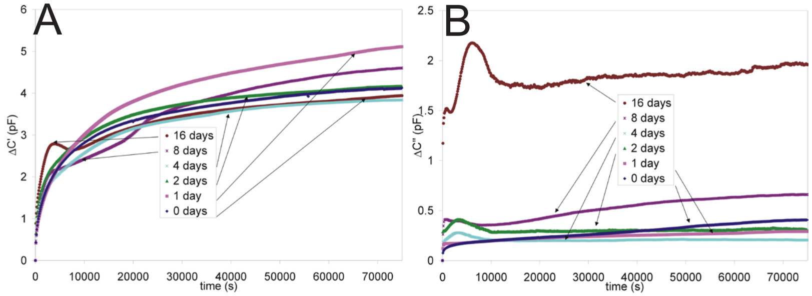

*Fig. 2a Cumulative degraded clear coating, $\Delta C'$ vs. time.*

*Fig. 2b Cumulative degraded clear coating, $\Delta C''$ vs. time.*

undegraded coating degradation times between 2-4 days causes similar water uptake. Most likely crosslinking dominates the process (despite the hydrophilic surface), keeping the water uptake the same due to a decrease in free volume. Longer degradation times show a clear difference in the shape of a bend (for 8 days) and a bump (for 16 days). Compared to the undegraded coating, longer degradation times does not result in a significant higher water uptake.

Although Δ*C*' does not show any difference for the 2 and 4 days, Δ*C*" clearly displays a bump. A large signal difference in Δ*C*" can be seen for 8 and 16 days UV degradation, but also for 1, 2 and 4 days a bump appears in the first 10.000 seconds, which makes it possible to discriminate from the undegraded coating. These results show that it is more interesting to use Δ*C*" to detect changes in coatings during uptake of water vapour, since the largest change can be found there. This emphasizes that the resistivity (Δ*C*") is more affected during degradation than the capacitative (Δ*C*') part of the coating, by movements of polar groups and water in the polymer matrix.

Instead of cumulative degradation with one sample, for comparison also non-cumulative (for every degradation a fresh sample) was performed. The result is shown in figure 3. In figure 3a the Δ*C*' is plotted against time and a clear trend for increasing degradation time and water sorption can not be observed. Degradation for 2 and 12 days show a higher signal than 4, 20 and 40, implying that the water uptake is lower than an undegraded sample (assuming that the capacitative part Δ*C*" is directly related to

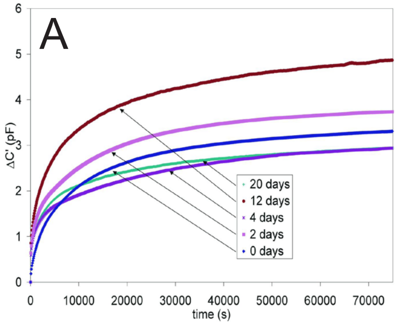

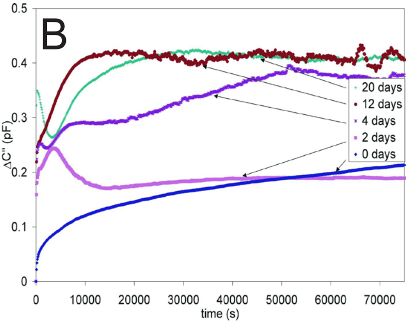

*Fig. 3a Non-cumulative degraded clear coating, ΔC' vs. time.*

*Fig. 3b Non-cumulative degraded clear coating, ΔC" vs. time.*

weight[33-34]. Similar to the cumulative curves in figure 2b, plotting Δ*C*" (figure 3b) shows that there are clear differences between the curves. Looking at the saturation level the trend is from low to high, 0, 2, 4, 12 and 20 days; and for the peak height in the first 10.000 seconds the trend is from low to high, 0, 2, 4, 12, 20 days. Also in the non-cumulative case it is clear that the resistive dielectric signal gives a more clear trend than the capacitative dielectric signal.

Comparing cumulative and non-cumulative degraded samples it can be seen that the capacitative signal shows the same trend for both coatings in the saturation area. A different trend is shown for 8 and 16 days cumulative, compared with 12 and 20 days non-cumulative; where the cumulative coating shows a dent at 8 days and a bump after 16 days degradation. When the samples were investigated with a microscope (figure 4), the undegraded coatings were undamaged, which was also the case after degradion (figure 4a), but after the DSA measurements the coatings showed cracks at the surface (figure 4b). Unfortunately the cumulatively degraded coatings were not monitored consistently with the microscope, but it is clear when cracks are present in the coating, further cumulative UV degradation and measurements with the DSA, results are different than when the cracks are not yet present.

Crack formation after DSA measurements is a result of stresses present at the surface of the coating by UV degradation, which are released after humidifying it during the DSA measurement. Humidity causes the coating to swell and lower its $T_g$[35-40]. During swelling the degraded part of the coating swells more than the bottom part, due to higher porosity and

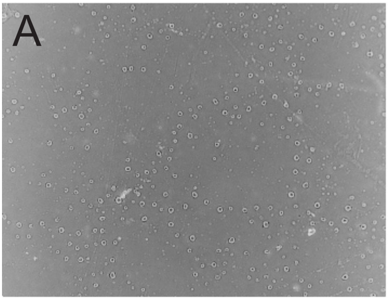

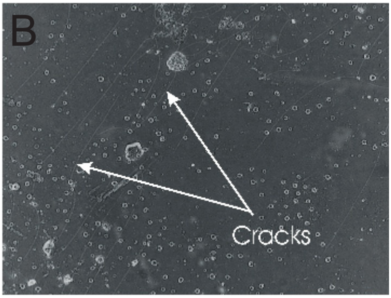

*Fig. 4a Degraded coating, before DSA measurement.*
*Fig. 4b Degraded coating (cracked), after DSA measurement.*

hydrofilicity. It is not expected that the cracks are being formed during swelling, but during the drying cycle, since the top layer releases the water more quickly causing a higher shrinkage, and most likely cracking, of the top layer. Also the fact that the top electrode is pressed on the coating surface, may facilitate crack formation.

In figure 2b it can be seen that the cumulative 16 days degraded sample shows a much higher signal than in figure 3b the 20 days degraded sample, suggesting that due to the fact the cracks are already present in the cumulative sample the resistive part of the coating increases more than when the cracks are not yet present, as is the case for the non-cumulative samples.

The stresses at the surface followed by crack formations of the clear coatings causes fluctuations in the DSA measurements.

The peaks that appear in both cumulative and non-cumulative measurements are result of desorption of water due to crack closure or stress relaxation by swelling of the degraded coating. Desorption has been discussed in a previous paper[34], and crack closure due to swelling has been described by Lundgren[41].

## Pigmented coating

In figure 5 the non-cumulative undegraded and degraded (figure 5a-b) pigmented coatings are shown for 0, 2, 4 and 40 days. Compared to the undegraded clear coatings (figure 3a-b), a lower value is expected for saturation Δ*C*’ and Δ*C*” for the pigmented coating (figure 5a-b), since the pigments do not contribute for the water sorption. Instead a higher value

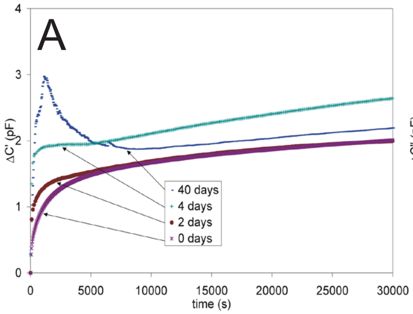

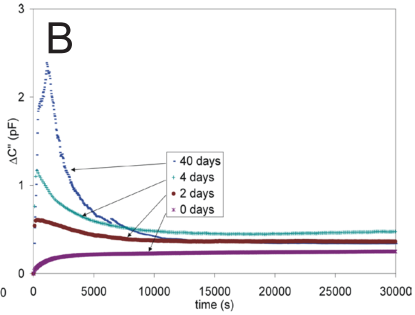

*Fig. 5a    Degraded pigmented coating, ΔC’ vs. time*

*Fig. 5b    Degraded pigmented coating, ΔC” vs. time* is found and this can be accredited to the thickness difference between clear coating (about 100 µm) and the pigmented coating (about 50 µm); A thinner coating results in a higher $\Delta C$' and $\Delta C$'' difference. For both $\Delta C$' and $\Delta C$'' an increasing peak is observed for longer degradation times as shown in figure 5a and 5b; similar to the degraded clear coatings, but more profound. Likely the pigments contribute to a better stress distribution inside the degraded resin, resulting in reproducible measurements of the DSA. No cracks were found before and after degradation and after the DSA measurements, supporting the assumption of a better stress distribution mentioned before. Therefore in the case of pigmented coatings there cannot be a crack closure mechanism causing desorption of water. Still during UV degradation scission of polymer chains causes a higher permeability of the resin. In a previous article it was shown that membranes with different porosities causes different desorption peaks during DSA measurements, due to pore closing as a result of swelling[34], which can also be the case for degraded pigmented coatings.

Considering that only the top layer degrades of both coatings, the pigmented coating gives a better resolution for the DSA measurements because of its lower thickness. Unfortunately a lower thickness could not be achieved with the clear coatings, due to dewetting and break up of the film.

### Diffusion coefficient of undegraded clear and pigmented coating

The undegraded clear and pigmented coating can be compared to find out what effect pigments and fillers have on the sorption rate of water vapour. Both coatings cannot be compared directly since the thicknesses are not the same, therefore the diffusion coefficients will be calculated and compared to each other.

The validation and explanation for the calculation of diffusion coefficients for DSA measurements is discussed in a previous article [34], therefore it suffices only to show the equation (1).

$$\frac{\Delta M_t}{\Delta M_{sat}} = \Phi\left(1-\frac{8}{\pi^2}\sum_{n=0}^{\infty}\frac{1}{\left(2n+1\right)^2}\exp\left(-\left(2n+1^2\right)\frac{\pi^2 Dt}{4d^2}\right)\right)+\left(1-\Phi\right)\left[1-\exp\left(-kt\right)\right] \qquad (1)$$

$M_t$ is the weight increase in time, $M_{sat}$ the weight increase at saturation, $d$ the half thickness [m], $D$ the diffusion coefficient [$m^2s^{-1}$], $t$ the time [s], $\Phi$ the equilibrium ratio constant which represents the ratio of the equilibriums of the first stage to that of the second stage in the sorption, and $k$ the rate constant of the relaxation process [$s^{-1}$].

For a clear coating the diffusion coefficient is 3.1x10-12 $m^2/s$ and for a pigmented coating 8.9x10-13 $m^2/s$. Since both coatings are composed of the same resin, the lower diffusion coefficient for the pigmented coating indicates that the presence of pigment and filler material slows down the sorption of water into the resin, likely due to the platelet shape of the filler material.

### Comparison between clear and pigmented coatings

Instead of the AH 1kHz dielectric bridge, a HP dielectric bridge is used, which is capable of frequency sweeps between 20 Hz-1 MHz.

An undegraded and degraded (40 days UV) clear and pigmented coating is measured with the DSA and is shown in figures 6a-d. To compare the signal heights of the clear coatings with the pigmented ones, $\Delta\varepsilon'$ and $\Delta\varepsilon''$ have been plotted against time, instead of $\Delta C'$ and $\Delta C''$. $\varepsilon'=C'd/\varepsilon_0 A$, where $\varepsilon'$ is the dielectric permittivity, $C'$ the capacitative part of the signal, $d$ the thickness [m], $\varepsilon_0$ the permittivity of vacuum [$J^{-1}C^2m^{-1}$] and $A$ the measured area [$m^2$], $\Delta\varepsilon' = \varepsilon_t' - \varepsilon_0'$, where $\varepsilon'_t$ is the permittivity at time $t$, and $\varepsilon_0'$ the permittivity in the dry state. $\varepsilon''$ and $\Delta\varepsilon''$ is found the same way, where $\varepsilon''$ represents the loss signal.

For the clear and pigmented undegraded coating the normalized sweeps $|\varepsilon'|$ are shown in figure 7a and 7c and $|\varepsilon''|$ in figure 7b and 7d. A similar result in figure 7a has been discussed in a previous paper, showing that the frequency overlap is a result of water penetrating the coating without interacting with the resin. Figure 7b shows the same result for $|\varepsilon''|$. For the pigmented samples it can be seen in figures 7c and 7d, that at frequencies 100 kHz and 1 MHz the curve deviates slightly from all other frequencies. This minor deviation might be the result of chemical or physical interaction of water with the pigments.

The frequency dependence is very prominent in figures 6a-d, which is not the case for undegraded samples. Furthermore, the maximum for clear and pigmented samples are both around 1200 seconds, which is also expected since the resins are the same.

Maximum peak height (Δε’ and Δε”) is obtained at low frequencies and decreases (even tends to disappear) at high frequencies for clear and pigmented samples. A high dielectric signal at lower frequencies could indicate hydrogen bonding of water with (degraded / oxidized) hydrophilic parts of the coating. Also, due to higher water uptake close to the surface of the coating, (electrode) polarization might be an issue at lower frequencies. The fact that the peak disappears in time suggests that another mechanisms is present. Water binds to the hydrophilic parts of the coating, causing a higher peak for lower frequencies, followed by desorption due to swelling of the coating. Already mentioned, the rise of the peak could be created due to polarization of water in large cavities/ pores, and fall after desorption of water due to swelling of the resin. One

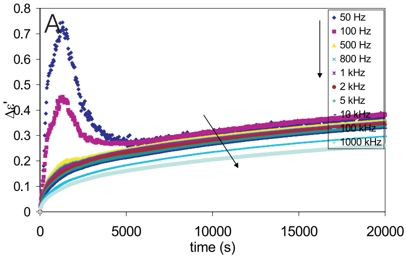

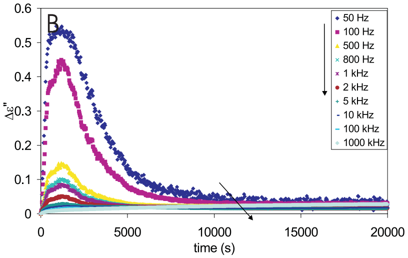

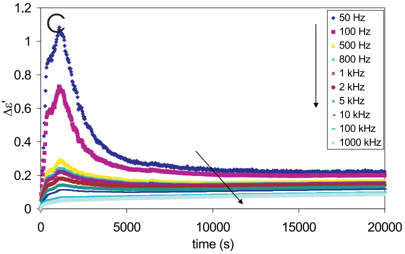

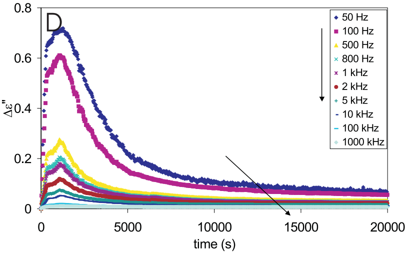

*Fig. 6a Frequency sweep (50 Hz-1 MHz) for a 40 days UV degraded clear coating, Δε’ vs. time.*

*Fig. 6b Frequency sweep (50 Hz-1 MHz) for a 40 days UV degraded clear coating, Δε” vs. time.*

*Fig. 6c Frequency sweep (50 Hz-1 MHz) for a 40 days UV degraded pigmented coating, Δε’ vs. time.*

*Fig. 6d Frequency sweep (50 Hz-1 MHz) for a 40 days UV degraded pigmented coating, Δε” vs. time.*

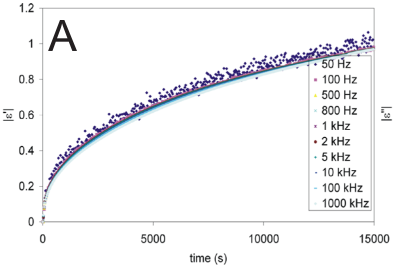

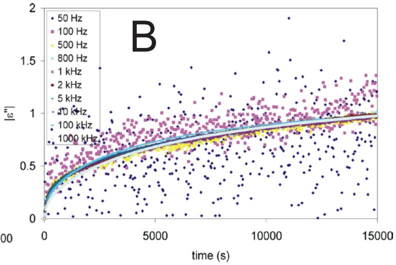

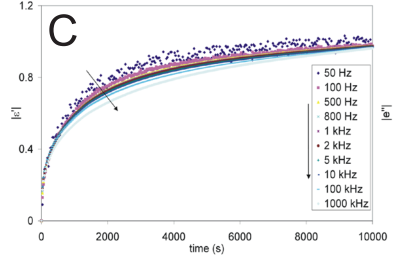

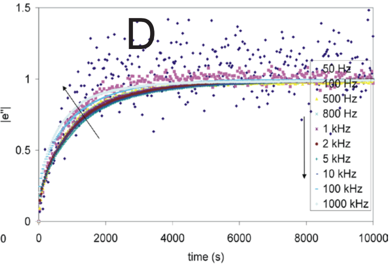

*Fig. 7a Normalized frequency sweep (50 Hz-1 MHz) for an undegraded clear coating, |ε'| vs. time.*
*Fig. 7b Normalized frequency sweep (50 Hz-1 MHz) for an undegraded clear coating, |ε''| vs. time.*
*Fig. 7c Normalized frequency sweep (50 Hz-1 MHz) for an undegraded pigmented coating, |ε'| vs. time.*
*Fig. 7d Normalized frequency sweep (50 Hz-1 MHz) for an undegraded pigmented coating, |ε''| vs. time.*

thing remains clear that lower frequencies give better resolution for water uptake in degraded coatings, indicating that a slow processes dominate the movements inside the polymer resin (with water) caused by the electric field.

### Simulation of data – pigmented coatings

To investigate whether the peak can be reproduced, several model systems have been chosen where an undegraded pigmented coating with a filter on top has been measured with the DSA. This way a simulation is created, where the filter on top of the pigmented coating artificially includes pores.

The filters used are porous polyethylene [porous PE] (porous PE Solupor Solupor:3p07A from DSM), cotton linters (cotton linters from

Schleicher&Schell Gmbh 595) and nitrocellulose (nitro cellulose 0.05 µm type VM from Millipore). These filters were already measured separately in a previous paper[34]. Nitro cellulose has very small pores (0.05 µm) and is semi hydrophilic, porous PE has a very open structure (3 g/m$^2$) and is hydrophobic; cotton linters have an open structure (78 g/m$^2$) and are hydrophilic. SEM pictures of these filters can be seen in figure 8a-c.

In figure 9a-f the DSA measurements are shown for the three model systems. For the pigmented coating with nitro cellulose (figure 9a ($\Delta C$')), desorption is not observed. In figure 9b ($\Delta C$'') a small peak can be found, indicating desorption, which is more pronounced at lower frequencies. No peak can be found for neither $\Delta C$' or $\Delta C$'', for the model system pigmented with porous PE, as shown in figure 9c-d. Finally for the pigmented coating with cotton linters, for both $\Delta C$' and $\Delta C$'', clear peaks can be found (figures 9e-f).

From these results it can be deduced that the peaks found in the degraded samples are most likely the result of increasing hydrophilicity and porosity due to UV degradation. Since porous PE (figure 9c-d) does not show desorption, either the size of the pores has influence on desorption (figure 8a), or the hydrophilicity, or both. The last option seems to be the most likely one, since hydrophilicity alone is not enough to cause high water uptake and eventually squeeze out enough water to cause a significant decrease of signal (otherwise it should already have been found for example for nylon, which is quite hydrophilic[42]). Also for a highly porous system that is very hydrophobic, water is not contained in high quantities and clustering does not occur; and therefore swelling is not likely to take place in order to squeeze out the water; as shown for porous PE. The amount of pores also seems to have an influence on the

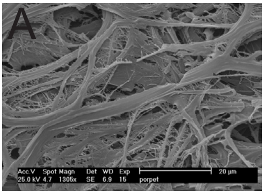

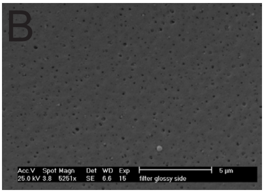

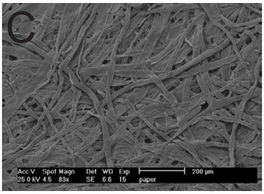

*Fig. 8a SEM picture of porous PE.*
*Fig. 8b SEM picture of nitro cellulose.*
*Fig. 8c SEM picture of cotton linter.*

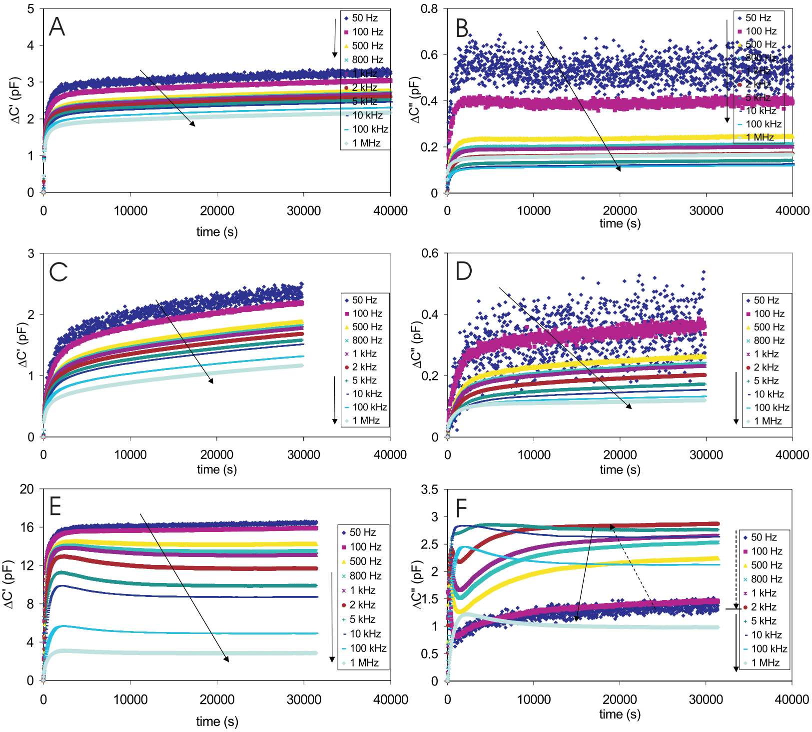

*Fig. 9a Frequency sweep (50`Hz-1 MHz) of model system undegraded pigmented coating with nitro cellulose, ΔC' vs. time.*
*Fig. 9b Frequency sweep (50 Hz-1 MHz) of model system undegraded pigmented coating with nitro cellulose, ΔC" vs. time.*
*Fig. 9c Frequency sweep (50 Hz-1 MHz) of model system undegraded pigmented coating with porous PE, ΔC' vs. time.*
*Fig. 9d Frequency sweep (50 Hz-1 MHz) of model system undegraded pigmented coating with porous PE, ΔC" vs. time.*
*Fig. 9e Frequency sweep (50 Hz-1 MHz) of model system undegraded pigmented coating with cotton linter, ΔC' vs. time.*
*Fig. 9f Frequency sweep (50 Hz-1 MHz) of model system undegraded pigmented coating with cotton linter, ΔC" vs. time.*

effect of desorption. Nitro cellulose has a low amount of pores, as shown in the SEM picture, figure 8b, and has only little desorption, whereas cotton linter shows a higher desorption due to higher porosity inside the cotton linters, figure 8c). To obtain more clarity on this, more research should be done on different pore sizes, pore densities and various levels of hydrophilicity.

## 5.4. Conclusions

The DSA is clearly capable of detecting differences between undegraded and degraded coatings, which makes this device useful as a non-destructive, in depth profiling, instrument for such purposes.

Degradation of clear and pigmented coatings affects the water sorption into these coatings, due to increased porosity and hydrophilicity. Also data fluctuations are found for UV degraded clear coatings that is caused by crosslinking, resulting in surface stress and eventually cracking during DSA measurements; which this is not the case for UV degraded pigmented coatings. Furthermore, the resistive part of the DSA signal is more sensitive for changes in water sorption of degraded coatings, instead of the capacitative part of the DSA signal.

DSA measurements on UV degraded clear and pigmented coatings show a desorption profile. Desorption is likely to occur due swelling of the coating, causing pores to shrink and water to be squeezed out. Higher porosity and hydrophilic regions, are induced by UV degradation.

Measurements at different frequencies shows that lower frequencies results in higher peaks, indicating that either polarization occurs at the electrodes or a water-hydrophilic interaction takes place.

Covering an undegraded pigmented coating with various (porous) filters supports the idea that porosity combined with the presence of hydrophilic regions are the cause of the peak that appears for DSA measurements on degraded samples. Porosity size and level of hydrophilicity are parameters that are responsible for the amount of desorption and are interesting for further investigation.

## References

1. Adams C.H., Taylor J.R., *Rubber World*, **131(1)**, (1954), 239–243.
2. Brand B.G., Nowacki L.J., Mirick W., Mueller E.R., *Journal Paint Technology,***62**, (1968), 37–42.
3. Vachon R.N., Rebenfeld L., Taylor H.S., *Textile Research Journal,* **38**, (1968), 716–728.
4. Blum G.W., Shelton J.R., Winn H., *Industrial and Engineering Chemistry,* **43**, (1951), 464–471.
5. Clark F. G., *Industrial Engineering Chemistry,* **44**, (1952), 2697–2709.
6. Dubois P., Hennicker J., *Plastics,* (1960), 428–430.
7. Dubois P., Hennicker J., *Plastics,* (1960), 474–478.
8. Reinhart F.W., Mutchler M.K., *American Society for Testing and Materials Bulletin,* (1956), 45–51.
9. Roxburgh C.M., *Journal Society Dyers and Colourists,* **84**, (1968), 518–519.
10. Tamblyn, J.W., Armstrong G.M., *Analytical Chemistry,* **25**, (1953), 460–465.
11. Feller R.L., Bailie C.W., *Bulletin of the American Group,* **6( 1)**, (1966), [pages not numbered].
12. Sherbondy V.D: in Koleske J.V. ed.; Paint and corrosion testing manual, (1995), 643-653.
13. Hicks L.S., Crewdson M.J.: in Koleske J.V. ed.; Paint and corrosion testing manual, (1995), 619-642.
14. Biggs S., Lukey C.A., Spinks G.M., Yau S.T., *Progr. Org. Coat*., **42**, (2001), 49-58.
15. Tidjani A., Pol. *Deg. Stab*., **68**, (2000), 465-469.
16. Gijsman P., Sampers J., *Die Angew. Makromol. Chemie*, **261/262**, (1998), 77-82.
17. Hardcastle K., Searle N.D.: in Rijntz R.A. ed., Plastics&Coatings, (2001), 189-240.
18. Martin J.W., Nguyen T., Byrd E., Dickens B., Embree N., *Pol. Degr. Stab*., **75**, (2002), 193-210
19. Nguyen T., Martin J., Byrd E., Embree E., *Pol. Degr. Stab.*, **77**, (2002), 1-16.
20. Bauer D.R., *J. Coat. Techn*., **74**, (2002), 33-38.
21. Bauer D.R., *Pol. Degr. Stab*., **69**, (2000), 297-306.
22. Mallon P.E., Li Y., Zhang R., Chen H., Wu Y. , Sandreczki T.C., Jean Y.C., Suzuki R., Ohdaira T., *Appl. Surf. Sci.*, **194**, (2002), 176-181.
23. Jacques L.F.E., *Prog. Polym. Sci*., **25**, (2000), 1337-1362.
24. Martin J.W., *Proc. of Corr. 97 Research Topical Symp*., (1997), 235-258.
25. Rabek J.F., Polymer Photodegradation, (1995), 433-598.

26. MacQueen R.C., Granata R.D., *Progr. Org. Coat.*, **28**, (1996), 97-112.
27. Biggs S., Lukey C.A., Spinks G.M., Yau S.T., *Progr. Org. Coat.*, **42**, (2001), 49-58.
28. Armstrong R.D., Jenkins A.T.A, Johnson B.W., *Corr. Sci.*, **37**, (1995), 1615-1625.
29. Perrin F.X., Irigoyen M., Aragon E., Vernet J.L., *Pol. Degr. Stab.*, **70**, (2000), 469-475.
30. Sugura M., Mitsuoka T., Murase A., *Pol. J.*, **33**, (2001), 617-620
31. Delobelle P., Guillot L., Dubois C., Monney L., *Pol. Degr. Stab.*, **77**, (2002), 465-475.
32. Lukey C.A., *Progr. Org. Coat.*, **41**, (2001), 129-134.
33. Giacomelli Penon M., Picken S.J., Wübbenhorst M., de Vos G., van Turnhout J., *Rev. Sci. Instr.*, **77** (2006), 115107
34. Giacomelli Penon M., Picken S.J., Wübbenhorst M., van Turnhout J., *J. Appl. Sci.*, **105**, (2007), 1471-1479.
35. Barrie J.A., in: J. Crank, G.S. Park (Eds.), Diffusion in Polymers, Ch. 8, (1968).
36. Adhikari B., Majumdar S., *Prog. Polym. Sci.*, **29**, (2004), 699-66.
37. Kondratowicz B., Narayanaswamy R., Persaud K.C., *Sensors and Actuators B*, **74**, (2001), 138-144.
38. Buchold R., Nakladal A., Gerlach G., Herold M., Gauglitz G., Sahre K., Eichhorn K.J., *Thin Solid Films*, **350**, (1999), 178-185.
39. Pradas M.M., Ribelles J.L.G., Aroca A.S., Ferrer G.G., Anton, J.S., Pissis P., *Colloid Polym. Sci.*, **279**, (2001), 323-330.
40. Turner D.T., *Polymer*, **23**, (1982), 197-202.
41. Lundgren J.E., Gudmundson P., *Comp. Sci. Techn*., **59**, (1999), 1983-1991.
42. Khanna Y.P., Han P.K., Day E.D., *Pol. Eng. & Sci*., **36**, (1996), 1745-1754.

# Chapter 6

## DIELECTRIC SORPTION ANALYSIS OF UV DEGRADED PIGMENTED EPOXY COATINGS AT ELEVATED PRESSURES*

*This chapter has been accepted in Polymer Degradation and Stability: soon to be published

### 6.1 Introduction

Life time prediction of organic coatings is focussed on estimating how long the coating keeps its protective barrier to the substrate from corroding, in order to know when a substrate should be recoated. For obvious economic (and environmental) reasons, industries prefer to recoat their buildings, boats, constructions, etc. as late as possible. On the other side, paint industries would like to sell their coatings with a warranty that their coating will survive an amount of years under certain, atmospheric, circumstances. Furthermore, in order to develop new high performance coatings, life time prediction is necessary to indicate whether the new coating has a better endurance than the current coating. Unfortunately, to investigate life time prediction the natural way, it would take more than 5 years[1] to get an impression of the performance of the coating. Without doubt this is much too long for newly developed coatings to appear on the market. Therefore industries started to degrade their coatings in laboratories, under more severe circumstances than natural weather is able to. Indeed the coatings degraded much faster, and results were available within several months[1]. However, the problem arose when the comparison was made between accelerated degradation and natural degradation. It appeared that there was not really a clear relationship between both types of degradation[2-6]. Up to date this problem has not yet been resolved[7-9]. In fact it has already been stated[10,11] that it is impossible to mimic natural weather on a laboratory scale. This is also the main reason that laboratory results do not comply with outdoor results. Although accelerated devices have been equipped with the possibility to cycle various parameters (temperature, humidity, intensity)[12], just like outdoors, still the correlation stays out.

The investigated parameters for accelerated degradation are temperature, UV source, UV intensity, humidity, day-night cycles and various concentration levels of salts, acids, bases[13-17]. Interestingly, one parameter that has never been thoroughly investigated is pressure. Of course this parameter is directly linked with concentration, and experiments have been performed for degradation at various concentration levels of oxygen[18,19]. In addition, high pressure degradation in combination with temperature was investigated[20,21]. But up to now the combination of UV radiation and pressure has not been found in literature.

In this paper a preliminary investigation was done on pigmented coatings that have been degraded with an UV source at various levels of pressure and duration. The degraded samples were measured with the dielectric sorption analysis (DSA), of which the device has already been described in a previous article[22]. The DSA has already proven to be able to measure differences in sorption curves for atmospheric degraded clear and pigmented coatings[23]. The results from this study show that elevated pressures have an accelerated effect on degradation. Furthermore, at certain frequencies the DSA is able to detect, besides water sorption and desorption, different molecular processes. These processes are polymer relaxation, water-hydrophilic group interaction and swelling.

## 6.2 Experimental

### 6.2.1 Materials

For UV degradation a fully commercial pigmented epoxy coating was used, kindly provided by Akzo Nobel, and is used as marine protective coating.

The coatings were air sprayed on glass plates and cured at ambient conditions. An end cure was done for 30 minutes at 110 ºC, to make sure the epoxy has fully reacted. The coatings were then released from the glass and dried under a dry nitrogen flow. The coatings have an average thickness of 60 μm.

### 6.2.2 DSA set-up

This technique involves the possibility of measuring the change in dielectric properties of the coating during moisture uptake. A more extensive description involving the principles of the dielectric sorption analysis (DSA) can be found elsewhere[22].

The dry flow was gaseous nitrogen (2% RH at 27 ºC) and the “wet” flow was humidified gaseous nitrogen (86% RH at 27 ºC), with a flow speed of 7 ml/s.

Absorption of “wet” gaseous nitrogen by the sample was achieved by a porous top electrode, while the bottom electrode was solid. The whole was placed in a closed compartment.

One frequency analyser used for these experiments was an Andeen Hagerling (high precision 1 kHz bridge, type 2500A), which was used for measurements at a single frequency. The Hewlett Packard (HP 4284A precision LCR meter) frequency analyser, with a frequency range between 20 Hz until 1 MHz, was used for frequency sweeps.

### 6.2.3 High pressure degradation set up

At the University of Twente, faculty of Chemical Technology a high pressure set up (figure 1) was built, and very kindly borrowed to us. The high pressure chamber can sustain a maximum of 100 bar and has a quartz window for UV degradation. The temperature (max 100 ˚C) was regulated by a heat belt, and the medium was air (Hoegst, 99.99% dry air). The UV source was a Philips PL lamp, of which the spectrum can be found in a previous article[24].

The pigmented coatings were degraded at 100 bar for 0, 1, 2, 3, 4, 15 days (a fresh coating for every degradation); and 1 bar for 40 days for comparison. The temperature was set at 40 ˚C.

To investigate the pressure dependency pigmented coatings were degraded at 1; 6,25; 12,5; 25; 50 and 100 bar for 2 days also at 40 ˚C.

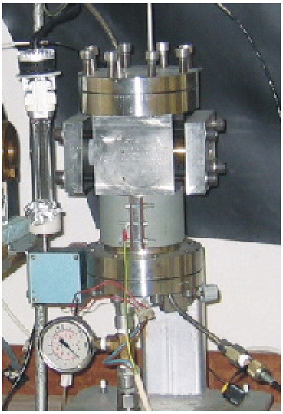

*Fig. 1 Picture of high pressure set*

## 6.3 Results and discussion

### 6.3.1 DSA measurements on degraded samples

**UV degradation at elevated pressures**

The results of the DSA measurements are shown in figure 2 for pigmented coatings, degraded from 1 to 100 bar for 2 days. It has already

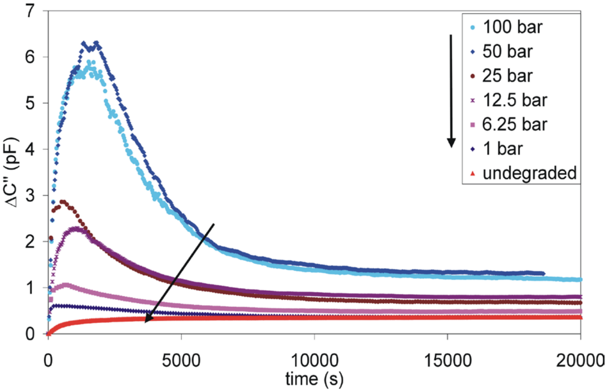

*Fig. 2 DSA permittivity measurements at 1 kHz for 2 days degradation at various pressures.*

been discussed[24] that the resistive (imaginary part of capacitance, *C*'') part of the dielectric signal is more sensitive than the capacitative (real part of capacitance, *C*') part. Therefore, only the signal difference $\Delta C''$ ($C_t''-C_{sat}''$) is shown.

A previous study[24] with DSA measurements and UV degraded coatings also showed that UV degradation causes hydrophilic groups and pores in the top layer of a polymer. When water vapour is blown across these degraded coatings, after a certain amount of time, desorption starts to occur. Desorption takes place due to swelling of the coating and water is being squeezed out of the pores. The peaks that appear in figure 2 are in this case also the result of desorption of water, causing the dielectric signal to decrease. The results also show that, with increasing pressures, the peak height increases. Since DSA measurements are directly related to the water ingress in the coating[22], the peak height suggests a higher water uptake with increasing pressure, followed by desorption. The saturation level (after > 20.000 seconds) is higher with increasing pressures, indicating higher water levels in the coating. It is believed that the size of the peak is related to the porosity (and amount hydrophilic groups) of the coating, therefore with increasing pressures a higher porosity (hydrophilic groups) is created. In order to find a relationship between elevated pressures and water sorption, the peak heights (with respect to the undegraded pigmented coating) are plotted against pressure in figure 3.

Figure 3 shows a clear linear trend up to 50 bar and remains saturated up to 100 bar. This trend can be explained by the linear relationship

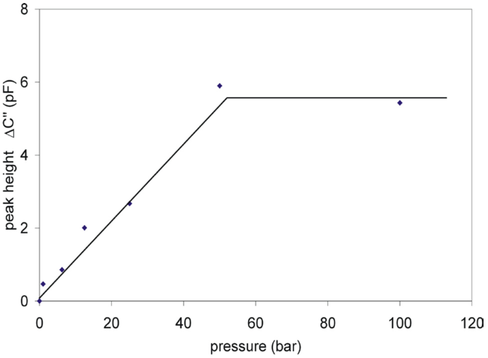

*Fig. 3 Relationship between UV degraded pressure and peak height.*

between pressure and air concentration in a polymer coating. Henry's law[25] states that for low pressures the concentration of air is linear with pressure. Also other experiments[26,27] with polymer systems have shown that air concentration is linear with pressure. The hypothesis behind this trend is, when UV "cuts" a polymer bond, either it recombines, cross-links, or oxidizes. When more oxygen is present in the polymer matrix, the likelihood for oxidation increases. In effect, more hydrophilic groups and a higher porosity of the polymer matrix are formed, which gives an explanation for the higher signal given by the DSA. The idea is that the abovementioned saturation level can be shifted to higher pressures (higher than 50 bar) by increasing the intensity of the UV source. The fact that saturation occurs at 50 bar signifies that, from that pressure on no further increase of degradation is possible with the current intensity of the used UV source (for equal degradation times). Another possibility is that air saturation has reached in the polymer at that pressure.

### UV degradation for various days

Pigmented coatings were UV degraded for 1, 2, 3, 4 and 15 days at 100 bar. The DSA measurements of these degraded pigmented coatings are shown in figure 4. In the same figure, also a 40 days UV degraded sample at 1 bar is plotted for comparison; where it clearly demonstrates the effect of elevated pressures by the height of the peak of for example

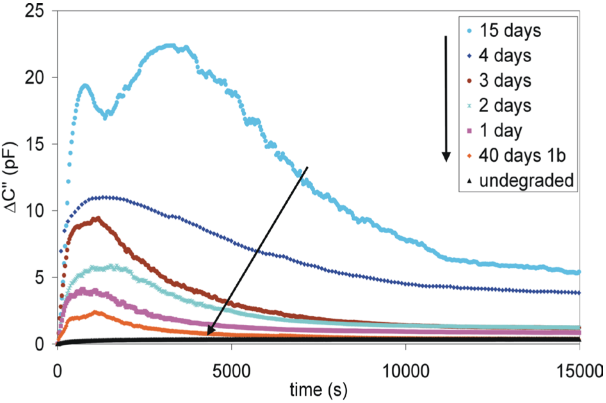

*Fig. 4 DSA permittivity measurements at 1 kHz after degradation at 100 bar for various days.*

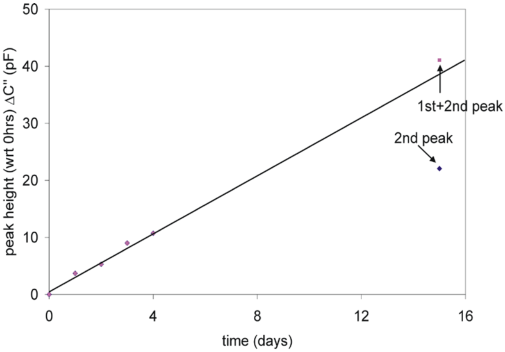

*Fig. 5 Relationship between amount of UV degraded days and peak height.*

at 100 bar already after 1 day. Interestingly for 100 bar 15 days degraded sample a double peak appears, which will be discussed later in this article.

In figure 5 the peak height, with respect to the undegraded sample, is plotted against the amount of degraded days. For degradation at 100 bar for 15 days, the peak height of the second peak is used to plot against the amount of degraded days. Up to 4 days the trend is quite linear and starts to deviate for 15 days. This deviation obviously occurs due to the fact that, after 15 days of UV degradation, the DSA measurement distinguishes the two peaks. For lower degradation times (for 1 to 4 days) these two peaks are likely also present in the DSA results, but they overlap. A linear trend can be found when the height of the 1st and the 2nd peak is added for the 100 bar 15 days (fig. 5), and supports the previous idea that for lower degradation times the two peaks overlap.

The appearance of a double peak for 15 days UV degradation can also be seen in Δ*C*' (the capacitative signal), see figure 6a; but not as clear as Δ*C*''. In case a similar plot is made as figure 5 with peak height Δ*C*', up to 15 days the same linear trend can be found like Δ*C*''.

The expectation is that this linear trend is not continuous, due to the fact that UV degradation only affects the surface of a pigmented coating. At some point the top layer will be degraded up to a maximum and starts to loose gradually the top layer; obviously even after 15 days at 100 bar this seems not to be the case.

### Explanation of double peak

Before discussing the double peak appearance with DSA, an important remark is that (all) peak(s) are reversible. In other words, when after the DSA measurement the coating is taken out, dried, and measured again again, the same double peak appears. Therefore chemical interaction or reaction with water is improbable.

Up to now frequency sweeps during DSA measurements seemed not to be necessary, because the degraded samples never showed a second peak. Also degradation at 1 bar for various days[23] showed that a frequency sweep did not add much extra information. At this moment, however, a frequency sweep might clarify the two peaks for the 100 bar 15 days degraded sample. In figure 6a and b Δ*C*' and Δ*C*" are shown vs time from 50 Hz to 1 MHz. It shows broadening of the peak for decreasing frequency for Δ*C*', but no double peak can be observed. However, Δ*C*" clearly shows that with decreasing frequency the 1st and 2nd peak becomes more pronounced. If only water sorption and desorption would take place, without any interaction with the polymer matrix, frequency independency would be the case (no shifting of peaks).

Obviously, for degraded samples with longer degradation times and at high pressure, other (molecular) processes start to play a role (besides water desorption) that are not only frequency dependent, but also frequency dependent in time with increasing absorption of water.

The clearest way of presenting frequency dependency is to plot

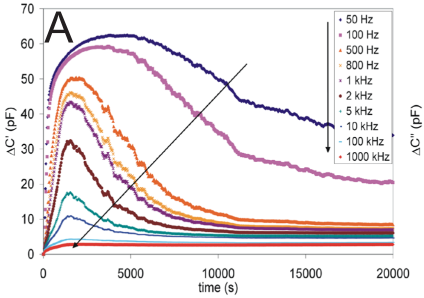

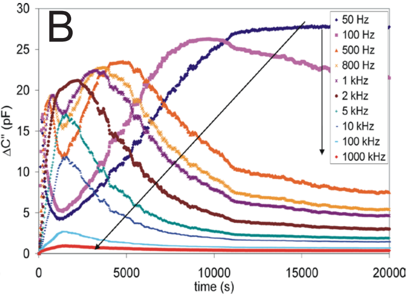

*Fig. 6a Time-frequency sweep of a DSA capacitance measurement for a 15 days UV degraded pigmented coating at 100 bar.*

*Fig. 6b Time-frequency sweep of a DSA permittivity measurement for a 15 days UV degraded pigmented coating at 100 bar.*

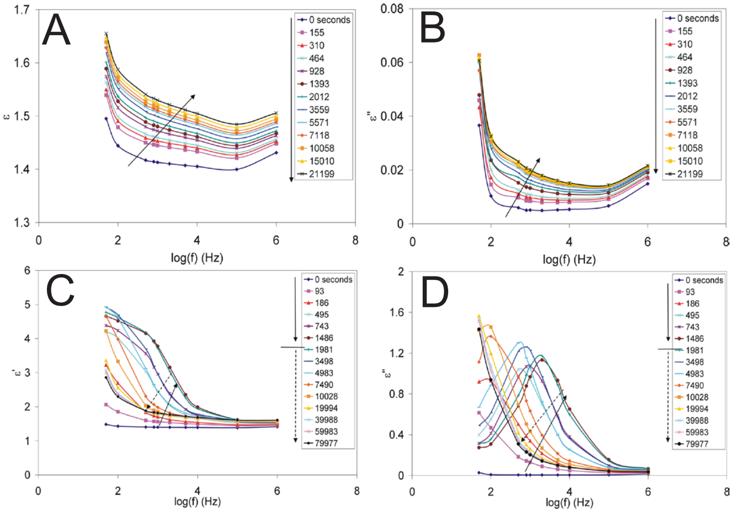

*Fig. 7a Frequency-time sweep of a DSA capacitance measurement for an undegraded pigmented coating.*
*Fig. 7b Frequency-time sweep of a DSA permittivity measurement for an undegraded pigmented coating.*
*Fig. 7c Frequency-time sweep of a DSA capacitance measurement for a 15 days UV degraded pigmented coating at 100 bar.*
*Fig. 7d Frequency-time sweep of a DSA permittivity measurement for a 15 days UV degraded pigmented coating at 100 bar.*

$\varepsilon'$ (dielectric permittivity, given by $\varepsilon' = C'd/\varepsilon_0 A$, where $C'$ is the real part of the capacitance, $d$ the thickness, $\varepsilon_0$ the vacuum permittivity and $A$ the area) and $\varepsilon''$ (dielectric loss, for which the same equation is used, but $C'$ is replaced by $C''$ the imaginary part of the capacitance) against frequency, see figure 7a-d. In figure 7a-b shows an undegraded sample for various times of water sorption; in figure 7c-d the same is plotted for a 100 bar 15 days degraded sample.

For the undegraded sample it is clear that with increasing sorption time $\varepsilon'$ and $\varepsilon''$ increases gradually for all frequencies with more or less the same increment; resulting that from t = 0 until t = 21000 seconds the frequency sweep shifts upwards.

For the degraded sample at t=0 $\varepsilon'$ and $\varepsilon''$ is the same as for the undegraded sample (also at t=0), but with increasing time the frequency dependency becomes very clear. Figure 7c shows that for $\varepsilon$' up to 200 seconds the signal is increasing for all frequencies, of which the low frequencies the fastest. Then from 200 seconds up to 1500 seconds the midrange frequency (around 5 kHz) increases rapidly, followed by a gradual decrease on all frequencies up to 80.000 seconds. The largest frequency dependency appear to happen in the mid- and low-range frequencies (below 10 kHz). For $\varepsilon$" (figure 7d), the trend appears to be more drastically, where from 200 seconds a peak appears around 100 Hz, and shifts to 5 kHz at 1500 seconds and shifts back to 100 Hz again at 10.000 seconds, after which the signal decreases again.

From 20.000 seconds on the sorption of water and (molecular) processes stabilizes. But between 0-20.000 seconds obviously multiple processes are taking place, due to the fact that, for various frequencies (from 50 Hz to 1 kHz) the signal first increases, then decreases, increases and finally decreases again.

For both $\varepsilon$' and $\varepsilon$" the two peaks appear, albeit that for $\varepsilon$" it is more pronounced, therefore $\varepsilon$" is used for further modelling of the data.

Both peaks are frequency dependent, as can be seen in figure 6b; for increasing frequencies it can be seen that both peaks decrease in height. Also the 1st peak moves to the right (starting from 154 seconds until 1578 seconds), and the 2nd peak moves to the left (from 13000 seconds until 1578 seconds). Furthermore from 5 kHz both peaks have recombined and do not shift anymore with increasing frequency.

The fact that two peaks appear, implicates that the dielectric permittivity somehow has to decrease in time. The decrease in signal, could be caused by several possibilities; either water is being squeezed out, the absorbed water forms clusters with hydrophilic regions that have a dielectric permittivity lower than water, or the freedom of movement of the polymer is restricted due to swelling (also decreasing the dielectric permittivity of water). Likely a combination of the three processes take place, since squeezing out of water is not frequency dependent; while the two other processes are. With increasing frequency the first peak moves to the right and indicates that, with increasing water uptake, the permittivity increases faster at low frequencies than at higher frequencies. The rise in the first peak can be attributed to cluster formation of water with hydrophilic regions, and relaxation and softening of the surface, and porous subsurface, layer of the coating. First at low water uptake levels the polymer is still rigid, but with increasing water level the polymer becomes more flexible and mobile.

The decrease in signal is due to a decrease of sorption of water due to surface swelling that slows down the diffusion of water through the pathway to subsurface regions. Even very low amounts of water might be squeezed out (giving a decrease of signal). Then due to increased cluster formation of water with the hydrophilic groups of the polymer, the mobility of clusters decreases and results in a decrease in signal. Remember that this only occurs for the low frequencies, the high frequencies do not monitor these processes.

From about 1550 seconds the slowing down of absorption becomes actually desorption of water, which is clearly shown for high frequencies (5 kHz and up), but not for the lower frequencies, where additional processes are monitored. Desorption of water has already been demonstrated in two previous articles[23,24] for UV (at atmospheric pressures) degraded coatings, and for several filters and membranes. Desorption occurs due to swelling and therefore decrease in size of pores, and the hydrophilic-water clusters have (with increasing time) less space to move and start to reorganize themselves into smaller clusters. The decreasing cluster size and water desorption are two processes that show either an increase in signal or decrease in signal. From 1 MHz to 5 kHz the cluster mobility is not monitored and only water desorption is detected. From 2 kHz to 100 Hz initially the process for cluster mobility dominates the water desorption and is characterized by an increasing signal. When the cluster mobility has stabilized, desorption starts to dominate and a decrease in signal is shown. A decrease of signal is not shown for 50 Hz, where the cluster mobility dominates the whole time.

An additional explanation for the rise in signal is the idea that the water is being squeezed in all directions (not only out of the polymer). This way water can penetrate to locations that are difficult to diffuse to; and show an increase in signal for the lower frequencies, either due to increase mobility due to relaxation, or the formation of hydrophilic-water clusters.

It becomes even more interesting, when a frequency sweep is shown for 100 bar and 3 days, see figure 8. It can be seen that only for

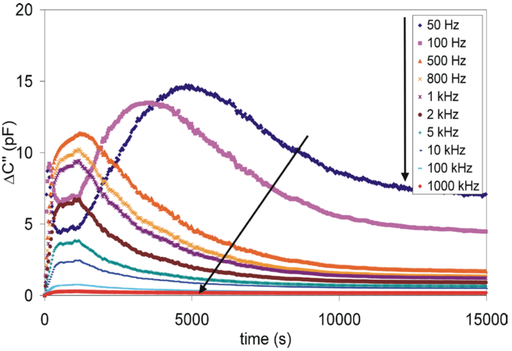

*Fig. 8 Time-frequency sweep of a DSA permittivity measurement for a 3 days UV degraded pigmented coating at 100 bar.*

50 and 100 Hz a double peak is shown (for Δ*C*''), whereas for 100 bar 15 days this is up to 2 kHz. Also the double peaks (for 50 Hz and 100 Hz) have shifted in time with increasing degradation time, for the 1st peak at 50 Hz from t = 123 s to t = 154 s, and for 100 Hz from t = 154 s to t = 154 s; and the 2nd peak at 50 Hz from t = 4800 s to t = 12000 s, and for 100 Hz from t = 3400 s to t = 9595 s. This data supports the idea that with increasing degradation times, higher frequencies start to monitor and distinguish processes between water and the polymer. It would also mean that eventually (with increasing degradation time) all frequencies could show a double peak. At frequencies where only one peak is seen, water desorption and other (molecular) processes are indistinguishable, and can be seen as a process that occurs simultaneously.

### Modelling of double peak

Fitting the two peaks give rise to some difficulties, since sorption and desorption of water occurs in time, combined with the frequency dependency of the water-hydrophilic groups, and relaxation of the polymer. Therefore a physical model to account for all these parameters is difficult to accomplish. At this moment a first, simplified, mathematical model to describe the processes is achieved by using four exponential terms, see equation (1).

$$c_1\left(e^{-a1\cdot t}-e^{-a2\cdot t}\right)+c_2\left(e^{-b1\cdot t}-e^{-b2\cdot t}\right) \tag{1}$$

The parameters $c_1$ and $c_2$ are permittivity constants to obtain the correct height of $\Delta\varepsilon$"; $a_1$, $a_2$ ($b_1$, $b_2$) are relaxation terms ($s^{-1}$) for the first peak (second peak), which are correlated to each other and $a_1 > a_2$ ($b_1 > b_2$); $t$ is time (s).

Equation (1) is only used to show that the two peaks can be mathematically described by two separate exponential peaks. Although both first exponential terms ($\exp(-a_1 t)$ and $\exp(-b_1 t)$) have no significant meaning, besides of course describing the increasing signals for peak 1 and 2 (when subtracted from the second exponential terms ($\exp(-a_2 t)$ and $\exp(-b_2 t)$); the second exponential terms ($\exp(-a_2 t)$ and $\exp(-b_2 t)$) give an estimation of the rate of swelling and relaxation ($a_1$ and $b_1$) of the polymer and therefore a rate of desorption of water for peak 1 and 2.

The used model (1) is only to illustrate the existence of two separate peaks which, when added, can actually fit the DSA signal; therefore only the 1 kHz curve is fitted for demonstration. The result of fitting a 1kHz ($\Delta\varepsilon$" vs $t$) with equation (1) is shown in figure 9, and illustrates that the two peaks can be quite accurately fitted with four exponential terms, with $c_1 = 4$, $c_2 = 1.27$, $a_1 = 0.002\ s^{-1}$, $a_2 = 0.001\ s^{-1}$, $b_1 = 0.00052\ s^{-1}$ and $b_2 = 0.00035\ s^{-1}$.

For the higher frequencies (5 kHz-1 MHz) the decrease in the permittivity signal is attributed to the desorption of water only, therefore this process can be fitted with only one exponential term; $c_3.\exp(-b_3.t)$, where $c_3$, $b_3$ and $t$ represent the same parameters as $c_2$, $b_2$ and $t$ in equation (1). Figure

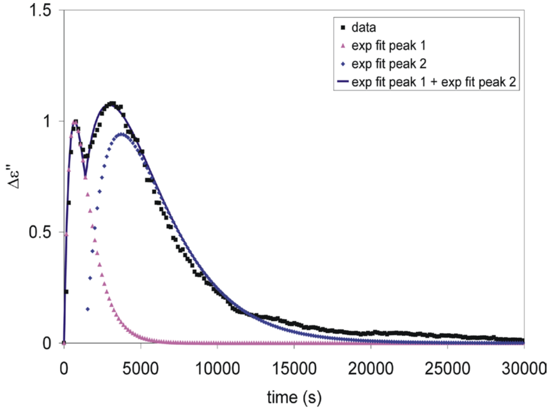

*Fig. 9 Exponential model fit of DSA permittivity measurement at 1 kHz for 15 days UV degraded pigmented coating at 100 bar.*

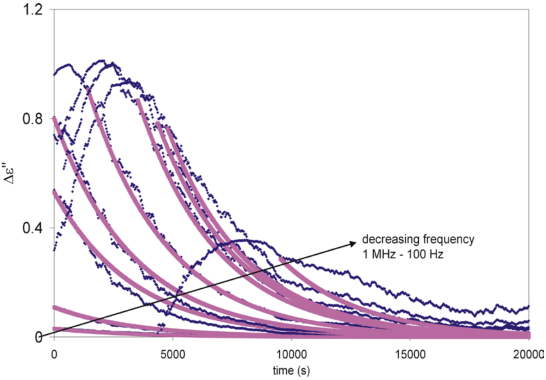

*Fig. 10 Single exponential term fit for DSA permittivity measurements at all frequencies for 15 days UV degraded pigmented coating at 100 bar.*

10 shows the fitting of the dielectric signal, due to desorption of water for all frequencies (except 50 Hz, since it is a straight line), with one exponential term. For all frequencies the same relaxation term has been used ($b_3 = 0.0003\ \mathrm{s}^{-1}$), except the multiplication term ($c_3$) increases with increasing frequencies (from 1 MHz-50 Hz, $c_3 = 0.0305; 0.109; 0.55; 0.8; 1.39; 2.5; 2.9; 3.2; 5; -$). The increase of $c_3$ with decreasing frequencies is likely a result of increased non-ohmic conduction[28].

For the higher frequencies the process is well described by an exponential term, and solely due to water desorption. For lower frequencies though a misfit can be seen, first of all by the appearance

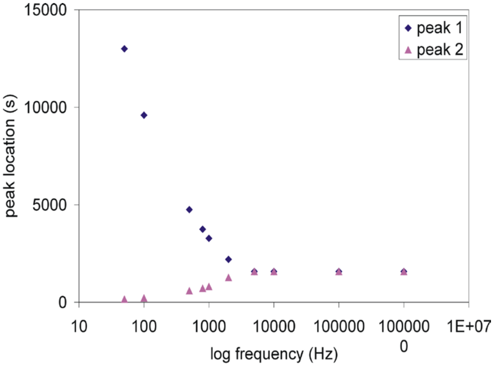

*Fig. 11 Single and double peak shifting in time at various frequencies, for 15 days UV degraded pigmented coating at 100 bar.*

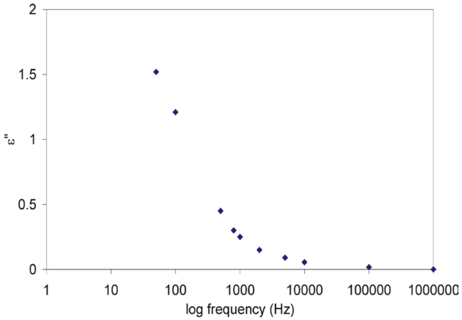

*Fig. 12 Saturation values at t=80.000 seconds for DSA permittivity measurements at all frequencies for 15 days UV degraded pigmented coating at 100 bar.*

of the peak earlier described. This misfit for lower frequencies indicates that other molecular processes take place (start to dominate) besides desorption of water.

The shifting of both peaks is shown in figure 11, and it appears (a little more clear for peak 1) that below 500 Hz the curve start to deviate from the linear behaviour found between 5 kHz to 500 Hz; and eventually both peaks combine from 5 kHz up to 1 MHz. This supports the idea that with frequencies between 5 kHz and 1 MHz only water (frequency independent) is probed, between frequencies of 2 kHz and 500 Hz water and molecular processes; and below that the molecular processes dominate (frequency dependent).

For longer times (above 20.000 seconds) it can be seen in figure 6b that the signal eventually stabilizes. The values of this stable signal are plotted against frequency (figure 12) and it shows a clear increasing (permittivity) signal with decreasing frequency. Of course the same trend can be found in figure 7d at $t = 80.000$ seconds. This dependency is similar to the increase of $c_3$ with decreasing frequency, already described in previous section. This increase in signal can not be attributed to electrode polarization, because a much higher increase in $\varepsilon'$ or $\varepsilon''$ should take place. Most likely, the increase in signal is due to non-ohmic conduction or polarization at inner boundaries[28].

## 6.4 Conclusions

Pressure can be considered as an accelerating parameter for coating degradation with an UV source; since it is clearly demonstrated that, with increasing pressures, an increasing water sorption behaviour can be found by DSA. A linear trend is found for this intensity up to 50 bar and at higher pressures the signal then saturated to a stable level. This acceleration effect is caused due to higher concentration, and increased activity (air is compressed, resulting in a higher energy level) of oxygen present in the polymer matrix and the surface. The idea is that the abovementioned saturation level can be shifted to higher pressures (higher than 50 bar) by increasing the intensity of the UV source.

Furthermore the effect of pressure is convincingly demonstrated when the DSA measurements are compared between a 1 bar 40 days and a 100 bar 1 day UV degraded sample; which shows that the effect of water sorption is much larger. With increasing times of UV degradation (at 100 bar) a linear trend up to 15 days is found. It is believed that this linear trend can not increase indefinite, because the UV degradation occurs only at the surface and top layer of the coating, and not throughout the whole coating.

The dielectric signal monitors only the desorption of water at high frequencies; whereas at lower frequencies also molecular processes can be detected. With increasing degradation times the DSA measurement is able to distinguish between water desorption, molecular processes (which evidently plays a role for the occurrence of desorption) and water interactions; which gives rise to the double peak in DSA measurements at lower frequencies. For shorter degradation times this double peak is also present, but they overlap.

The rise in the first peak can be attributed to cluster formation of water with hydrophilic regions, relaxation and softening of the surface, and porous (sub) surface layer of the coating. After a short time the pathway to subsurface regions becomes more difficult due to surface swelling, and the rate of sorption of water decreases. Water might be squeezed out at low levels by surface swelling, but also in the mean time the cluster size of water with hydrophilic groups of the polymer increases; slowing down the mobility and therefore decreasing the dielectric permittivity.

Desorption is caused by a decrease in size of pores due to polymer matrix swelling. Reduction in pore size means that also the hydrophilic-water clusters have (with increasing time) less space to move. In effect, the once increasing cluster sizes now start to redistribute, and smaller cluster sizes is the result with higher mobility. The increased mobility and desorption are two processes that show either an increase in signal or decrease in signal and can be monitored, dependent with which frequency is being measured. From 1 MHz to 5 kHz the increased mobility was not monitored and only the desorption was detected. From 2 kHz to 100 Hz initially the increasing mobility dominates the desorption was characterized by an increasing signal, after which the desorption dominates, showing a decrease in signal. Whereas for 50 Hz the increasing mobility dominates the whole time.

A first simplified mathematical model is used to show that the two peaks can be fitted by two curves, both represented by two exponential terms.

Fitting only the decreasing signal of the 2nd peak shows that, when a constant relaxation term is used, all curves can be fitted. Higher frequencies results in a good fit, indicating that only water desorption is monitored (and is negligible for molecular influences), but lower frequencies displays a less good fit due to effects by molecular processes.

After t = 80.000 seconds a stable and saturated value is achieved. This value increases with decreasing frequency, and likely non-ohmic conduction occurs. To account for the conductivity, Johnscher[28] or the continuous-time-random walk approximation[28] can be used for this, but lower frequencies are necessary for this and are for future measurements, since the current device is not able to reach these low frequencies.

The effect of pressure and duration of degradation is clearly demonstrated by DSA measurements. The DSA has proven to be quite adequate to measure, non destructively, differences in degraded polymer coatings.

In order to get a clear understanding behind all physical / chemical processes occurring during water sorption on degraded coatings, it would be desirable that the processes can be separated. By trying to understand these processes individually, models can be derived for each separate process. Finally by combining all models a best fit can be made to get an idea in which ratio each process has an influence on the dielectric signal. This means that the sorption / desorption of water, relaxation and swelling of the polymer, and the formation of hydrophilic-water clusters should be individually investigated.

One way to attempt this is to perform temperature and frequency sweeps, during sorption of water in time. Temperature sweeps are interesting because then the relaxation terms can be determined. However, this implies that the DSA device should be upgraded for such purposes, which is left for future work.

## References

1. Johnson B.W. and McIntyre R., Progr. Org. Coat., 27, (1996), 95-106.
2. McEwen D.J, Verma, M.H., and Turner R.O., J. Coat. Techn., 59(755), (1987), 123-129.
3. Association of automobile industries, J. Coat. Techn., 58(734), (1986), 57-63.
4. Martin J.W., Progr. Org. Coat., 23, (1993), 49-70.
5. Shah C.S, Patni M.J., and Pandya M.V., Polymer Testing, 13, (1994), 295-322.
6. Sims J.A., J. Coat. Techn., 59(748), (1987), 45-53.
7. Martin J.W, Nguyen T., Byrd E., Dickens B., and Embree N., Pol. Degr. and Stab., 75, (2002), 193-210.
8. Bauer D.R., J. Coat. Techn., 74(924), (2002), 33-38.
9. Sherbondy V.D: in Koleske J.V. ed.; Paint and corrosion testing manual, (1995), 643-653.
10. Burroughs W.J., Weather cycles: real or imaginary?, (1994).
11. Scott J.L., J. Coat. Techn., 49(633), (1977), 27-36.
12. Brennan P. and Fedor C. Sun, ultraviolet and accelerated weathering, (1995), 85-93.
13. Schulz U., Trubiroha P., Schernau U., and Baumgart H., Progr. Org. Coat., 40, (2000), 151-165.
14. Colin X., Marais C., and Verdu J. A, Polymer Testing 20, (2001), 795-803.
15. Gu X., Rahavan D., Nguyen T., VanLandinham M.R., and Yebassa D., Pol. Degr. Stab., 74, (2001), 139-149.
16. Dubois C., Monney L., Bonnet N., and Chambaudet A., Composites: Part A 30, (1999), 361-368.
17. Kotnarowska D., Progr. Org. Coat., 37, (1999), 149-159.
18. Vink P., Koster T.P.M., Fontijn H.F.N, and Mackor A., Pol. Degr. Stab., 48, (1995), 155-160.
19. Botelho G., Queirós A., and Gijsman P., Pol. Degr. Stab., 73, (2001), 431-435.
20. Seguchi T., Hashimoto S., Arakawa K., Hayakawa N., Kawakami W., and Kuriyama I., Radiat. Phys.Chem. 17, (1981), 195-201.
21. Tsotsis T.K., Keller S., Bardis J., and Bish J., Pol. Degr. Stab., 64,(1999), 207-212.
22. Giacomelli Penon M., Picken S.J., Wübbenhorst M., de Vos G., and van Turnhout J., Rev. Sci. Instrum., 77, (2006), 115107.
23. Giacomelli Penon M., Picken S.J., Wübbenhorst M., and van Turnhout J.,.

Pol. Degr. Stab., **92**, (2007), 1247-1254.
24. Giacomelli Penon M., Picken S.J., Wübbenhorst M., and van Turnhout J.,. J. Appl. Pol. Sci., **105**, (2007), 1471-1479.
25. Henry W., Phil.Trans., 93, (1803), 274-276.
26. Tammann G. and Bochow K., Z. Anorg. Chem., (168), (1927), 322-324.
27. Newitt D.M. and Weale K.E., J. Chem. Soc., (1948), 1541-1549.
28. A.Schönhals and F.Kremer: in F. Kremer and A. Schönhals eds.; Broadband Dielectric Spectroscopy, Springer (2003), 59-96.

# Chapter 7

## WATER SORPTION IN UV DEGRADED NANOCOMPOSITE ALKYD COATINGS BY DIELECTRIC SORPTION ANALYSIS

### 7.1 Introduction

Automotive coatings have come a long way in the past few decades. Lower costs, reduced air pollution and better performance continue to be the key drivers in automotive coatings. Reduced air pollution can be achieved by using high solid coatings, powder coatings or water borne coatings. Lately more focus has been given to water borne coatings, since high solids are generally more viscous and powder coatings cannot be applied in all cases. For property enhancement the use of nanoparticles has been an interesting development, which resulted in the term nanocomposites. As nanoparticle, clay has become an interesting ingredient, and has been investigated on its benefits. With clay particles the colloidal stability, mechanical properties, thermal stability and flame retardancy of the coating improved[1-12]. Furthermore a low percentage of clay resulted in better anti-corrosive properties than without them[2]; and can be explained by the fact that clay particles enhance the molecular barrier property for water and oxygen. Clay particles are disk shaped, thus it is thought that they increase the tortuosity of the diffusion pathway.

Besides improvement of the mechanical properties, also the weathering resistance is an important parameter. Weathering (up to 4800 hours) of UV cured polyurethane-acrylic coatings and UV curing of waterborne acrylate coatings (with and without stabilizers) have been studied by Decker et. al.[13,14]. They showed that with stabilizer at least 2000 hours was necessary to see a small difference (FTIR); without stabilizer about 8 hours (at 70 ºC and 100% humidity) was necessary to find yellowing of the coating. He et. al.[15] investigated acrylic coatings with $TiO_2$ and nano-$TiO_2$ and found that nano-$TiO_2$ was an excellent shield for UV light. Furthermore Morrow[16] saw that degradation occurs around the particles (acrylic coating with silica particles).

However, to our knowledge, no research can be found on water sorption for short (up to 40 hrs) UV degraded samples (acrylic resin), and with different amounts of clay particles (laponite, 0-6%). Short term UV degraded samples will be examined in this paper with the DSA set up; and the sensitivity of the DSA will be probed, and compared with ATR-FTIR, UV-VIS and contact angle measurements. Detecting quantifiable changes at low degradation times is useful for life time prediction of coatings, and performance of different coating systems, in an early time frame; making it possible to increase the pace for coating development.

From the preliminary results it will become clear that with ATR-FTIR, contact angle measurements and UV-VIS, no differences can be found between coatings with different amount of clay particles. The DSA however, is able to detect sorption differences between % of clay and increasing degradation. Fitting full sorption curves to calculate diffusion coefficient values do not show large differences or a clear trend. But by fitting short time sorption curves, clear differences were found. The best method was to calculate the slope of the initial sorption curve, when the data was plotted on a log-log scale. Clear trends were found for increasing degradation times, and increasing % of clay particles.

Furthermore, to calculate the amount of water uptake, two different models, Brasher and Kingsbury and Landau, Lifschitz, Looyenga (LLL), have been used. Only one model appeared to give reliable values.

## 7.2 Experimental

### 7.2.1 Preparation of nanocomposite coating

The acrylic resin (Setalux 6768 AQ-40) bought from Akzo-Nobel BV, was used as top coat for metal. The Laponite clay particles (Districhem B.V.) were high-shear stirred into the polymer resin at high speeds, as this was the easiest way of exfoliation, very fast and cost effective. 0, 2, 4 and 6 weight percentages of total solids content coatings were made. Coatings above 6 wt% of solid content showed cracking when dried, hence it was decided no more than 6 wt% of solids should be used. More detailed information concerning preparation of the nanoparticle coating solution can be found in ref. 17.

The solutions were applied on to a PP plate using a doctor blade applicator with 250 micrometer gap and left to cure in air for 1 week.

Then they were degassed in an oven at 80 ºC for 24 hours and dried in a nitrogen ($N_2$) box for 24 hours. The coatings were then carefully pealed off. The thickness of the free-standing films ranged from 25-60 micrometer.

### 7.2.2 UV degradation of nanocomposite coating

The samples have been degraded with a Philips PL-S UV lamp (9 W) at a distance of 10 cm, at room temperature. The spectrum of this lamp is given in a previous article[18]. The samples are rotated around the lamp, to assure that all samples receive the same amount of radiation.

### 7.2.3 Expansion measurements

Swelling is an interesting parameter for nanocomposites with different % of clay (besides the fact that it has minor affects on dielectrical measurements); therefore the increase in thickness was measured using a Linear Variable Differential Transformer (LVDT) coupled to a Keithley ® multi-meter. The same amount and rate of humidity was supplied as the DSA measurements. The dry flow was gaseous nitrogen (2% RH at 27 ºC) and the "wet" flow was humidified gaseous nitrogen (86% RH at 27 ºC), with a flow speed of 7 ml/s.

### 7.2.4 DSA measurements

DSA measurements were performed to investigate the water vapor sorption behavior of the coatings at various clay % and degradation times. The measurement technique is based on measuring real time the dielectric value of the coating during water vapor uptake. More information concerning this device can be found in a previous article[19,20]. The parameters concerning the gas and flow are mentioned in section 7.2.3 (expansion measurements). A Hewlett Packard (HP 4284A precision LCR meter) frequency analyser, with a frequency range between 20 Hz until 1 MHz, was used for frequency sweeps.

The DSA measurements were performed with the same procedures, and parameters, as previous articles[19,20]; except for one detail. Degraded (20 hours of degradation) nanocomposite coatings tended to stick to the top electrode and causes the measurement to fail due to excessive noise. Short chain polymers are created due to scissoring by UV degradation near the surface of the coating, and humidity causes the short chain polymers to soften (lowering of Tg) and start to stick to the top electrode. The top electrode sticking was prevented by using a 20 micrometer (aluminum) spacer.

### 7.2.5 Contact angle measurements

Contact angle measurements were performed with a Kruss (GmbH, Hamburg) contact angle instrument. The measurements were done at room temperature (20 °C) by using a sessile drop technique. The sessile drop method is an optical contact angle technique used to estimate wetting properties of a localized region on a solid surface. The angle between the baseline of the drop and the tangent at the drop boundary is measured. The angle was measured against an illuminated background using the optical protractor. On every sample six different spots were measured and difference from the average value was no more than 5 degrees. The measuring liquid used was milli Q® water.

### 7.2.6 Ultra Violet – (Visible) spectroscopy (UV-VIS)

The absorbance and transmission spectra of the films with and without nanoparticles, and degraded and un-degraded, in the range of 200 to 700 nm were determined using an UVICON-XL (Bio-tek instruments) spectrometer.

### 7.2.7 Attenuated Total Reflectance – Fourier Transformed Infrared spectroscopy (ATR – FTIR)

A Thermo Nicolet Nexus 470 FT-IR Spectrometer (bench) fitted with a Continuum infrared microscope was used for ATR-FTIR spectroscopy. Selected peak areas were measured using the Omnic programme, also from Thermo-Nicolet. Exactly the same wave number points were used every time on each spectrum to obtain the peak area.

The graphs were then used to evaluate the effect of UV degradation on the films. The wavenumber of interest was 1725-1700 cm$^{-1}$, which is related to the C=O stretch and is an indication of the amount of de-esterification of the alkyd coating.

## 7.3 Results

### 7.3.1 Expansion measurements

It was found that the swelling for virgin films were between 1.5 to 3.4%, these values are negligible for the DSA measurements. The initial thickness of the coatings was measured and an average was used. It is interesting to note that the swelling decreases with solid content (figure 1), and although this is not in the scope of the project, the decreasing swelling could help the adhesion of the coatings to the substrates. The expansion curves are also shown in figure 2. The expansion curves have the same shape as that of the DSA curves, and for future research it would be interesting to see whether these curves coincide with DSA curves. Worth mentioning is that no differences could be found for expansion measurements between undegraded and degraded samples.

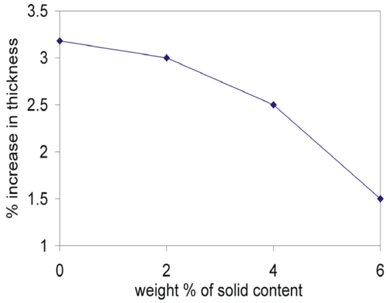

*Fig. 1 Variation of film swelling with increasing % solid content.*

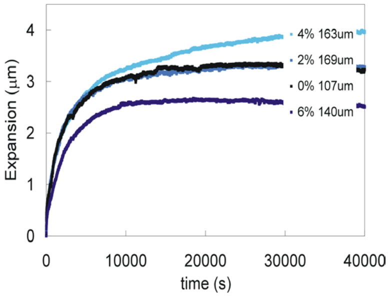

*Fig. 2 Expansion curves measured with a LVDT (0-6%).*

## 7.3.2 DSA measurements

### 7.3.2.1 DSA measurements on undegraded nanocomposite coatings

DSA results for the 0% and 4% nanocomposite coatings are shown in figure 3a-d. It can be seen that for both clay percentages the height of the dielectric signal increases with decreasing frequency. For higher clay percentage the 1 kHz signal increases (both Δ*C*' and Δ*C*") even more than 0% clay, and is likely the result of the charged layers of laponite causing an increase in dielectric signal due to polarization[18]. Polarization is caused due to the negative charged layer and attracts the positive polar side of the water to counter charge. Due to this interaction, ionic movement occurs at lower frequencies. Normalizing the frequency sweeps (figure 4a-d), gives an indication whether the water interacts with the coating or clay particles. 0% clay results in an almost perfect overlap and little to no interaction is taking at various frequencies. For 4% a small difference is found between frequencies and interaction is taking place (during the water uptake) of water with the (charged) clay particles. A

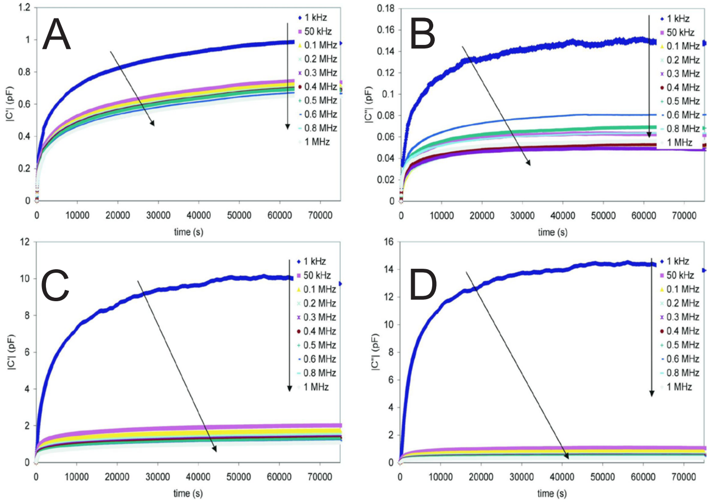

*Fig. 3a ΔC' vs t for 0% acrylic coating undegraded.*
*Fig. 3b ΔC" vs t for 0% acrylic coating undegraded.*
*Fig. 3c ΔC' vs t for 4% acrylic coating undegraded.*
*Fig. 3d ΔC" vs t for 4% acrylic coating undegraded.*

possibility is that water is being attracted to these nano-particle sites, causing this interaction.

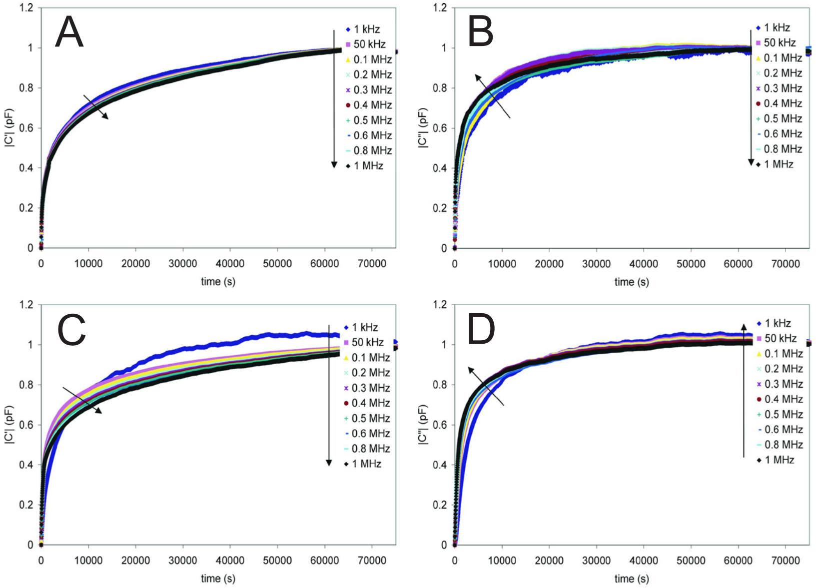

*Fig. 4a* *|C'| vs t for 0% acrylic coating undegraded.*
*Fig. 4b* *|C"| vs t for 0% acrylic coating undegraded.*
*Fig. 4c* *|C'| vs t for 4% acrylic coating undegraded.*
*Fig. 4d* *|C"| vs t for 4% acrylic coating undegraded.*

### *7.3.2.2 DSA measurements on degraded nanocomposite coatings*

Figure 5a-d shows the DSA measurements for 0 and 4% nanocomposite, degraded for 20 hours under a UV lamp. After 20 hours a decreasing signal is shown for Δ*C*' (4%, 1kHz, and 6% [not shown]) and for Δ*C*"(0% 1 kHz, and 2% [not shown]). So the decreasing signal changes from 0-2% for Δ*C*' to 4-6% for Δ*C*". The reason for this decreasing signal is unclear and needs further investigation in the future. Possibly the signal decrease change from Δ*C*' to Δ*C*", after 20 hours of UV degradation, is related to the interaction of clay particles with the water and degraded polymer material around these clay particles.

Figure 6a-b show the results of 0 and 4% degraded from 0 to 20 hrs. For 0% the water sorption increases with longer degradation times. For 4% the same trend is found, with exception of 10 hrs of degradation. The initial slope of the 10 hrs degradation curve (figure 6a, 1 kHz) shows a higher increase than 0-5 hrs degradation, but the after about 2000 seconds the sorption rate decreases below that of 0-5 hrs. This slower sorption rate could be related to the swelling/ collapse of the resin[21], causing a slower and lesser increase in water uptake.

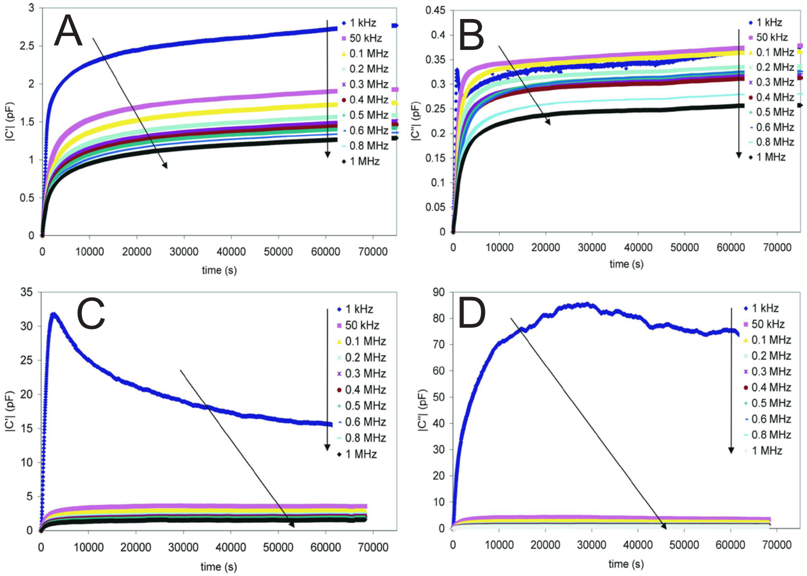

*Fig. 5a* $\Delta C'$ *vs t for 0% acrylic coating degraded 20 hrs.*
*Fig. 5b* $\Delta C''$ *vs t for 0% acrylic coating degraded 20 hrs.*
*Fig. 5c* $\Delta C'$ *vs t for 4% acrylic coating degraded 20 hrs.*
*Fig. 5d* $\Delta C''$ *vs t for 4% acrylic coating degraded 20 hrs.*

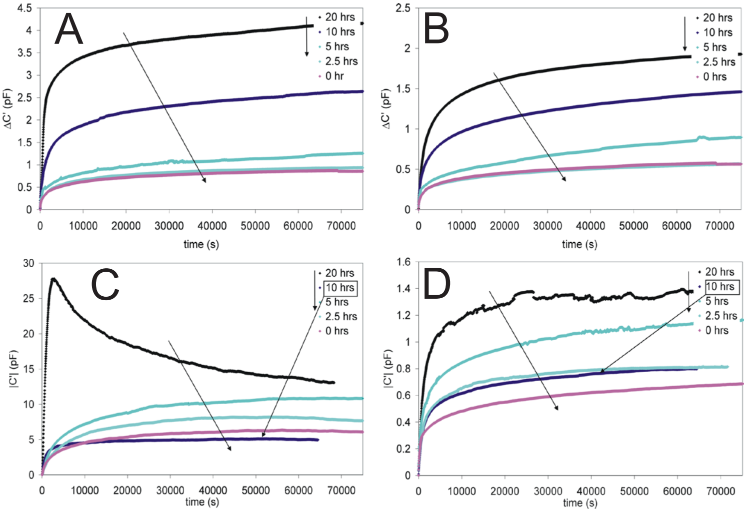

*Fig. 6a* *$\Delta C'$ vs t for 0% acrylic coating (0-20 hrs degraded) at 1 kHz.*
*Fig. 6b* *$\Delta C'$ vs t for 0% acrylic coating (0-20 hrs degraded) at 1 MHz.*
*Fig. 6c* *$\Delta C'$ vs t for 4% acrylic coating (0-20 hrs degraded) at 1 kHz.*
*Fig. 6d* *$\Delta C'$ vs t for 4% acrylic coating (0-20 hrs degraded) at 1 MHz.*

### *7.3.2.3 Calculation of % of water uptake*

The water uptake of the undegraded and degraded samples is shown in figure 7a-b. Two models were used for this: Brasher-Kinsbury (BK)[22] and LLL model[19] and are given in equation 1 and 2.

$$\Phi = \left( \frac{\log\left( C_t \big/ C_0 \right)}{\log 80} \right) \tag{1}$$

$$\varepsilon_t'^{1/3} = \nu_w \cdot \varepsilon_w'^{1/3} + (1-\nu_w)\cdot \varepsilon_d'^{1/3} \tag{2}$$

For equation 1, $\Phi$ is the volume fraction of water absorbed by the film, $C_t$ the capacitance (pF) of film at any time $t$, $C_0$ the capacitance (pF) of dry film (at time $t = 0$) and *80* is permittivity of water.
For equation 2, $\varepsilon_t'$ is the total dielectric permittivity of the saturated signal, $\varepsilon_w'$ the dielectric permittivity of water (assumed to be *80*), $\varepsilon_d'$ is the dielectric permittivity of dry coating and $v_w$ the volume fraction of water at saturation.

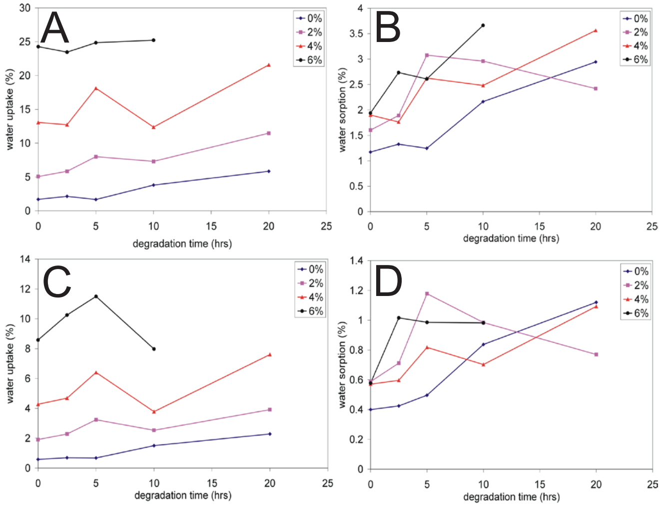

*Fig. 7a Water uptake(%) vs degradation time (0-6% clay), Brasher-Kingsbury, at 1 kHz.*

*Fig. 7b Water uptake(%) vs degradation time (0-6% clay), Brasher-Kingsbury, at 1 MHz.*

*Fig. 7c Water uptake(%) vs degradation time (0-6% clay), LLL, at 1 kHz.*

*Fig. 7d Water uptake(%) vs degradation time (0-6% clay), LLL, at 1 MHz.*

As comparison both figures are given for 1 kHz and 1 MHz, to display the frequency effect. For the Brasher-Kinsbury (or LLL) equation, no restriction for the frequency is required[23], as long as $\varepsilon$ for water is equal to 80. This is true when there is no interaction between water and the resin, or no polarization occurs for lower frequencies. For nanoclay filled alkyd water-nanoparticle-resin interaction seems to occur, due to the to the presence of the charged clay particles. Polarisation effects and resin interaction are neglegible at higher frequencies, therefore 1 MHz (and higher frequencies) seems to be the correct frequency to use to calculate the percentage of water uptake.

When the two models are compared with each other (1 MHz) another discrepancy is found, the LLL model is systematically too low compared to BK. The water uptake for acrylic coatings are according to the literature about 2 wt%[24] and therefore the Brasher Kinsbury model is the correct one in this case. In another article[19] the LLL model was used, and it becomes clear that one has to be careful which model to use; which was already discussed by Bosma[25]. An important observation is that there is a clear trend for all compounds, that with increasing degradation time the sorption of water also increases, independent of the chosen model or clay %.

### *7.3.2.4 Sorption models*

#### *Model 1*

The diffusion coefficient has been calculated by using equation (3). The

$$M_t = M_{\infty,F} \cdot \left(1 - \frac{8}{\pi^2}\sum_{n=0}^{\infty}\frac{1}{(2n+1)^2}\exp\left(-(2n+1^2)\frac{\pi^2 Dt}{4d^2}\right)\right) + \sum_i M_{\infty,i}\left[1-\exp(-k_i t)\right] \quad (3)$$

first term is the Fickian diffusin term and the second term is the additional gradual uptake brought about by the long-term relaxation of the sample due to structural rearrangements induced by water.

$M_t$ is the weight increase in time, $M_{\infty,F}$ is the equilibrium amount of sorption in the unrelaxed polymer [mg/g], $d$ the half thickness [m], $D$ the diffusion coefficient [$m^2s^{-1}$], $t$ the time [s], $M_{\infty,i}$ the equilibrium sorption of the ith relaxation process [mg/g], and $k_i$ the relaxation rate constant of the ith relaxation process [$s^{-1}$].

This equation has already been used in previous articles[18-20] for DSA measurements. In figure 8a-b the diffusion coefficient trend is shown with increasing degradation times for 1 kHz and 1 MHz. As can be seen, 1 MHz results in an unclear trend (besides 0%,). Only 1 kHz shows an increasing trend for longer degradation times and higher % clay particles. Possible explanation for the fact that 1 kHz does result in a trend, and

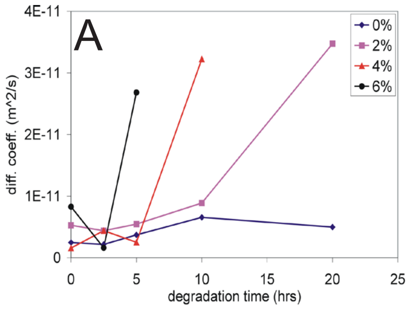

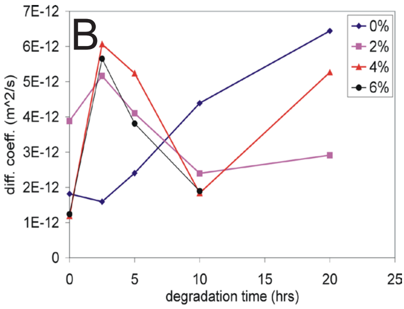

*Fig. 8a Diffusion coefficient vs degradation time (0-6% clay) at 1 kHz.*

*Fig. 8b Diffusion coefficient vs degradation time (0-6% clay) at 1 MHz.*

1 MHz not, is that the lower frequency range is sensitive for water interactions with the resin-clay particles.

However, to investigate short term degradation it is not necessary to fit the total sorption curve, and calculate a diffusion coefficient. The initial slope, and in this case particularly the first 1000 seconds, should be sufficient to find a trend.

*Model 2*

Balik[26] already found another way to calculate the diffusion coefficient, which is given in in equation 4, for $a$=½.

$$M_t = M_\infty \frac{4}{d}\left(\frac{Dt}{\pi}\right)^a \tag{4}$$

$M_t$ is the weight after time $t$ (g), $M_\infty$ is the weight after infinite time (g), $d$ is the thickness of the coating (m) and in a previous article[19] it was found that $M$ can be substituted for ΔC', $D$ the diffusion coefficient (m$^2$/s), $t$ the time (s) and for $a=1/2$ we have Fickian diffusion. Now by simply plotting the sorption curves in $t^{1/2}$ the slope can be calculated and used in equation 4. When the sorption curves are plotted in $t^{1/2}$ , the first 100 seconds resulted in a straight line (for both 1kHz and 1MHz), followed by a second straight line with a different slope from 100 to 1000 seconds (figure 9). Above 1000 seconds the straight line started to deviate. It seems that the first 100 seconds is either the stabilization time of the set up, or surface effects of the film that causes a different diffusion profile in the first seconds. This due to the fact that when the slope values are

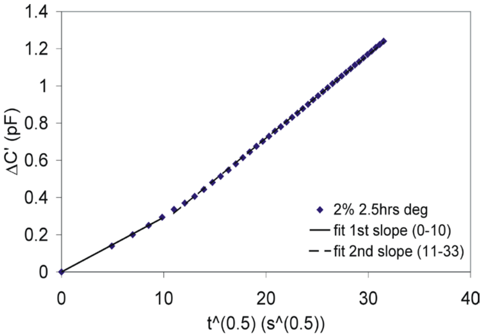

*Fig. 9 ΔC' vs $t^{1/2}$ for 2% acrylic coating (2.5hrs degraded) at 1kHz, showing slope difference between 0-32 $s^{1/2}$.*

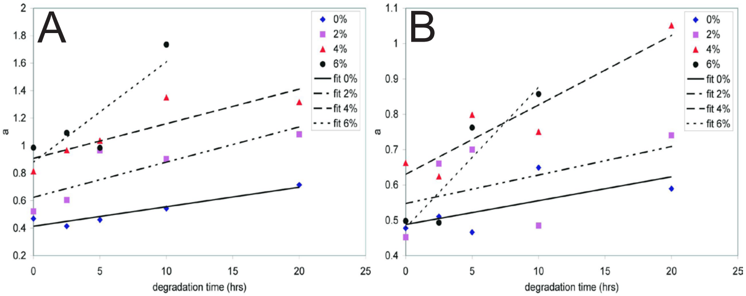

*Fig. 10a Logarithmic diffusion coefficient (2nd slope fit) vs degradation time (0-6% clay) at 1 kHz, and its exponential fit.*
*Fig. 10b Diffusion coefficient (2nd slope fit) vs degradation time (0-6% clay) at 1 MHz, and its linear fit.*

compared with each other of the first slope (0-100 seconds), no trend could be found between the different samples. The second slope, however, does show a trend with increasing degradation times; and also with increasing % of clay particles, as shown in figure 10a-b. Increasing the degradation time results in higher diffusion coefficients, which is the result of higher hydrophilicity, and more cavities caused by scissoring of the resin. Since the clay particles have affinity for polar particles, the water has easier access to them after degradation, resulting in a higher diffusion coefficient. Also in an article[15] it has been mentioned that clay particles are UV absorbers. Therefore, it it might be possible that the bonding between resin and clay particle are affected during UV degradation. This causes a higher water uptake with increasing % of clay particles with the same amount of UV degradation. For 0 and 2% (1 kHz) it seems that there is a linear trend with increasing degradation time, whereas for 4 and 6% (1 kHz) it started to deviate into a more exponential shape (the figure (10a) has been plotted on an exponantial axis). For 1 MHz there is a linear trend for 0-6%, but there is no trend with increasing % of clay. The results do not give clear trends and therefore a different approach was applied, described in model 3.

### *Model 3*

Another way of approaching the initial slope, is by calculating the slope when the data are plotted on a log-log scale. For this the

following empirical relation was used, $C_t'=Kt^{a.}$, where $C_t'$is the dielectric permittivity (F), $t$ is the time in (s), $K$ is a constant and a the scaling exponent. The scaling exponent $a$ can be calculated by plotting the initial sorption curves logarithmic and fitting the slope. When the fitted curve results in a slope $a=½$ normal Fickian diffusion takes place. The slope is calculated from 0-400 seconds and in this case no slope deviation was found between 0-100 seconds and 100-400 seconds; above 400 seconds non-linear deviations where found for higher degradation times.
In figure 11a-b the slope values (a) are shown graphically. From 0-4% (undegraded) the values increase from 0.5 to 1 (1 kHz) and for 1 MHz they are about 0.5, but 4% deviates (0.66), which is likely a deviation. The 1 MHz data shows that interaction between clay particles and water is not measured, which is the case for 1 kHz. If only the sorption of water is being investigated for this system, and not the interaction, 1 MHz frequency should be used. For UV degraded coatings (fig. 11a-b), it can be seen that for longer degradation times the diffusion profile changes in a linear trend from Fickian (0.5) to a more frontal (=1), showing that water penetrates the degraded coating more easily (as well for 1 kHz as 1 MHz). Interestingly, for 1 kHz and 1 MHz, with increasing clay content and degradation time the slope is also increasing which was not demonstrated by the previous model 2. This could indicate that the clay particles are UV absorbers and facilitates the water absorption for higher clay content at the same duration of UV degradation.

Figure 12a-b shows the slope values as fitted in figure 11a-b versus clay %, and in this case both 1 kHz and 1 MHz are increasing

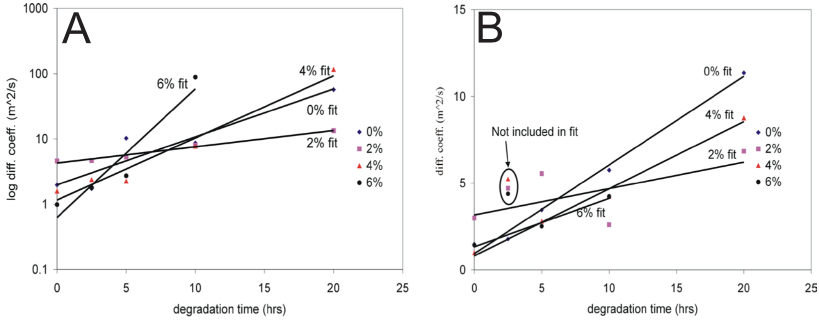

*Fig. 11a Fitted value (a) vs degradation time (0-6% clay) at 1 kHz.*
*Fig. 11b Fitted value (a) vs degradation time (0-6% clay) at 1 MHz.*

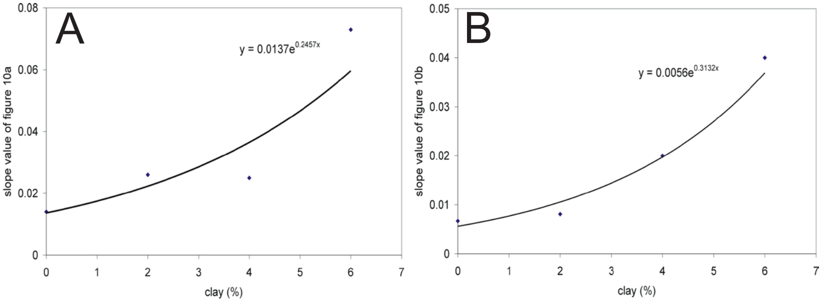

*Fig. 12a Slope values of figure 10a vs clay (%) (1 kHz).*
*Fig. 12b Slope values of figure 10b vs clay (%) (1 MHz).*

with increasing clay percentage, suggesting that, from degradation from 0 to 20 hours, the water uptake increases more with higher clay %. An exponential fit has been made and its equation is shown in figure 12a-b [inlay]. Although more values are necessary to create a reliable fit, a first impression indicates that the fitted values for 1 kHz and 1 Mhz are more or less of the same order. So out of the three models, it seems that only this model for both 1 kHz and 1 MHz a similar trend was found.

### 7.3.3 Contact angle measurements

Contact angles on polymer surfaces are not only influenced by the interfacial tensions according to Young's equation but also by many other phenomena, such as surface roughness, chemical heterogeneity, sorption layers, molecular orientation, swelling, and partial solution of the polymer or low-molecular constituents in the polymer material. Although static contact angle is no longer considered to be adequate for absolute surface characterisation, it can be taken as a comparative parameter for surface affinity for water in this project.

Variation of surface properties with respect to water affinity after UV degradation is more clearly seen in both, dielectric measurements and contact angle measurements. Decreasing contact angle shows increasing affinity of film surface towards water, as shown in figure 13. Figure 13 also shows that there are no detectable differences between clay %, which is explained by the fact that no clay particles are at the surface of the coating. The roughness of the coatings were not compared.

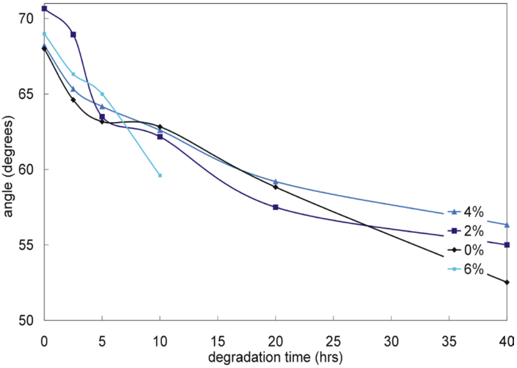

*Fig. 13 Contact angle vs degradation time (0-6% clay).*

### 7.3.4 UV-VIS measurements

First the effect of UV-VIS on solid content is investigated, followed by degraded samples.

#### *7.3.4.1 Effect of solid content: (addition of Laponite nanoparticles).*

Figure 14 illustrates the ultraviolet – visible spectra for the nanocomposite acrylic coatings and for pure acrylic coatings studied in

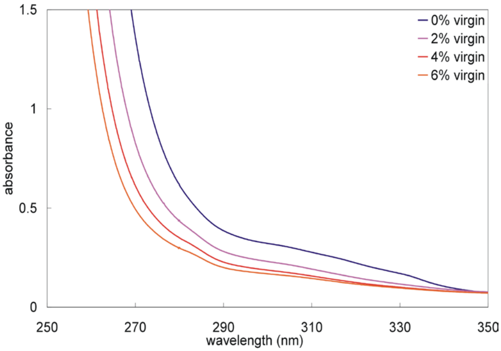

*Fig. 14 UV absorbance spectra of virgin coatings with various solids content (weight %).*

this project. The results show that there is a decrease in absorption in the region 250 to 350 nm with increasing solid content. Similar results were obtained when acrylic/nano-$TiO_2$ composite latex was prepared by the stirring and mixing[15]. However, when in situ polymerization method was used for the same acrylic/nano-$TiO_2$ composite latex, an increase in absorption was observed. This optical change was attributed to the quantum size effect of the nanoparticles. That is, when the particle size is reduced to the nanoscale, the big specific surface area makes the atoms and electrons at the surface behave differently than the particles in the interior of the coating. Under UV irradiation, the electrons are exited and transfer from the valence band to the conductance band, causing UV absorbance. Thus nanocomposites should be prepared by the in situ polymerisation technique to improve weatherability.

### *7.3.4.2 Effect of UV degradation.*

Figure 15a-d shows the effect of exposure to UV, since ‘yellowing’ of the coatings would occur because of exposure to UV irradiation. The accelerated degradation time was too short compared to studies by Decker [14] and visual observation did not show any colour changes in the degraded films. However, the UV absorption spectrum showed absorption in the range 270-300 nm, which shows that there is slight yellowing of the sample. The absorption at 300 nm is plotted against hours of degradation (figure 16a) and against weight percentage of solid content in figure 16b. Results show that no clear differences can be found between various clay%. This can be explained that yellowing is caused by degradation of the resin and not by the clay particles.

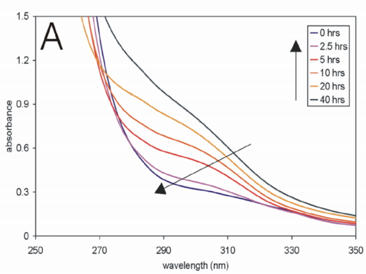

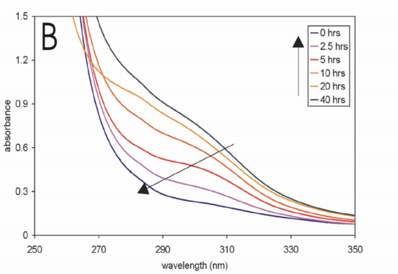

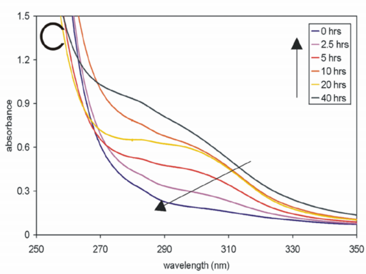

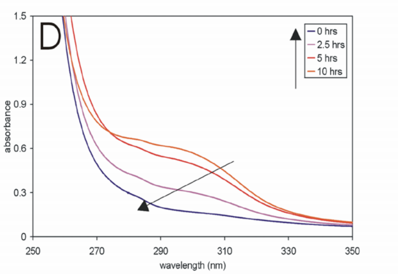

*Fig. 15a UV absorption spectra of coatings with 0% clay for various degradation times.*

*Fig. 15b UV absorption spectra of coatings with 2% clay for various degradation times.*

*Fig. 15c UV absorption spectra of coatings with 4% clay for various degradation times.*

*Fig. 15d UV absorption spectra of coatings with 6% clay for various degradation times.*

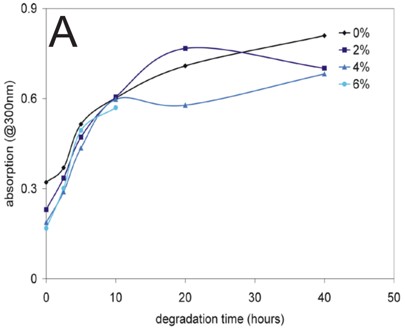

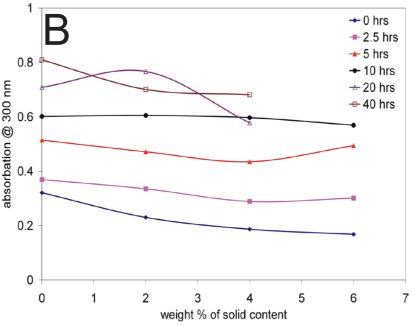

*Fig. 16a UV absorption of coatings at 300 nm. variation of absorption of 0, 2, 4 and 6 percentage solid content coatings with hours of degradation.*

*Fig. 16b UV absorption of coatings at 300 nm. Variation of degraded coatings with increasing percentages of solid content.*

### 7.3.5 ATR-FTIR measurements

Ester group (1728 cm$^{-1}$) was monitored by following the changes in peak areas. Figure 17 shows the ATR/FTIR peaks of 0 wt% samples before and after exposure to UV irradiation for various hours relative to each other.

Figure 18 shows ester change for films degraded up to 40 hours (only for 0 and 6%) and with varying contents Laponite nanoparticles. De-esterification in acrylic films may be associated with the beta scission of the ester side groups or unzipping/loss of volatile chain fragments. No differences can be seen between 0 and 6%, due to the same arguments given for the UV-VIS results.

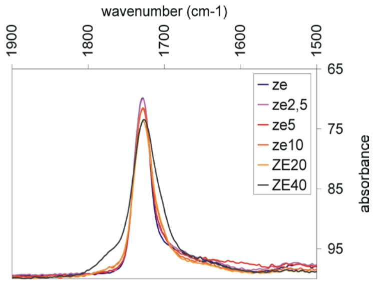

*Fig. 17 ATR-FTIR spectra of 0% clay samples at various degradation times.*

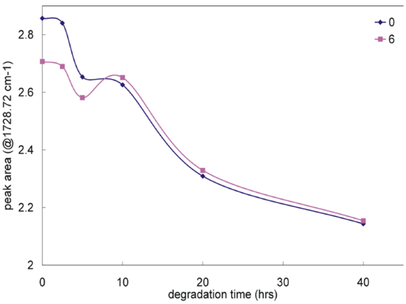

*Fig. 18 FT-IR peak area changes for ester group (1728 cm-1) with exposure to UV irradiation time in hours.*

## 7.4 Conclusions and discussion

ATR-FTIR and contact angle measurements are able to detect changes with increasing degradation time, but are limited to surface analysis; which means that no intrinsical differences can be found between coatings with different amount of clay particles. The same holds for UV-VIS, because it only analyses the resin. DSA, however, is able to detect differences between % of clay and increasing degradation. Fitting the whole sorption curve, folllowed by plotting the diffusion coefficient value versus degradation time did not show large changes or a trend. When shorter sorption times were investigated, clear differences could be found by linear fitting. Linear fitting resulted in an increasing slope for increasing degradation. Fitting these increasing slopes (with increasing degradation time) for different clay % resulted in an unclear trend for as well as 1kHz as for 1MHz. The last approach, based on calculating slope when the data is plotted on a log-log scale, resulted in clear trends, and showed to be the most useful technique to investigate the nanocomposites used for this project. Therefore, this model seems to be very promising for future use. Furthermore, for calculating the total water sorption, it appeared to be important which model was used, due to polarization within the sample. Brasher and Kingsbury seemed to be the most suitable for this system. Due to the fact that these conclusions are based on preliminary results, more research will be necessary to understand the mechanism(s) occuring during water sorption in short UV degraded nanoclay filled coatings.

## References

1. Y.S. Choi, M. Xu, I.J. Chung, Polymer **46**, 531 (2005)
2. H. Wong, K.Chang, H. Chu, S. Liou, J. Yeh, J. Appl. Polym. Sci **92**, 2402 (2004)
3. T.H. Kim, L.W. Jang, D.C. Lee, H.J. Choi, M.S. Jhon, Macromol. Rapid Commun **23**, 191 (2002)
4. J. Yeh, S. Liou, C. Lai, P. Wu, Chem. Mater. **13**, 1131 (2001)
5. J. Yeh, S. Liou, C. Lai, P. Wu, Chem. Mater. **14**, 154 (2002)
6. K.E. Strawhecker, E. Manias, Chem. Mater. **14**, 2943 (2000)
7. D. Wang, J. Zhu, Q.Yao, C.A. Wilkie, Chem. Mater. **14**, 3837 (2002)
8. Y.K. Kim, Y.S.Choi, K.H.Wang, I.J.Chung, Chem. Mater. **14**, 4990 (2002)
9. T. Lan, P.D. Kaviratna, T.J. Pinnavaia, Chem. Mater. **6**, 573 (1994)
10. H. Tyan, Y. Lui, K. Wei, Chem. Mater. **11**, 1942 (1999)
11. Z. Wang, T.J. Pinnavaia, Chem. Mater. **10**, 3769 (1998)
12. J.W. Gilman, C.L. Jackson, A.B. Morgan,R. Jr. Hayyis, E. Manias, E.P. Giannelis, M. Wuthenow, D. Hilton, S.H. Philips, Chem. Mater. **12**, 1866 (2000)
13. C. Decker, I. Lorinczova, J.C.T. Research **1**, 247 (2004)
14. C. Decker, F. Masson, R. Schwalm, Polym. Degr. Stab. **83**, 309 (2004)
15. Q. He, L. Wu, G. Gu, B. You, High Perf. Polym. **14**, 383 (2002)
16. A.M. Morrow, N.S. Allen, M. Edge, D. Aldcroft, H. Jones, Polym. Degr. Stab. **69**, 143 (2000)
17. M. L. Nobel, E. Mendes, S. J. Picken, J. Appl. Polym. Sci. 103, 687 (2007)
18. M. Giacomelli Penon, S.J. Picken, M. Wübbenhorst, J. van Turnhout, Pol. Degr. Stab., **92**, (2007), 1247-1254.
19. M. Giacomelli Penon, S.J.Picken, M.Wubbenhorst, G.deVos, J. van Turnhout, Rev. Sci. Instr. **77**, 115107 (2006)
20. M. Giacomelli Penon, S.J. Picken, M. Wübbenhorst, J. van Turnhout,. J. Appl. Pol. Sci., **105**, (2007), 1471-1479.
21. M. Giacomelli Penon, S.J. Picken, M. Wübbenhorst, J. van Turnhout, Pol. Degr. Stab., accepted.
22. D.M. Brasher, A.H. Kingsbury, J. Appl.Chem. **4**, 62 (1954)
23. U. Rammelt, G. Reinhard, Progr. Org. Coat. **21**, 205 (1992)
24. E.E. Rose, D.D. Joginder, R. Green, J. Cornell, Journal of Dental Research. **35**, 697 (1954)
25. T.J. Bosma, T. Lebey, V. Pouilles, I. Chernerie, Bui Ai, N. Rieux, J. Phys. D.: Appl. Phys. **28**, 1180 (1995)
26. C.M. Balik, Macromolecules **29**, 3025 (1996)

# Chapter 8

## WATER SORPTION IN NATURALLY DEGRADED COILCOATINGS BY DIELECTRIC SORPTION ANALYSIS

### 8.1 Introduction

During outdoor exposure, a well known phenomenon of steel is corrosion. This is also the reason that the surface is coated with a protective layer, like paint. But even paint has not the ability to protect steel for an infinite time, and at some point in time the organic layer has to be replaced. One question that remains is, when should it be replaced? The industry prefers to recoat the steel before it starts to corrode and influence the mechanical properties of the construction. Not surprisingly it is an expensive operation to stop a process plant for several days or weeks to have it (re-)painted. Therefore it is desirable to monitor and evaluate the quality of the coating and the steel, in order to estimate the planning of when (and where) to have the coating renewed. Various instruments are able to analyse an organic coating, such as FTIR, micro-(nano-) hardness, DSC, UV-VIS, SEM, DRS, WAXS, etc.[1-8].

The quality of the coating is mostly related to the ability to resist permeation of water and ions, since they are responsible for corrosion (together with oxygen)[9] of steel or other metal substrates. It is a well known fact that organic coatings are not impermeable to absorption of a certain amount of water[10-13]. Pigments and other additives are added to function as barrier (increase the tortuous path)[9,14] (and, of course, as cheap filler, colour, or to inhibit corrosion, etc.). With this knowledge it is interesting to use a measurement device that can monitor this water diffusion behaviour in time, to have an idea of the changing diffusion behaviour of a coating with (degradation) time. For this we have developed a device that simultaneously monitors the dielectric behaviour of the coating and the water sorption. It has already been used extensively on various organic materials and membranes and artificially degraded coatings[15-17]. Our purpose is to show that the DSA technique can also be applied to naturally degraded coilcoatings. It will become clear that already after three months of natural weathering a difference can be detected. Furthermore, interestingly, the sorption behaviour of the naturally degraded samples show similar trends as the artificially degraded ones, for which a desorption profile was found[16]. Conclusively, the DSA set up is a sensitive and versatile device that is applicable to a broad range of systems for which the sorption of water vapour has to be investigated.

## 8.2 Experimental

### 8.2.1 Materials

From Corus we received a polyester coilcoating used for panels in building constructions. The commercial system consists of an aluminium substrate with a polyester topcoating. Normally, when these coilcoatings are used outside, a primer is used between the aluminium and the topcoat. In this case it was deliberately decided not to use this system, otherwise the degradation would take too much time. The thickness of the polyester topcoat is 15 micrometer. The coilcoating process guarantees high uniformity of the coating, and this was also the reason for using this system for natural degradation tests and subsequent DSA measurements.

### 8.2.2 DSA set-up

The DSA set up has already been extensively described[18] and needs no further explanation. The DSA set up monitors real time the water vapor sorption of a sample dielectrically. The flow speed of both dry and wet nitrogen flow is 7 ml/s. The gas temperature is 27 ºC, the dry gas is about 2% RH and the wet gas is 86% RH. The dielectric analyser used for these experiments is a HP frequency analyser with a frequency range between 20 Hz until 1 MHz. The set up is placed in a temperature conditioned ambient room at about 24.5 ºC (±1 ºC).

### 8.2.3 Natural degradation

The panels were degraded for 0; 0.25; 2 and 2.5 years in Delft. The panels were mounted under a 45º angle facing south. The starting date for this degradation test was April 2003.

### 8.2.4 Micro ATR-FTIR

To investigate changes in chemical composition before and after degradation, micro ATR-FTIR was used. For this we used a Thermo Nicolet Nexus 470 FT-IR Spectrometer (bench) fitted with a Continuum infrared microscope.

### 8.2.5 SEM

For surface analysis SEM was conducted to see whether any differences could be found before and after 2.5 years of degradation. The used SEM device was a SEM Philips XL20 microscope.

## 8.3 Results

### 8.3.1 DSA

In figure 1a and 1b the DSA $\Delta C'$ and $\Delta C''$ sorption curves are shown between frequencies of 50 Hz and 1 MHz, for an undegraded coilcoating,. $\Delta C'$ represents the difference between the $C_t'$ in time and $C_{dry}'$. $C_t'$ is the real part of capacitance for time $t$ in [F] and $C_{dry}'$ is the real capacitance of a the dry coilcoating in [F]. $\Delta C''$ is calculated the same way as $\Delta C'$, and is the imaginary or loss part of the capacitance. For $\Delta C'$ the coating shows a normal water vapour sorption behaviour

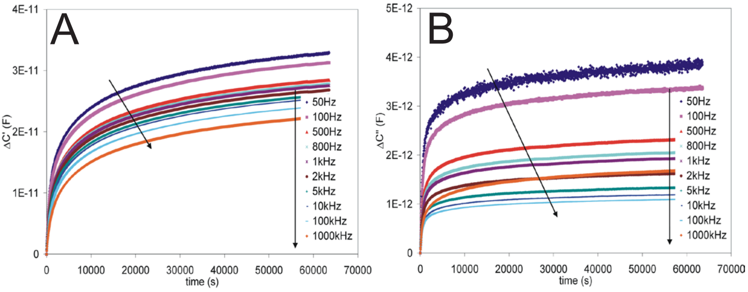

*Fig. 1a,b Sorption curve (a. $\Delta C'$ vs t, and b. $\Delta C''$ vs t) for an undegraded coilcoating.*

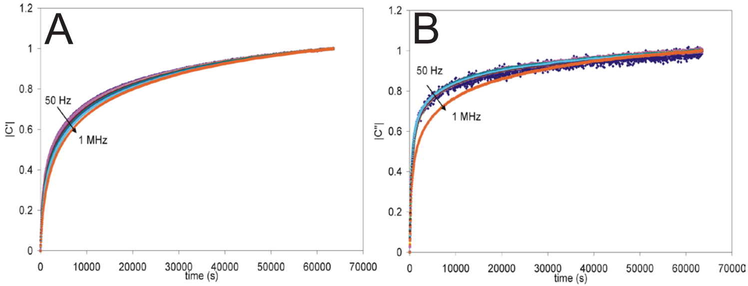

*Fig. 2a,b  Normalized sorption curve (a. $|C'|$ vs t, and b. $|C''|$ vs t) for an undegraded coilcoating.*

like previous studies[15-17]. $\Delta C''$ shows a similar trend, except for 1 MHz, where it would be expected that the signal would be below 100 kHz. Obviously for a particular, but unkown, reason the loss is higher at that frequency. Intermediate and higher frequencies would be necessary to clarify this, but it will become clear that this does not influence the results for degraded samples.

Also normalized data is shown in figure 2a and b for $\Delta C'$ and $\Delta C''$ given by $|C'|$ and $|C''|$. For this the data is divided by the (nearly fully) saturated $\Delta C'$ and $\Delta C''$ value at time 64000 seconds. Presenting data this way gives an idea whether the water in the coating has interaction with the polymer matrix.  For $|C'|$ there is a slight trend from low to high frequencies, but overall the effect is very small and one can assume that there is no interaction. For  $|C''|$ the overlap from 50 Hz to 100 kHz is very good and for these frequencies there is no interaction. At 1MHz there is a discrepancy and it might be possible that for this frequency the water and the polymer matrix interact with water in pores or water-polymer clustering.

It becomes more interesting when the coilcoatings had been naturally degraded, and for clarity the frequencies have been plotted separately in figure 3a-j. A first general remark is that, for all frequencies and both $\Delta C'$ and $\Delta C''$, differences in sorption behaviour can be seen at various degradation times. The lower frequencies (100 Hz and 1 kHz) show more scatter for longer degradation times, and is probable due to higher sensitivity for interactions between water and the degraded top layer. In a previous article[15] it was already discussed that a peak starts to appear from low to high frequencies for short to longer degradation

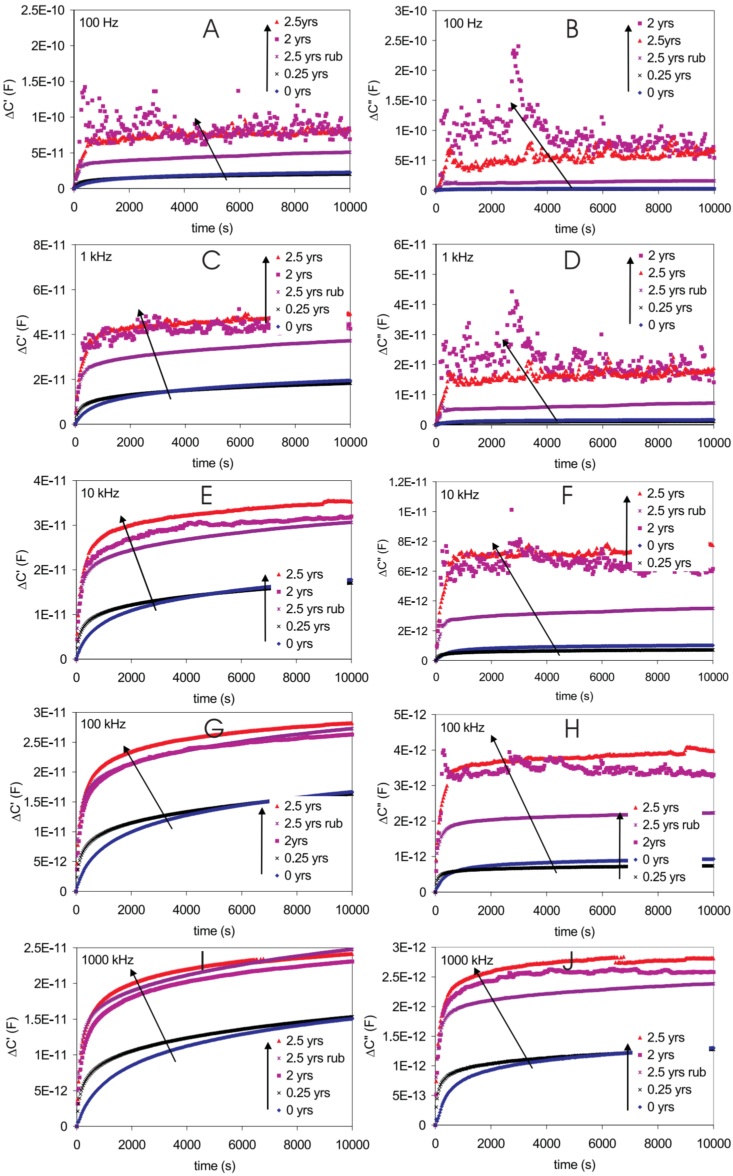

*Fig. 3a-j Sorption curves (ΔC' vs t and ΔC'' vs t) at different frequencies (100 Hz-1 MHz) for degraded coilcoatings (0, 0.25, 2 and 2.5 years).*

times. Also for these two frequencies a peak seems to be present. Most likely this peak is caused either by desorption of water, due to swelling of the coating causing the pores in the top layer to squeeze out the water[16]; or by interaction of water with the degraded polymer matrix, causing a decrease in the capacitance (*C*')[17]. Longer degradation times result in a higher total amount of water sorption. Already after 3 months a difference in water sorption can be detected with the DSA. None of the coatings were cleaned after degradation, but they do become dirty after several years of degradation. By eye the surface seemed not very dirty, but with SEM (see figure 4a, undegraded surface and 4b degraded surface) a fouling layer could be found. Therefore one coating (2.5 yrs degradation) was cleaned to see whether this had effect on the DSA measurement. The coating was cleaned by rubbing it with a water saturated tissue. From figure 3a-j it shows that due to the rubbing, the total amount of water in the coating is

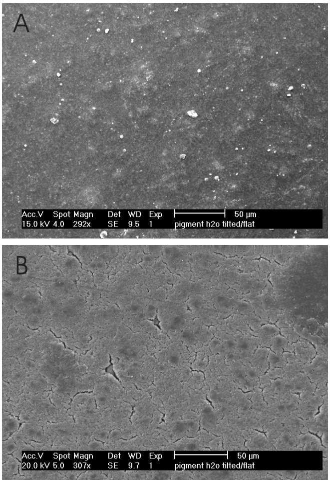

*Fig. 4a,b SEM photo's of an undegraded (a) and 2.5 years degraded (b) coilcoating.*

lower. Most likely this is because the degraded top layer is partially being removed, resulting in lower water uptake; or that the fouling layer adds to the total water uptake. Based on the fact that the uptake is still more than the undegraded coating, it can be seen that not the whole degraded layer is removed after this cleaning procedure.

### 8.3.2 ATR-FTIR

In figure 5 the results of the ATR-FTIR measurements are shown. Unfortunately the device was only able to measure the spectrum of the undegraded sample clearly. For the degraded samples only the 1725 $cm^{-1}$ peak remains visible, which decreases already after 3 months, but then remains stable up to 2 years. Even after cleaning the surface, by rubbing the surface with a tissue with water, of the 2.5 yrs degraded coating and measuring again did not result in a better quality spectrum. Since the ATR-FTIR is only useful for surface characterization, most likely the pigment particles reach the surface after 2.5 yrs of degradation. Which makes the ATR-FTIR unsuitable to measure the coating degradation.

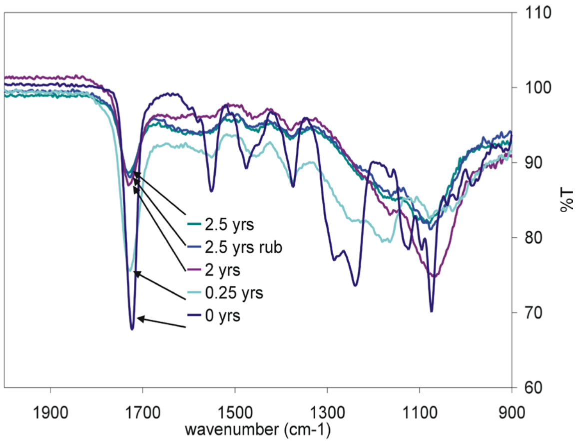

*Fig. 5 ATR-FTIR of 0, 0.25, 2 and 2.5 years degraded coilcoating.*

## 8.4 Conclusions and outlook

Already after 3 months of natural weathering a difference in the DSA sorption behaviour could be found. Most importantly, similar results were seen between natural weathering of coilcoatings and artificially degraded coatings, which show first an increase of water sorption; followed by a desorption profile. The initiation of a desorption profile was found for longer degraded samples. This profile indicates that either “squeezing” out of water occurs, or that clustering of water occurs, which lowers the capacitance (C’). The only difference between artificial and natural degraded samples is that DSA measurements on natural degraded samples are noisier; especially for the longer degraded samples (2 and 2.5 years). This scatter is presumably the result of dirt accumulated on the surface, also known as fouling, and can be reduced by cleaning the surface with a wet tissue. Cleaning the surface might induce the removal of a part of the degraded layer, resulting in a lower signal, resulting in almost complete disappearance of the desorption behaviour. Whether part of the degraded layer has been removed by cleaning is an issue which needs to be investigated further. Nevertheless, even after cleaning the surface a higher uptake of water is found and this indicates that not the whole degraded layer was removed. Future measurements are necessary to find the influence of the fouling layer on DSA measurements, and longer degraded samples should reveal the further development of the desorption profile.

Besides the fact that the DSA has the potential of measuring differences between natural degraded samples; the major advantage is the possibility to investigate the condition of the coating after natural weathering, which could not be done with the ATR-FTIR.

## References

1. Rabek J.F., Polymer Photodegradation, (1995), 433-598, Chapman and Hall, Weinheim.
2. MacQueen R.C., Granata R.D., *Progr. Org. Coat.*, **28**, (1996), 97-112.
3. Biggs S. et al., *Progr. Org. Coat.*, **42**, (2001), 49-58.
4. Armstrong R.D., Jenkins A.T.A, Johnson B.W., *Corr. Sci.*, **37**, (1995), 1615-1625.
5. Perrin F.X., Irigoyen M., Aragon E., Vernet J.L., *Pol. Degr. Stab.*, **70**, (2000), 469-475.
6. Sugura M., Mitsuoka T., Murase A., *Pol. J.*, **33**, (2001), 617-620
7. Delobelle P., Guillot L., Dubois C., Monney L., *Pol. Degr. Stab.*, **77**, (2002), 465-475.
8. Lukey C.A., *Progr. Org. Coat.*, **41**, (2001), 129-134.
9. Florio J.J., Miller D.J. ed., Handbook of coating additives, (2004), 127-144 (by Coughlin R.) Marcel Dekker, New York
10. Krevelen D.W. van, Properties of Polymers, (1972), pp.295-297, Elsevier, New York
11. Comijn J., Polymer Permeability, (1985) (whole book), Elsevier, New York.
12. Osswald T., Menges G., Materials Science of Polymers for Engineers, (2003), pp. 571-584 (permeability properties of polymers), Hanser Gardner Publications, Ohio
13. van der Wel G.K., Adan O.C.G., Progr. Org. Coat. **37** (1999),1-14.
14. Marcus P., Corrosion Mechanisms in Theory and Practice 2nd ed., (2002), 683-729 (de Wit, J.H.W. van der Weijde D.H., Ferrari G.), Marcel Dekker, NewYork.
15. Giacomelli Penon M., Picken S.J., Wübbenhorst M., and van Turnhout J.,. J. Appl. Pol. Sci., **105**, (2007), 1471-1479.
16. Giacomelli Penon M., Picken S.J., Wübbenhorst M., and van Turnhout J.,. Pol. Degr. Stab., **92**, (2007), 1247-1254.
17. Giacomelli Penon M., Picken S.J., Wübbenhorst M., and van Turnhout J.,. Pol. Degr. Stab., accepted.
18. M. Giacomelli Penon, S.J. Picken, M. Wubbenhorst, G. de Vos, J. van Turnhout, Rev. Sci. Instr. **77**, 115107 (2006)

# Chapter 9

# CONCLUSIONS AND OUTLOOK

## 9.1 Conclusions

The original goal of this research was to investigate new ways of predicting the life-time expectancy of organic coatings. Since this topic is too ambitious to finish within a PhD project which lasts four years, the idea changed into the exploration of the possibilities and opportunities that were aimed in the direction of the main goal. Therefore two different approaches were studied for their feasibility. The first approach was to optimise an existing measurement device, or to build one, which is able to detect (physical or chemical) changes of a coating as early as possible. In this way it would become possible to use this technique as an early-warning system for coatings, and quick evaluation of coatings would be possible. For this a set-up has been built which was baptized as DSA or Dielectric Sorption Analysis. The basic principle of this technique is the sorption of water and simultaneously measuring the changes of the dielectric properties of the coating. Secondly the accelerated degradation devices were critically analysed on the parameters used to increase the degradation of coatings. It appeared that basic parameters like UV radiation, temperature and humidity are commonly used, along with salt spray, day and night cycles, acid rain simulation and other similar techniques. One parameter remained absent however, which was the atmospheric pressure. All other parameters were increased: UV dose, temperature, humidity cycles, etc., but the atmospheric pressure remained 1 bar. Based on this the decision was made to investigate the effect of pressure on UV degradation. This combined approach resulted in a useful measurement device and a novel method to degrade coatings. An overview of each separate chapter is briefly given below. As already mentioned, this research started from ground zero with the aim to push this topic into a different direction than the approaches used thus-far. While at least an alternative direction has been given, still a lot of further work remains to be done, as is discussed below.

## 9.2 Outlook

Firstly, the DSA technique can be developed further in such way that temperature and humidity can be controlled simultaneously. This feature can be used to evaluate degraded coatings, but, of course, can also be used to evaluate separation membranes, permeability, food packaging, etc. These are very interesting fields to investigate, since at various temperatures the diffusion behaviour and affinity of the polymer chains with water and their mobility can differ. Furthermore, by measuring the diffusion behaviour at different humidity levels, the (non) linearity of the coatings can be revealed. Another interesting option is to use another liquid, instead of water, to humidify films. This way particles with different polarity, molecule size, affinity with polymer, etc. can be studied.

Secondly, the investigation of pressure in relation with UV degradation has initiated, and is far from finished. Large steps have been made to extreme pressures, and a closer look is necessary with smaller pressure steps; in order to derive a more accurate model than the one proposed here. Also measurements at different temperatures, with the presence of water, under various UV intensities and using a lamp that mimics the solar spectrum should be done. In addition, further establishing the relationship between natural degradation and the accelerated pressure technique is a necessary, and crucial, step.

As can be seen still a lot of research is possible, and hopefully this will also be done in the future, as interesting results might come out.

# SUMMARY

The objective of this project was to improve the correlation between accelerated and natural weathering, making it possible to make better estimations to predict the life time of organic coatings.
One approach was based on developing a measurement device, that was able to detect at an early stage (physical or chemical) changes in an organic coating. In this way an organic coating can be degraded under less agressive/ intensive accelerated degradation parameters; making the circumstances more close to natural weathering. Or the coating can be weathered naturally. The device constructed for this has lead to the so-called dielectric sorption analysis (DSA) and is described more elaborately in chapter 3.
The other approach focused on the possibility to increase the correlation between natural degradation and the accelerated weathering machines. Closer investigation revealed that all parameters (UV, humidity, temperature etc.) were present, except pressure. Pressure is an important parameter, since it determines the amount of photo-oxidation in the coating during UV degradation. Therefore a closer investigation was started into this parameter. The results of the effect of pressure can be found in chapter 6. Below the contents of the separate chapters are briefly summarized.

**Abstract chapter 3**
The sorption of water vapour in Kapton® (polyimide) films has been investigated with a new method, dielectric sorption analysis (DSA). The technique is based on high-resolution time-resolved, capacitance measurements performed during exposure of an organic coating to humidified nitrogen. The basis of the method is described together with experimental details related to the capacitance measurement, long-term stability, reproducibility and other characteristics of the set-up. The technique allows the determination of the sorption/desorption and diffusion characteristics of a coating on a time scale varying from seconds to days. Mass transport properties derived from complementary weight measurements are in good agreement with the DSA results. Real-time monitoring of the moisture sorption in organic coatings demonstrates the potential of the technique in the field of non-destructive coating inspection and testing.

**Abstract chapter 4**
The sorption of water vapour in various organic coatings (PI, PA6.6, epoxy, PMMA and LDPE) and filters (PVDF, PTFE, porous PE, and nitro cellulose) has been investigated by Dielectric Sorption Analysis (DSA). The technique is based on high-resolution time-resolved, capacitance measurements performed during exposure of an organic coating to humidified nitrogen. The DSA technique can distinguish between all samples and the diffusion coefficient and maximum sorption is calculated for all samples. A frequency sweep with a dielectric analyser shows that in all cases the water has no interaction with the polymer films, except for PA6.6. For PA6.6 it is assumed that electrode polarization takes place. For filters a frequency sweep shows in two cases electrode polarization (porous PE, cotton linter), two cases no interaction (PTFE, nitro cellulose) and two

cases an intermediate effect (PVDF 0.22 µm, PVDF 0.45 µm). The filters show a desorption profile likely due to the swelling of the filters causing vapour to be pressed out of the pores of the filters. Mass transport properties derived from complementary weight measurements on epoxy films are in good agreement with the DSA results.

**Abstract chapter 5**

Degraded clear and pigmented epoxy coatings were investigated by dielectric sorption analysis. Differences in the dynamics of absorption behaviour, due to increased hydrophilicity, crosslinking and porosity, can be found between UV degraded and undegraded epoxy coatings, while at longer degradation times a desorption behaviour is observed. Desorption is caused by swelling of the coating and shrinking of pore size, squeezing out the excess of water. This desorption phenomena has been reproduced by model system measurements of pigmented coatings with various filters on top. Due to crack formation during DSA measurements, clear coatings show fluctuating results. Crack formation is a result of release of tension of the UV degraded clear coating by humidified nitrogengas. Pigmented coatings do not show this behaviour and a clear increasing absorption trend is found for longer degradation times. In case of desorption a frequency sweep shows larger peaks for lower frequencies. This may be due to electrode polarisation or the interaction of water with hydrophilic groups formed during degradation. Even though the mechanism is not fully understood, we conclude that dielectric sorption analysis is suitable for non-destructive investigation of degraded coatings and paints.

**Abstract chapter 6**

Epoxy pigmented coatings were UV degraded for various days at elevated pressures. The pressures varied between 1 and 100 bar. The relationship between degradation and pressure was investigated with dielectric sorption analysis (DSA). Differences in dynamics of absorption behaviour for degraded polymer occur due to increased hydrophilicity, crosslinking and porosity. Degradation at all pressures show first sorption followed by desorption of water. Desorption is caused by swelling of the coating and shrinking of pore size, squeezing out the excess of water. The amount of water sorption and desorption from 1 to 50 bar increases linearly. From 50 bar no further increase of degradation is found, which is likely due to saturation of the degradation process.

For UV degradation at 100 bar with increasing degradation times, an increasing linear trend was found for the water sorption and desorption behaviour. At lower frequencies double peaks are found as a result of water desorption, polymer relaxation, water-hydrophilic cluster interactions and polymer swelling. Besides water desorption all other processes are highly frequency dependent. With a simple model it is shown that the two peaks can be fitted by two independent curves. The desorption of water in the 2$^{nd}$ peak can be fitted for all frequencies with a single exponential term. For lower frequencies the exponential fit starts to deviate due to the influence of the other processes, whereas at higher frequencies only the effect of water is measured.

**Abstract chapter 7**

Water sorption in (short) UV degraded alkyd coatings containing nanoparticles has been investigated by DSA, contact angle measurements, UV-VIS and ATR-FTIR. The clay % of these coatings varied between 0-6%. Only DSA measurements appeared to be able to distinguish between the various clay particle filled alkyd coatings. Three methods have been used to fit the and analyse the (diffusion data of the) DSA measurements, and only one was found to be useful for future quantification of (short) degraded organic coatings. This method was based on calculating the initial slope for data plotted on a log-log scale. The other two methods, full diffusion curve fits and linear fit, did not result in a clear trend. The total water sorption of the coatings was calculated with two models, Brasher-Kinsbury (BK) and Landau, Lifschitz, Looyenga (LLL). It could be concluded that care should be taken which model is used for which coating system.

**Abstract chapter 8**

Sorption behaviour of naturally degraded (0, 0.25, 2 and 2.5 years) polyester coilcoatings on steel were investigated. The chemical degradation was investigated with ATR-FTIR. The results show that an increase in sorption can be found for longer degradation times. Also the start of a desorption profile can be seen, similar to previous measurements on artificially degraded samples. Cleaning of the surface appeared to be necessary as SEM pictures showed clear fouling of the surface. Surface cleaning resulted in a drop of the water sorption level, but it still remained higher than for undegraded samples. Furthermore the ATR-FTIR was not useful for measuring 2 and 2.5 years degraded coatings, showing the advantage of the DSA measurement. Future measurements are necessary to further investigate fouling of the surface and the development of a desorption profile after longer degradation times.

# SAMENVATTING

Het doel van dit project was de correlatie tussen versnelde en natuurlijke verwering te verbeteren, zodat het mogelijk wordt de levensduur van organische coatings beter te kunnen voorspellen.
Een essentieel deel van de aanpak was gebaseerd op de ontwikkeling van een meetapparaat, dat in staat is in een vroeg stadium (fysische of chemische) veranderingen in een organische coating te detecteren. Op deze manier kan een organische coating gedegradeerd worden met minder agressieve en intensieve versnelde degradatie parameters; zodat de omstandigheden dichter bij de natuurlijke verwering komen. Of de coating kan onder natuurlijke omstandigheden verweerd worden. De methodiek die hiervoor ontwikkeld werd, is de zogenaamde dielektrische sorptie analyse (DSA) en is in meer detail beschreven in hoofdstuk 3.
Een belangrijk ander onderdeel van de aanpak werd geconcentreerd op de mogelijkheid de correlatie tussen natuurlijke degradatie en versnelde verwering te verbeteren. We realiseerden ons dat alle parameters (UV, vochtigheid, temperatuur etc.) aanwezig waren, behalve druk. Druk is een belangrijke parameter, aangezien het de hoeveelheid zuurstof, dus de foto-oxidatie in de coating bepaalt gedurende UV degradatie. Daarom werd een nader onderzoek geïnitieerd naar deze parameter. De resultaten van het effect van druk kunnen gevonden worden in hoofdstuk 6. Hieronder wordt de inhoud van de afzonderlijke hoofdstukken kort samengevat.

**Samenvatting hoofdstuk 3**
De sorptie van waterdamp in Kapton ® (polyimide) film werd onderzocht met een nieuwe methode, dielectrische sorptie analyse (DSA). De techniek is gebaseerd op hoge-resolutie tijd-oplossende, capaciteitsmetingen uitgevoerd gedurende blootstelling van een organische coating aan vochtig stikstofgas. De basis van de methode wordt beschreven, samen met experimentele details gerelateerd aan de capaciteitsmeting, langeduur stabiliteit, reproduceerbaarheid en andere karakteristieken van de opstelling. De techniek maakt het mogelijk om de sorptie / desorptie en diffusiekarakteristieken van een coating te bepalen, op een tijdschaal variërend van seconden tot dagen. Massatransport eigenschappen afgeleid van complementaire gewichtsmetingen zijn in goede overeenstemming met de DSA resultaten. Het in de tijd monitoren van de vochtsorptie in organische coatings demonstreert de potentie van deze techniek in het veld van niet-destructieve coating inspectie en testen.

**Samenvatting hoofdstuk 4**
De sorptie van waterdamp in een aantal organische coatings (PI, PA6.6, epoxy, PMMA en LDPE) en filters (PVDF, PTFE, poreuze PE en nitro cellulose) werd onderzocht door middel van dielektrische sorptie analyse (DSA). De techniek is gebaseerd op hoge resolutie tijd-oplossende, capaciteitsmetingen, uitgevoerd gedurende blootstelling van een organische coating aan vochtig stikstofgas. De DSA techniek kan onderscheid maken tussen alle monsters en de diffusiecoëfficiënt en maximum sorptie worden berekend

voor alle monsters. Metingen bij verschillende frequenties met een dielectrische analyser lieten zien dat in alle gevallen het water geen interactie heeft met de polymeer films, behalve PA6.6. Voor PA6.6 wordt aangenomen dat er elektrodepolarisatie plaatsvindt. Voor filters laten metingen bij verschillende frequenties in twee gevallen elektrodepolarisatie (poreuze PE, katoen snippers), in twee gevallen geen interactie (PTFE, nitro cellulose) en in twee gevallen een tussen effect zien (PVDF 0.22 mm, PVDF 0.45 mm). De filters laten een desorptie profiel zien, waarschijnlijk door de zwelling van de filters wat ertoe leidt dat het vocht uit de holtes van de filters wordt gedrukt. Massatransport eigenschappen afgeleid van complementaire gewichtsmetingen op epoxyfilms zijn in goede overeenstemming met de DSA resultaten.

**Samenvatting hoofdstuk 5**

Gedegradeerde blanke en gepigmenteerde epoxy coatings werden onderzocht door middel van dielektrische sorptie analyse. Verschillen in de dynamiek van absorptie gedrag, door verhoogde hydrofiliteit, vernetting en porositeit, konden worden gevonden tussen UV gedegradeerde en ongedegradeerde epoxy coatings, terwijl bij langere degradatietijden een desorptie gedrag werd geconstateerd. Desorptie wordt veroorzaakt door zwelling van de coating en het krimpen van de holtes, zodat het overschot aan water eruit wordt geperst. Dit desorptie fenomeen kon gereproduceerd worden door te meten aan een modelsysteem van gepigmenteerde coatings met verscheidene filters er bovenop geplaatst. Door scheurvorming gedurende de DSA metingen, lieten de blanke coatings fluctuerende resultaten zien. Scheurvorming is een gevolg van spanningsrelaxatie van de UV gedegradeerde coating door het vochtige stikstofgas. Gepigmenteerde coatings laten dit gedrag niet zien en een duidelijke absorptie trend kon gevonden worden bij langere degradatietijden. In geval van desorptie laat een frequentie sweep dan hogere pieken zien bij lagere frequenties. Dit kan komen door elektrode polarisatie of de interactie van water met hydrofiele groepen gevormd tijdens de degradatie. Ondanks het feit dat het mechanisme niet geheel verklaard is, kunnen we concluderen dat dielektrische sorptie analyse geschikt is voor niet-destructief onderzoek aan gedegradeerde coatings en verven.

**Samenvatting hoofdstuk 6**

Gepigmenteerde epoxy coatings werden UV gedegradeerd voor een aantal dagen bij verhoogde drukken. De drukken varieerden tussen 1 en 100 bar. De relatie tussen degradatie en druk werd onderzocht met dielektrische sorptie analyse (DSA). Verschillen in dynamiek van absorptiegedrag voor een gedegradeerd polymeer vinden plaats door verhoogde hydrofiliteit, vernetting en porositeit. Degradatie bij elke druk liet eerst sorptie gevolgd door desorptie zien van water. Desorptie wordt veroorzaakt door zwelling van de coating en het krimpen van de holtes, zodat overtollig water eruit wordt geperst. De hoeveelheid watersorptie en desorptie verloopt lineair van 1 tot 50 bar. Vanaf 50 bar wordt er geen verdere verhoging van de degradatie gevonden, wat waarschijnlijk door verzadiging van het degradatieproces komt.

Voor UV degradatie bij 100 bar met toenemende degradatietijden, werd een lineaire trend gevonden voor watersorptie en desorptiegedrag. Bij lagere frequenties werden dubbele pieken gevonden als een gevolg van waterdesorptie, polymeerrelaxatie, water hydrofiele clusterinteractie en polymeerzwelling. Naast watersorptie zijn alle andere processen sterk frequentie afhankelijk. Met een simpel model kon worden aangetoond dat de twee pieken gefit kunnen worden met twee onafhankelijke krommen. De desorptie van water in de 2e piek kan gefit worden voor alle frequenties met een enkele exponentiele term. Voor lagere frequentie begint de exponentiele fit af te wijken door de invloed van de andere processen, terwijl bij hogere frequenties alleen het effect van water wordt gemeten.

**Samenvatting hoofdstuk 7**

Watersorptie in (kort) UV gedegradeerde alkyd coatings met nanodeeltjes werd onderzocht met DSA, contacthoek metingen, UV-VIS en ATR-FTIR. De percentages kleideeltjes in deze coatings varieerden tussen 0-6%. Alleen de DSA meting bleek in staat verschillen te meten tussen de verschillende met kleideeltjes gevulde alkyd coatings. Drie methoden zijn gebruikt om te fitten en vervolgens de (diffusiedata van de) DSA metingen te analyseren; en slechts één werd geschikt bevonden voor toekomstige kwantificering van (kort) gedegradeerde organische coatings. Deze methode is gebaseerd op de berekening van de initiële helling van de data geplot op een log-log schaal. De andere twee methoden, volledige diffusie curve fitten en een lineaire fit, leidde niet tot een duidelijke trend. De totale watersorptie van de coating werd berekend met twee modellen, Brasher-Kinsbury (BK) en Landau, Lifschitz, Looyenga (LLL). Er kon worden geconcludeerd dat voorzichtigheid is geboden welk model wordt gekozen voor welk coatingsysteem.

**Samenvatting hoofdstuk 8**

Sorptiegedrag van natuurlijk verweerde (0, 0.25, 2 en 2.5 jaar) polyester coilcoatings op staal werd onderzocht. De chemische degradatie werd onderzocht met ATR-FTIR. De resultaten laten zien dat een verhoging van sorptie gevonden kan worden voor langere degradatietijden. Ook het begin van een desorptie profiel kon gezien worden, gelijk aan voorgaande metingen op kunstmatig gedegradeerde samples. Schoonmaken van het oppervlak bleek nodig aangezien SEM foto's duidelijk vervuiling lieten zien van het oppervlak. Het schoonmaken resulteerde in een verlaging van het watersorptie niveau, maar dit bleek nog steeds hoger te zijn dan voor ongedegradeerde monsters. Tevens bleek ATR-FTIR niet geschikt om 2 en 2.5 jaar gedegradeerde coatings te meten. Dit laat het voordeel zien van de DSA. Toekomstige metingen zijn nodig om de vervuiling van het oppervlak verder te onderzoeken en de ontwikkeling van het desorptieprofiel voor langere degradatietijden vast te leggen.

## Curriculum Vitae

Massimiliano Giacomelli Penon werd op 21 april 1973 geboren te ‘s-Gravenhage. Na het behalen van het VWO diploma aan het Stevin College te ’s-Gravenhage in 1992 is hij aan de universiteit te Leiden Scheikunde gaan studeren. Twee jaar later waren de gedachten veranderd, en na een korte tussenpauze in de vorm van de diensplicht (de laatste) werd in 1996 de opleiding Materiaalkunde begonnen aan de Technische universiteit Delft. De studie werd afgerond in 4,5 jaar en het afstudeerproject werd gedaan bij Philips Natlab onder begeleiding van dr. Johan Feenstra en dr. Menno Prins. Het project bestond uit het onderzoeken naar de oplading van fluoropolymeren bij het aan en uitschakelen van een elektrisch veld t.b.v. nieuwe röntgenfilters voor medische apparatuur. Direct daarna werd hij aangenomen bij Fokker Aerostructures om te werken aan het Glare project, waarin werd gekeken naar het belang van de legpatronen van prepreg glasfibres in Glare en de verbetering van het Glare productieproces. De onderzoekskriebels waren echter nog niet gestild en na 6 maanden werd de beslissing genomen een promotieonderzoek te doen bij prof. Jan van Turnhout in 2002, met het onderwerp “Accelerated life time prediction of organic coatings”. Tijdens het aflopen van het contract aan de universtiteit, verlengde Materials Innovation Centre (dr. Rik Breur) mijn contract voor 6 maanden om mijn proefschrift af te kunnen schrijven en tevens onderzoek te doen voor naar inhibitor-mechanismen door biofilms op staal. Dit contract werd daarna verlengd voor een jaar, bij C-Cube International door ir. Guus Coolegem. Het werk verschoof toen meer naar het gebied van meetapparatuur voor kwaliteitsmetingen aan, en karakterisering van, coatings; en projectuitvoering voor klanten.
Per 1 januari 2008 zal hij bij Avery Dennison gaan werken als Senior Development Engineer bij de afdeling Product Development & Adhesive Technology of Roll Materials Europe.

# Acknowledgements

Het begon allemaal bij prof. Jan van Turnhout, en daarom begin ik bij hem. Ik ben hem dankbaar dat hij mij een promotie heeft aangeboden, en ook dat hij mij alle vrijheid bood om onderzoek te doen. Dankzij hem ben ik nu een zelfstandig onderzoeker geworden. Op de juiste momenten heeft hij mij ook bijgestaan om oplossingen te verzinnen voor gerezen problemen. Prof. Stephen Picken verdient eveneens mijn waardering en dank voor zijn hulp een creativiteit om mij door de welbekende “dips” heen te trekken. Ook hij heeft op de juiste momenten zijn steun gegeven. Michael Wübbenhorst is tijdens mijn promotie naar de zuiderburen vertrokken, maar we hebben het contact niet verloren. Hij was altijd bereid hulp te bieden wanneer dat nodig was.

Tijdens mijn promotie was er een begeleidingscommissie, en de heren die daar lid van waren verdienen ook de nodige aandacht. De hele commissie bestaande uit; prof. Hans de Wit, ir. Gabriele Ferrari, ing. Leo van der Ven, Kees van Vliet, dr. Jan Breen en dr. Patrick van Veenendaal, ben ik dankbaar voor de vrijheid die geboden werd om dit project uit te voeren. Ondanks het feit dat er bedrijven bij waren, werden niet de wensen van het bedrijfsleven voorop 5gesteld, maar telde vooral het belang van het onderzoek. Prof. Hans de Wit ben ik zeer dankbaar voor het feit dat hij een oogje in het zeil hield tijdens mijn promotie. Zijn kritische kijk op de resultaten heeft er mede toe geleid dat ik gedurende de hele promotie alert bleef. Gabriele Ferrari heeft ook vele malen het belang van het afmaken van mijn promotie voorop gesteld. Dat Den Helder de meeste zonuren van Nederland heeft, kan wel eens kloppen aangezien de keren dat ik er ben geweest de zon altijd scheen. Leo van der Ven is een razend enthousiast commissielid geweest en heeft altijd veel interesse getoond in het onderzoek. Helaas was Kees van Vliet niet de hele promotie periode aanwezig, maar ik stel zijn praktijkervaring en zijn pragmatische aanpak zeer op prijs. Ook de openheid die het bedrijf heeft getoond is het noemen waard. Dr. Jan Breen heeft zijn chemische kennis, en zijn kennis over de veroudering van polymeren, ingebracht in mijn project. Dr. Patrick van Veenendaal kwam later in dit project, en heeft dit project financieel in goede banen laten lopen.
Tom Bos was mijn “mede-” promovendus, waar het onderzoek mee is uitgevoerd. Helaas zat hij permanent in Den Helder, dus veel contact is er niet geweest, ook doordat hij later in dit project is gestapt. Toch waren de momenten wanneer we contact hadden erg nuttig en zinvol en heb ik ook veel van hem over coatings geleerd.

Een persoon, die een grote invloed heeft gehad op het afronden van mijn promotie is prof. M. Wessling. Hij was zo vriendelijk mij zijn hoge druk opstelling uit te lenen, waar ook hij zijn onderzoek op heeft uitgevoerd. De opstelling zal nu weer terugkeren naar zijn rechtmatige eigenaar, tot er weer een promovendus opduikt die hem graag wil gebruiken.
Mijn waardering gaat ook uit naar prof. de With, die zijn interesse heeft getoond in dit onderwerp door kritische vragen te stellen en een aantal opmerkingen plaatste, zodat het geheel leesbaarder is geworden.

De PME groep, dat later de NSM groep werd, is een gezellige groep waar altijd tijd was om de druk af te laten. Uiteraard begin ik met mijn kamergenoten Plamen en Zeynep, waarvan ik alleen zeg: we hebben het fort lang gehouden! Verder wil ik Wilco, Mirko, Chris, Stefan, Seb, Arek, Daniel, Telma, Stefan, Ceren, Louise, Marcel, Daniele, Hayley en Otto bedanken voor de gezelligheid ook buiten die van de werksfeer. Een speciale dank gaat uit naar Plamen die zo goed als een broer van me is geworden, we hebben een hoop samen meegemaakt. Ook zal ik niet de wijnavonden vergeten in een kamer die ik verder niet zal noemen. Voor Gerard is een normaal bedankje niet voldoende, aangezien hij me altijd terzijde heeft gestaan, alhoewel het niet altijd duidelijk was of dit leedvermaak was of oprechte meelij; eerlijk gezegd ga ik uit van het eerste, maar het was nodig “to separate the boys from the men!” Dankzij Gerard heeft het project ook nooit stilgestaan. Piet wil ik bedanken voor het altijd in staat zijn om meetapparatuur voor me op te snorren en software + ondersteuning. Ook Ben heeft mij altijd met raad en daad bijgestaan op mijn vraag naar onderdelen en gevoelige situaties omtrent veiligheid. Uiteraard vergeet ik Wolter en Eduardo niet alhoewel we nooit elkaars paden gekruist hebben, vaktechnisch gezien. Karin en Wil wil ik bedanken voor hun hulp en gezelligheid de afgelopen jaren.

Een grote dank gaat uit naar dr. Rik Breur, voor het uitreiken van zijn hand op het moment dat ik het nodig had om mijn proefschrift af te ronden. Mede dankzij hem heb ik het ook voor elkaar gekregen.

Voor Guus gaat een bijzonder dank voor zijn vertrouwen om met mij verder te gaan, en de lessen die ik geleerd heb en het gelach dat wij hebben gehad; dit zal zeker niet de laatste keer zijn.

Verder van de mensen van de materiaalkunde opleiding gaat een speciaal bedankje naar Patricia, die gelukkig nog contact heeft met de oude garde; en zondermeer ook blijft houden. Verder heeft Frederik altijd tijd voor me gemaakt om mij verder te helpen op de, nu hetende, surfaces and interfaces. Dit geldt ook voor Jeroen, die de “voorganger” van Frederik was.

Furthermore, I would like to thank a number of people for the happy and joyful evenings; Celia, congratulations for your pronounciation of Hoegaarden, but most importantly for being a friend. Nuno and Fernando, Mattijs and Hannelore Daniel and Sonia, Arek and Ola, Christoph and Cristina, Erik and Agatha, Judith and John, Cem and Zeynep for the many outgoing and “gezellige” evenings / dinners.

Aan Pares en Rachna, dat we altijd de “happy campers” zullen blijven en ook wat vaker zullen ontmoeten.

To Nick and Nicola, a lot of luck and happiness in England with your children. Thanks for the nice evenings and Nick for the squash.

I would like to thank my second family, Antonio, Eduarda and Fabio, for their support and confidence in the past years; and for opening my eyes to a second world. Their optimism, joy of life and gastronomy is a true blessing and an example.

Mijn vader en moeder, “tweede vader en moeder” Ron en Aad, “broer(tje)” Wes en Gerda wil ik bedanken voor hun grenzeloze steun in elk opzicht en vertrouwen in mij, er zijn geen woorden voor die dat kunnen uitdrukken, maar waarvan ik gelukkig weet dat dat ook niet nodig zal zijn.

Finally I thank Cristiana for her trust, support, “gezelligheid”, (world) experience, humour, thoughts and future.

# Publications

## Scientific papers

M. Giacomelli Penon, S.J. Picken, M. Wübbenhorst, G. de Vos and J. van Turnhout. Dielectric water sorption analysis. Review of Scientific Instruments 77, 115107, 2006.

M. Giacomelli Penon, S.J. Picken, M. Wübbenhorst and J. van Turnhout. Vapour diffusion in porous/non porous polymer coatings by dielectric sorption analysis. Journal of Applied Polymer Science 105, 1471-1479, 2007.

M. Giacomelli Penon, S.J. Picken, M. Wübbenhorst and J. van Turnhout. Water sorption in UV degraded clear&pigmented epoxy coatings by DSA. Polymer Degradation and Stability 92, 1247-1254, 2007.

M. Giacomelli Penon, S.J. Picken, M. Wübbenhorst and J. van Turnhout. Dielectric sorption analysis of UV degraded pigmented coatings at elevated pressures. Polymer Degradation and Stability, accepted, 2007.

## Presentations and poster presentations

| | | |
|---|---|---|
| Fair | ESEF Jaarbeurs Utrecht (March 2006) | invited speaker |
| Workshop | IOP OT TPA Maarssen (June 2005) | invited speaker |
| Congress | Dutch Polymer Days Lunteren (Februari 2005) | presentation |
| Workshop | SigmaKalon-Sigma Coatings (June 2004) | presentation |
| Workshop | Akzo Nobel Coatings (May 2004) | presentation |
| Congress | Dutch Polymer Days Lunteren (Februari 2004) | poster |
| Workshop | Surface Technologie Vlieland (October 2003) | presentation |
| Workshop | TNO corrosie (April 2003) | presentation |
| Congress | Dutch Polymer Days Lunteren (Februari 2003) | poster |
| Congress | IDS&DRP Leipzig Duitsland (October 2002) | poster |
| Congress | Dutch Polymer Days Lunteren (Februari 2002) | poster |